Borehole seismic methods for opencast coal exploration

Kragh, J. Edward

Borehole Seismic Methods For Opencast Coal Exploration

by

J. Edward Kragh

A Thesis submitted in partial fulfilment of the requirements for the degree of Doctor of Philosophy

Geological Sciences

The University of Durham
1990

Abstract

Borehole seismic methods for opencast coal exploration

By

J. Edward Kragh

Surface seismic techniques lack the resolution to image the top 100m or so of the earth's surface necessary for opencast coal exploration. The work reported in this thesis is the development of borehole seismic methods making use of the closely spaced boreholes that are routinely drilled by British Coal.

The first method investigated was to use a tomographic technique to observe any reduction in seismic velocities above old workings, and hence infer the presence of old workings. In order to obtain clear images of the subsurface, it was necessary to interpret the field data for the presence of headwaves, and to pick the later arrival direct waves for the tomographic inversions. However, independent data obtained from uphole surveys showed that there was no measurable reduction in the seismic velocity above old workings for strata below the water table, and the tomographic method was abandoned in favour of borehole seismic reflection methods.

Fifteen hole-to-surface seismic reflection surveys were acquired using down-hole explosive charges as sources and a linear spread of surface geophones passing through the borehole position as receivers. A complete package of processing software was developed for processing the data, and eight of the surveys are presented in this thesis. The final migrated and stacked sections delineate a washout and faulting at both large and small scales. The vertical resolution of the data is high due to the wideband temporal frequencies in the data, typically up to 300Hz.

The hole-to-surface method is compared to the crosshole seismic reflection method, which was developed in parallel by M. J. Findlay. The relative merits of the two techniques are discussed, and suggestions are made to improve the acquisition of the data to make both methods applicable to a wider variety of problems. Although the vertical resolution of the hole-to-surface method is lower than the crosshole method, this could be more than compensated for by extending the hole-to-surface method to three-dimensions, using areal arrays of surface geophones around the borehole.

Acknowledgements

Firstly I would like to thank my supervisor Dr Neil Goulty. This work would not have been possible without him.

I would also like to thank all those in the department who have helped to make this work possible, in particular the technicians, the computer brains and those who helped with the fieldwork.

I am grateful to the British Coal Cooperation's Opencast Executive for providing the boreholes, and to its staff for their professional assistance.

I acknowledge the NERC for my postgraduate award.

Finally, thanks to Shell for correcting some of me grammar!

Contents

Chapter I

Introduction

The aim of the research reported in this thesis was to develop borehole seismic methods which may be used in the exploration of shallow coal deposits, especially in the context of the opencast coal mining industry in the U.K.

This first chapter discusses opencast coal mining and the geophysical methods that have previously been used in site exploration. The borehole seismic methods reported in the following chapters are then introduced.

1.1 Opencast coal mining

Opencast coal mining was first carried out in the U.K. in 1942, as a wartime expedient. Mine depths were only a few metres. Now, a typical site is mined to 100m depth (the deepest yet is 215m at the former Westfield site in Scotland), and produces up to 5 million tonnes of coal. This is small by world standards, due to the urban environment of the U.K., with site boundaries restricted by features such as roads, railways, buildings and water courses. Opencast coal mining currently produces approximately 15 million tonnes of coal per annum. This is 15 % of the U.K. total production.

Coal produced from opencast mining is generally of higher quality and is cheaper than coal produced by deep mine methods. It is much less wasteful than long-wall mining, which only recovers 45% of coal in place. Current figures suggest that it is 30% cheaper per unit of energy produced (L. Knight pers. comm). Opencasting is also a safer method of mining and can mine coal which is too shallow, and seams which are too thin, to be mined safely or profitably by deep mine methods. Shallow coal seams which have previously been worked underground can be worked by opencasting. It is estimated that there are currently 300 million tonnes of shallow coal reserves in the U.K. which could be extracted by opencast mining.

In England and Wales the majority of opencast sites are supervised by the British Coal Opencast Executive. Approximately 1 million tonnes of coal per annum is mined by small, private, licensed mines. British Coal sites are worked by civil engineering companies who tender for each site on the basis of a detailed specification provided by the Opencast Executive.

After a site has been worked, British Coal are obliged to restore the land. This may be for agricultural, industrial or leisure purposes.

1.1.1 Site exploration

The initial stage of exploration involves the assessment of known geological information. Maps of the prospective site are studied, along with old mine plans and results from neighbouring opencast sites. Regional, geographic and economic constraints must also be considered.

Once the feasibility of a profitable mine is established, then the exploration may proceed. Sites are explored by drilling a grid of boreholes. The boreholes are drilled using a tricone bit with an airflush system. Compressed air brings the rock fragments to the surface which are logged with depth by the driller. One in every four or five holes is cored to measure rock quality.

A typical strategy is initially to drill on 120m centres. This is then reduced to 60m and subsequently to 30m, or less, in areas with faults and old workings. In 1988 three quarters of a million metres were drilled for British Coal Opencast Executive, mostly in holes less than 100m deep. The boreholes are geophysically logged by a logging contractor using natural gamma and density tools. The logging tools are run inside a 2-inch (approximately) internal diameter steel casing, known as the logging casing, which is lowered into the borehole immediately after drilling.

Data are combined from all boreholes to give information on drift thickness, horizon lithology, and coal seam depths and thicknesses. A structural map is drawn and an estimate is made of the site reserves. If site reserves turn out to be less than predicted, the contractors may make a financial claim on British Coal. If site reserves are more than predicted then the contractor stands to make an excessive profit. An accurate site specification is thus in the interests of British

Coal. No geophysical surveying technique is routinely used to aid the exploration and the site specification is based solely on the borehole information and geological knowledge.

Faults can be inferred from horizon levels in boreholes, and directly from 'missing section' where a borehole cuts a fault plane. If faulting is intense then this can affect the extraction of the coal. Faults commonly mark the boundaries of old workings, as deep mining was sometimes abandoned when a fault was encountered. At the shallow depths of opencast mining, old workings are usually pillar and stall type, where pillars of coal are left in situ to prevent subsidence. This can leave up to 70% of the coal. The presence of old workings, in one or more of many seams, rarely makes a site uneconomic, though estimation of reserves is difficult. Mine plans may not exist and a dense grid of boreholes is necessary to delineate the structure of the old workings. Figure 1.1 shows two photographs of exposed pillar and stall workings.

The ratio of the overburden thickness to coal thickness, the overburden ratio, is an important factor in determining the economic viability of a site. This averages 15:1 and rarely exceeds 25:1.

1.1.2 Geophysical exploration work

Geophysical methods are well established as an essential tool for oil exploration. Their acceptance into the coal industry has been quite recent. Reflection seismology has been used for coal exploration for deep mines since the mid 1970's (Ziolkowski 1979, Ziolkowski and Lerwill 1979, Ziolkowski 1981, Goulty and Ziolkowski 1985). Average seam depth is 500m and seismic reflection sections to 1000m depth are required. These data generally fail to image the top 100m or so necessary for opencast exploration.

Even with appropriate acquisition parameters, the seismic reflection method fails to image shallow depths. With receivers close to a shallow source, there can be interference from refracted arrivals and surface waves, which may mask the shallow reflected energy. The shots and receivers are both located in the near surface, which is highly attenuating, and this gives rise to low frequency data (e.g. Bredewout and Goulty 1986). The drilling of deeper shot holes to overcome these

Figure 1.1 Exposed pillar and stall workings (courtesy of Bullen and Partners Consulting Engineers).

problems is not economically viable, as the reflection method might as well be abandoned in favour of drilling boreholes only.

Brabham (1986) applied the reflection technique, without success, to the opencast method. No reflections shallower than 100m were seen, the data suffered from much ground roll noise, and wavelengths of approximately 20m were obtained (see also Bredewout and Goulty 1986).

Other geophysical techniques are used in coal exploration. In-seam seismics are routinely used for mapping deep seam continuity (e.g. Krey 1963, Mason et al. 1980, Buchanan 1983, Jackson 1985), though this technique has not been succesfully applied to shallow seams. Seismic inversion techniques have been used on in-seam seismic data (e.g. Mason 1981) and vertical seismic profile techniques are used to give high resolution seismic sections in Coal Measures, as demonstrated by Greenhalgh and Suprajitno (1985) and used with success by Jackson et al. (1989). For the particular application of opencast coal exploration Goulty and Brabham (1984) and Brabham (1986), used refraction seismics to estimate overburden thickness, detect faults and drift channels, and to pinpoint areas of previous opencast excavation.

Geophysical techniques can be costly in both acquisition and processing. There can also be long time spans between acquiring the data and seeing the final results. The time and cost of a technique must not be outweighed by the alternative of drilling further boreholes to gain the extra information. There are some particular circumstances, such as where drilling is not permitted, where there are buildings or roads etc, or where access is limited by safety considerations, that the success of the technique is of major importance, since further drilling may not be carried out. In order to be useful, a geophysical technique must be high resolution and be able to make a contribution in one or more of the following ways:

- Identify small faults and sedimentary features too small to be seen from the borehole information.

- Accurately map large faults and associated splays to locate site boundaries and identify stability problems at site boundaries.

- Position the boundary between solid coal and worked coal.

It is also necessary for the technique to be cost-effective and to have access where drilling is not permitted. At present no technique is available that satisfies these criteria.

1.2 The Coal Measures

The Coal Measures, or Westphalian, is the name given to those Carboniferous rocks which occur above the Namurian, and together they form the Upper Carboniferous (325-280 Ma).

In Northern England the Coal Measures consist of interbedded shales, mudstones and sandstones with seatearths and coals, deposited in a cyclic fashion. The majority of the coal seams are less than 2m thick (Goossens et al. 1974). In North Western England the Coal Measures are harder and with a higher seismic velocity than in the east due to their haematite content, formed by percolating ground water. Originally the Coal Measures were divided into the Upper, Middle and Lower Measures but with locally defined boundaries. In 1927 the three subdivisions Westphalian A, B and C were erected with marine band boundaries. In 1935 the Westphalian D was erected on the basis of floral evidence.

Almost all workable coal is found in the Upper Carboniferous. Some workable coal is found in other parts of the Carboniferous, such as the Scremerston and Limestone coal group of the Lower Carboniferous in Northumberland (Trueman 1954).

1.3 Collapse of strata above old workings

Collapse of strata above old workings is commonplace in the U.K., and the size and type of collapse will depend upon the size and type of the old workings. Garrard (1984) carried out a statistical study on the collapse of old mineworkings, and found the collapse to be generally a form of arching above the cavity, with the greatest collapse at the centre of the workings, and the state of the collapse proportional to the width of the workings. Garrard found almost all of the old workings he examined to be in some state of collapse.

Figure 1.2 shows two photographs of collapse into old workings. Figure 1.2a is from East Chevington opencast coal site in Northumberland, and figure 1.2b is

a

b

Figure 1.2 Collapse features above old workings. (a) From East Chevington opencast coal site in Northumberland. (b) From a civil engineering site in Durham (courtesy of Bullen and Partners Consulting Engineers.)

from a civil engineering site in Durham.

1.4 Borehole seismic techniques presented in this thesis

Previous work in surface seismics (Goulty and Ziolkowski 1985) had shown that seismic velocities may be lowered above old workings, due to the collapse of the overlying strata. The first idea examined in this project was to use the tomographic technique to observe any reduction in seismic velocities above old workings, and hence infer the presence of the old workings. This proved to be unsuccessful, partly due to the limited resolution of the tomographic images obtained, but mainly because there was no measurable reduction in velocities above old workings for strata below the water table, as demonstrated by data from uphole surveys.

The second part of the project was to use the hole-to-surface seismic reflection technique (i.e. multi-offset vertical seismic profiling with a downhole source). This makes use of the exploration boreholes, and is a logical development of surface seismic reflection surveying, which does not have the resolution necessary for opencast coal exploration (Brabham 1986). A complete package of processing software was developed for these surveys, and a total of 15 surveys were carried out. High resolution seismic sections are presented which contain strong reflections obtained from coal seams, and delineate structural and stratigraphic features. The method is compared to the crosshole seismic reflection method developed in parallel by Findlay (1990).

Further development, of both the hole-to-surface and crosshole techniques, will make the methods applicable to a wider variety of problems; in particular, the potential advantages of extending the hole-to-surface method to three-dimensions are discussed.

The project fieldwork was carried out over three years, starting in the late summer of 1987. Data were collected specifically for this project, and for other related research projects (Findlay 1990, Goulty et al. 1990, Beattie 1990). A total of six British Coal opencast exploration sites were visited during the three-year period, in Yorkshire, Northumberland and in Cumbria, though only reconnaissance surveys were carried out on some visits. Data from the sites at Highthorn

(Northumberland); Gawber, Tinsley Park and Lowther South (Yorkshire); and Lostrigg (Cumbria) are presented in this thesis (figure 1.3).

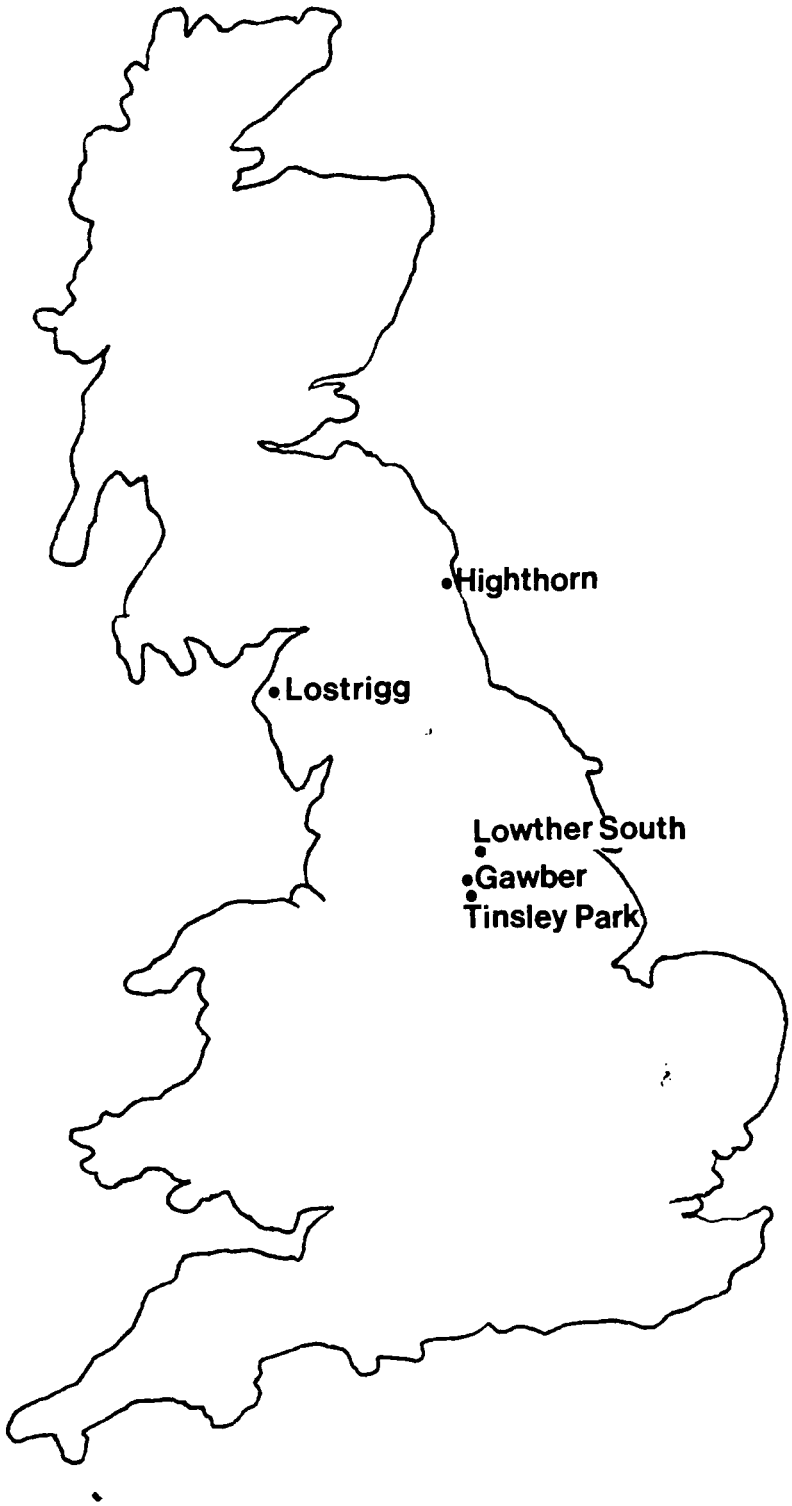

Figure 1.3 Site location map.

Chapter II

Tomography

2.1 Introduction

Seismic tomography uses observed traveltime or amplitude measurements, and inverts these to obtain estimates of the seismic velocity or attenuation in a given area of investigation. The result is a two-dimensional cross-section of the survey area. There have been numerous applications of seismic tomography in geology, engineering and in medicine. For a review of the methods with an application to exploration seismology, see Worthington (1984). More recently there has been interest in the oil industry in using tomography for monitoring enhanced oil recovery processes in producing oil fields (e.g. Macrides et al. 1988, Bregman et al. 1989, Justice et al. 1989).

The purpose of the tomography work was to see if old mineworkings could be detected either directly, or by observation of lower rock velocities associated with the collapsed strata above the old workings. The ability of the tomographic technique to produce velocity images of shallow Coal Measures strata, had previously been demonstrated by Findlay (1987).

2.2 Data acquisition

Figure 2.1 shows the typical field geometry used for a tomographic survey and the resulting curved raypaths. Two boreholes are required, typically spaced 40-50m apart. Small explosive charges of approximately 25g were used as sources. These were fired at successive depths below the water table in one borehole, at 4m intervals. The source apparatus and triggering mechanism are the same as for the hole-to-surface work and are described in section 4.2.1. The shooting technique was also similar to the hole-to-surface work, with the deepest shots being fired first to minimize the risk of aborting the survey due to blocking the borehole. The receiver array consisted of a string of twelve hydrophones spaced at 4m intervals, which was suspended below the water table in the second borehole.

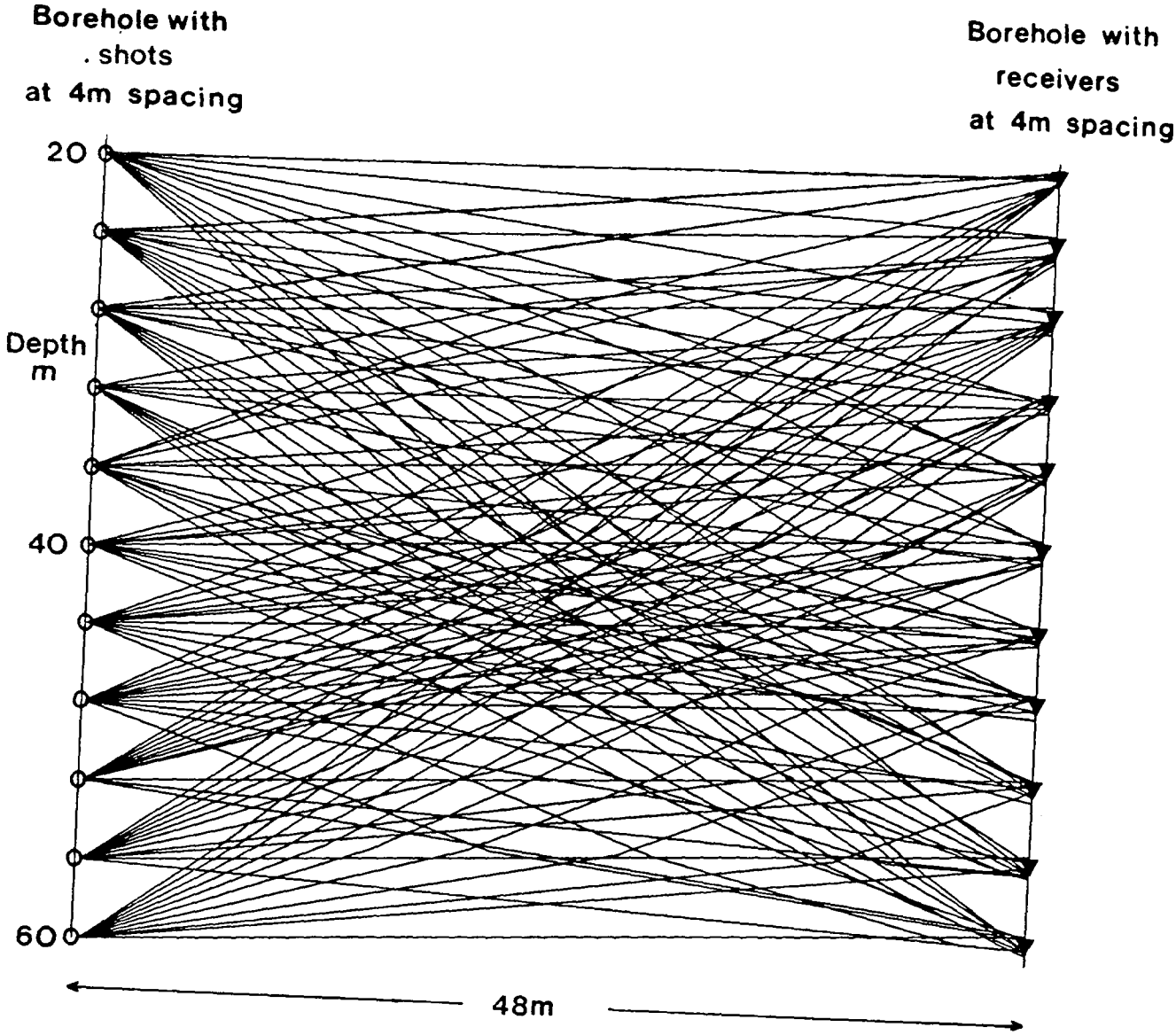

Figure 2.1 Typical field geometry used for a tomographic survey and the resulting curved raypaths. Both shots and receivers must be below the water table.

Typically a total of twelve shots was fired for each survey, and three or more surveys with 12 source and 12 receiver positions could be acquired in one day.

2.2.1 Borehole deviation

Accurate positioning of sources and receivers is important in tomographic work. If each borehole were to deviate by 1m laterally in opposite directions, and the borehole spacing were 40m, this would give a 5% error in source-to-receiver spacing, and hence in velocity calculation.

Borehole deviation was measured using a pendulum style inclinometer. Dip readings were taken at 2m depth intervals with the inclinometer at two perpendicular azimuths. This was achieved by running the inclinometer inside a grooved aluminium tube which keeps the azimuth fixed at all depths. The tube was lowered into the borehole and secured before each inclinometer run. The values of dip and azimuth were converted to Cartesian coordinates by the method of Howson and Sides (1986). Source and receiver positions were calculated to an accuracy of about 10cm.

2.3 Data processing

The data were recorded with a Nimbus 12-channel enhancement seismograph, on to magnetic tape, in modified SEG-D format. The data were transferred to the Durham University NUMAC (Northumbrian Universities Multiple Access Computer) Amdahl 5860 mainframe computer where they were reformatted for processing. The data were recorded as individual shot records with 12 channels and 1024 samples. The sample interval was 0.05 ms, and the first breaks were picked to an accuracy of $\pm$ 1 sample.

2.3.1 SIRT

Tomography relies on there being a line integral relationship between the observed data and the field to be imaged. In the case of traveltime ray tomography this line integral is

$$t_k = \int_{raypath\ k} g(x,z)ds$$

where t_k is the traveltime of the ray, ds is an element of length, and $g(x,z)$ is the slowness (reciprocal velocity) at position coordinates (x,z). There are many methods available for solving such integrals. Matrix inversion methods, Fourier transform and convolution methods have been used and documented by many authors (e.g. Ivansson 1985, East 1988). Hatton et al. (1986) give a good introduction to all these methods.

The data presented in this thesis were inverted using the Simultaneous Iterative Reconstruction Technique or SIRT (Gilbert 1972). Many traveltime tomography datasets have been inverted using various forms of iterative reconstruction techniques (e.g. Dines and Lytle 1979, Mason 1981, McMechan 1983). The SIRT method can cope with any shot and receiver geometry and can be used with curved-raytracing algorithms.

The area to be imaged is divided into Cartesian cells assigning a constant slowness g_i to each cell, i. The above integral can then be approximated by

$$t_k = \sum_i g_i s_i \tag{2.1}$$

where s_i is the path length in cell i.

Equation (2.1) may be written in matrix form

$$\underline{t} = \mathbf{A}\underline{g}$$

where the matrix $\mathbf{A}$ consists of all the s_i values, each row representing one raypath. This is the basic equation for the SIRT method.

Starting with equation (2.1) we have

$$\hat{t}_k = \sum_i g_i s_i$$

where $\hat{t}_k$ is the estimated traveltime for an initial estimate of the slowness field g_i. We can then represent the true slowness field as a perturbation of this

$$t_k = \sum_i (g_i + \Delta g_i) s_i$$

The traveltime error Δt_k is then

$$\Delta t_k = t_k - \hat{t}_k = \sum_i \Delta g_i s_i \tag{2.2}$$

Dines and Lytle (1979) proposed minimizing the arbitrary criterion

$$c = \sum_i \Delta g_i{}^2$$

subject to 2.2 to obtain

$$\Delta g_i = \frac{\Delta t_k s_i}{\sum_i s_i{}^2} \tag{2.3}$$

This is the basis of the reconstruction algorithm, and is implemented on a computer as follows

o The region to be imaged is divided into Cartesian cells, and an initial value of slowness is assigned to each cell.

o Raypaths are then traced through this region to calculate the estimated traveltime of each ray, and the path length of each ray in each cell.

o The slowness field is then updated using equation (2.3). This update is done after all rays have been traced, the final update being a simple average of all the Δg_i values for a given cell.

The whole process is then iterated until some criterion is satisfied, such as the field no longer changing significantly, or the residuals in the traveltimes being of the order of the 'noise' in the data. Initial velocity fields were calculated by a simple back-projection of the traveltime data (Wong et al. 1983).

A computer program written by Dyer (1988) was used to invert the traveltime data. This was implemented on the NUMAC mainframe computer by Wye (1986), and a curved-raytracing algorithm, Raysyn (Cassel 1982), was modified by Findlay (1987) for use with the tomographic software.

Chapter III

Tomography in shallow Coal Measures strata

3.1 Introduction

Ten tomography surveys were acquired at Tinsley Park, a British Coal opencast exploration site in Yorkshire, and six tomography surveys were acquired at Gawber, a British Coal opencast exploration site also in Yorkshire. These surveys were acquired in ground above both solid and worked coal seams, and in ground above solid-to-worked boundaries. The data were acquired and processed as described in chapter 2.

3.2 Tomography results

Only a single tomography experiment is discussed and presented in this thesis. This was acquired from Tinsley Park, and the data were carefully recorded without saturation so that they might also be processed by the crosshole reflection method (section 6.1). In all the other surveys acquired at Tinsley Park and Gawber, the arrivals saturated soon after the first breaks, due to the 10-bit fixed-gain amplifier on the recording system being turned up to enable the first breaks to be picked with maximum accuracy. This was unfortunate because as explained and demonstrated below, first breaks which are headwaves should be ignored, and the arrival times of direct waves picked instead.

Two near-vertical boreholes were used with a separation of 54m. 22 shots were fired in one borehole from 22m to 64m depth, at a separation of 2m. 23 receiver positions were occupied in the other borehole from 22m to 66m depth, again at a 2m separation. This was achieved by shooting from all shot positions into the 12-channel hydrophone array, then shifting the hydrophone array by 2m and firing a second shot in each of the shot positions. The water table was at 20m depth and the boreholes were blocked below 67m, corresponding to the depth of a worked seam.

Figure 3.1 shows the coal seam details from the stratigraphic logs in the two boreholes. There is a 1.6m coal seam with its base at 42m. This is the Meltonfield Seam. The Two Foot Seam lies at approximately 57m d· ·th, and the worked seam at 67m depth is the Winter Seam.

Figure 3.2 shows the result of processing the first break data using the SIRT method. Data from alternate source and receiver positions have been used to produce this section, giving 11 source positions from 22m to 62m depth, and 12 receiver positions from 22m to 66m depth. The inversion was carried out using 4m square cells, and 5 iterations were performed. The resulting section shows a very poor image of plane parallel layers, which is expected from the stratigraphic logs. Velocity artifacts are seen around the edges of the section, and the 1.6 m coal seam at 42m depth is hardly apparent. Surveys acquired above solid and worked seams show no differences in velocity, and all share the same poor resolution and velocity artifacts.

Figure 3.3 shows two further inversions of the dataset. In figure 3.3a all shot and receiver positions have been used. This gives 506 raypaths (compared to 132 raypaths previously) but there is almost no improvement in the final image. Clearly, increasing the number of raypaths has little effect. In figure 3.3b all shot and receiver positions have again been used, but the cell size for the inversion has been reduced to 2m square. Although this section is slightly noisier, there is little difference again.

3.2.1 A simple model study

A simple model study was carried out to try to understand the results obtained at Tinsley Park. The model consists of 11 shots and 11 receivers at 4m spacing in two boreholes 44m apart. Direct traveltimes from sources to receivers were calculated by raytracing, and the resulting data inverted using the SIRT algorithm. A 4m square grid was used for the inversion and a curved-raytracing algorithm used.

Figure 3.4 shows the results of the model study. Figure 3.4a shows the model contoured using a 4m square cell size, and indicates the best resolution obtainable with the chosen cell size. The velocity shading key is the same as for figures 3.2

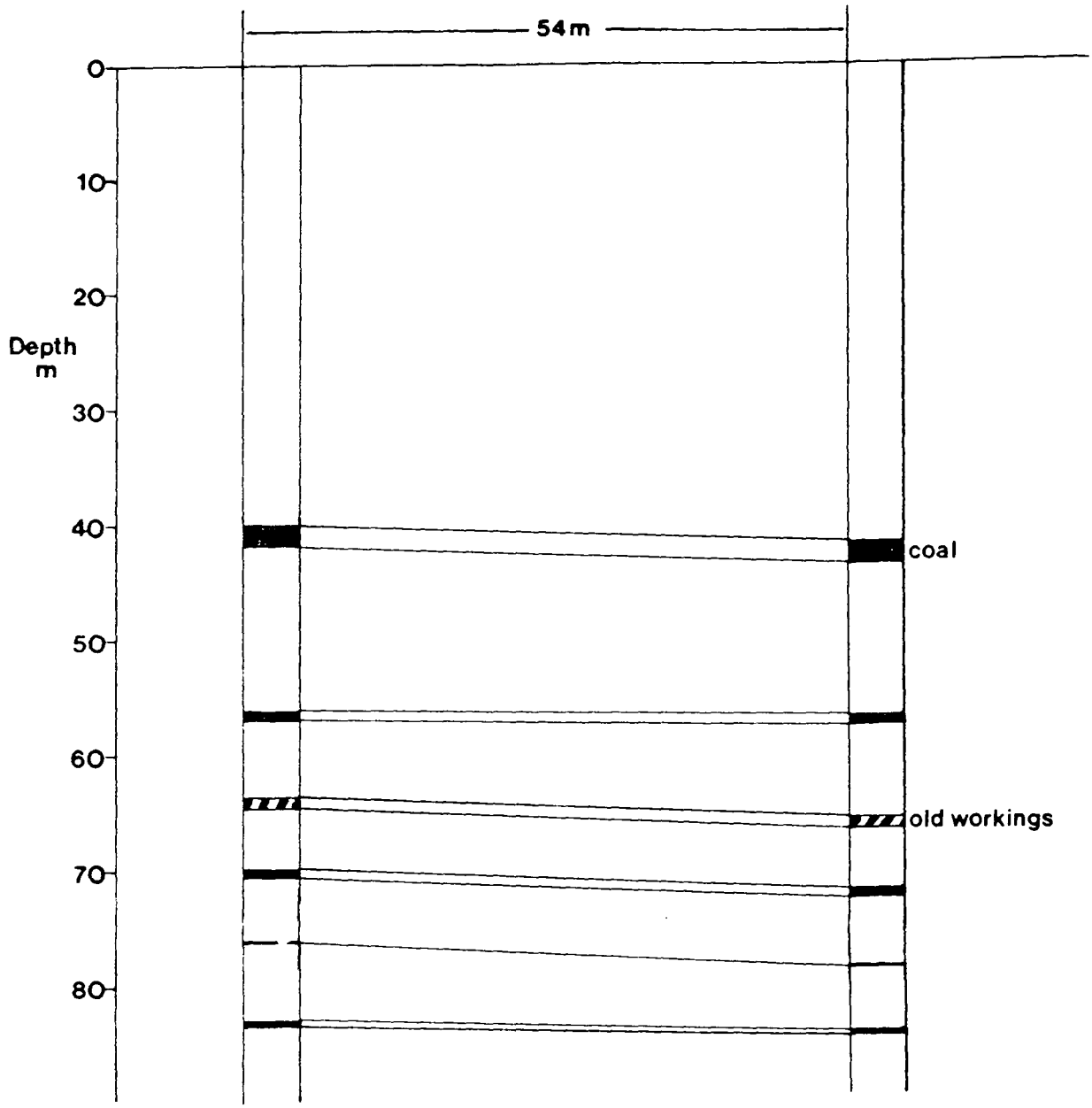

Figure 3.1 Coal seam details from the stratigraphic logs for the two boreholes at Tinsley Park.

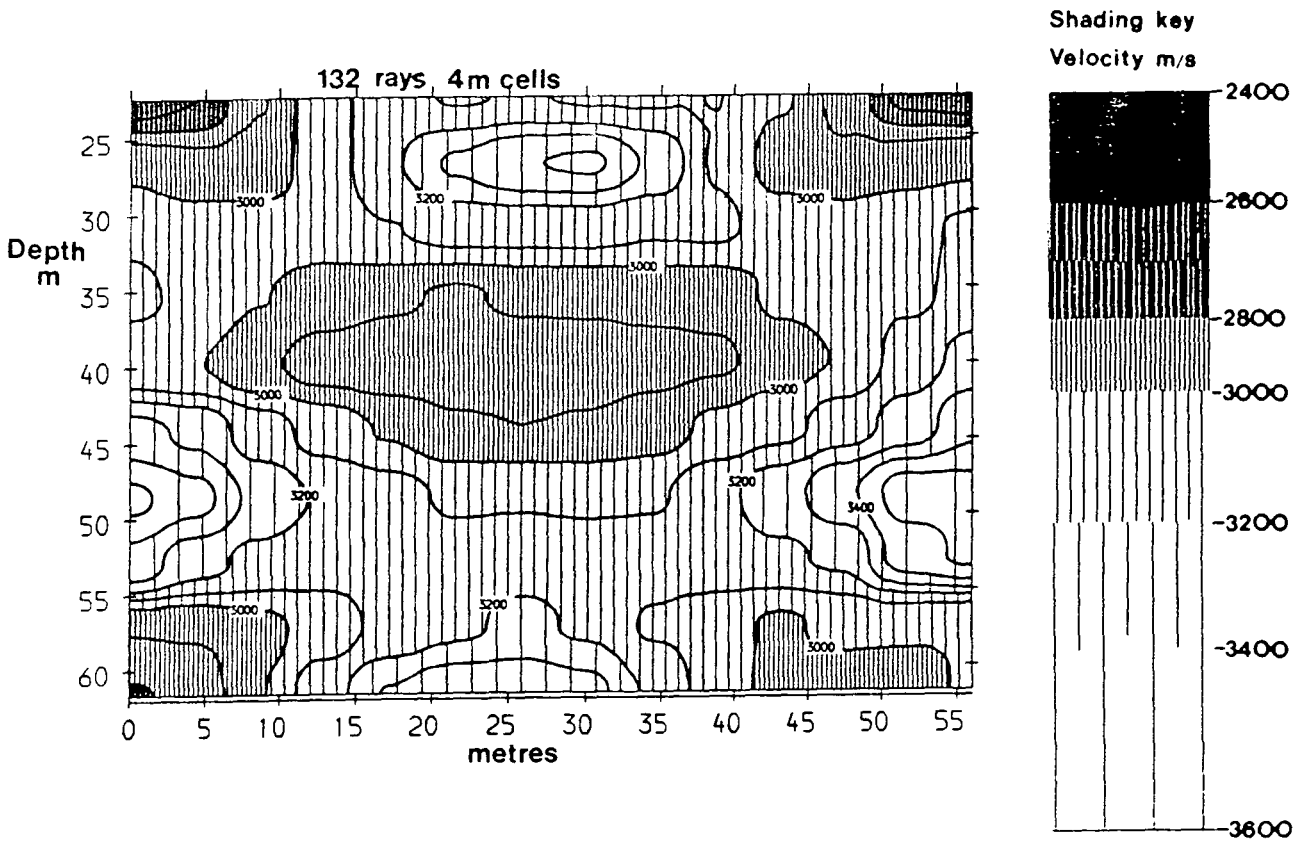

Figure 3.2 Tomographic velocity field resulting from processing the first break data using the SIRT method. Alternative shot and receiver positions have been used.

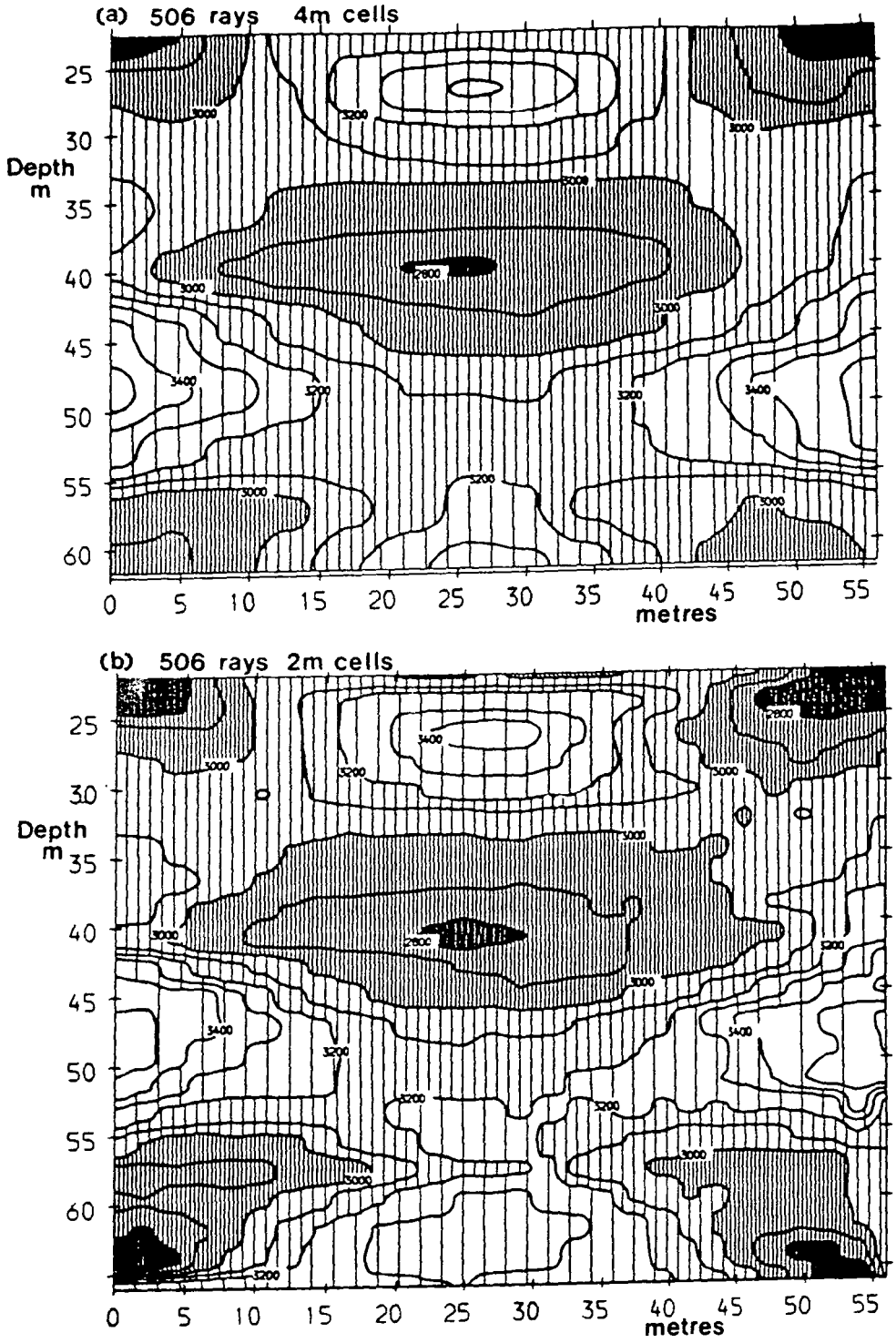

Figure 3.3 Tomographic velocity fields resulting from processing the first break data using the SIRT method. The velocity shading key is the same as for figure 3.2. (a) All shot and receiver positions have been used. (b) All shot and receiver positions have been used and the cell size for the inversion has been reduced to 2m.

and 3.3. There is a thin low velocity unit representing a coal seam, and a thin high velocity unit near the base of the model. Figure 3.4b shows the resulting inversion after 9 iterations. Some small artifacts are seen but overall the inversion is very accurate. Figure 3.4c shows the resulting inversion after headwave traveltimes were calculated and substituted for the slower direct wave traveltimes. The effect is dramatic. Both the high velocity unit and the low velocity unit are completely smeared out, and the section has a very similar appearance to the real data inversion of figures 3.2 and 3.3.

3.2.2 Interpretation of the field data

With the results of the model study in mind, it was decided to try to interpret the field data for the presence of headwaves. Using the stratigraphic logs and the unfocused velocity field of figure 3.3 as a guide to where headwaves may be expected, the data were repicked, ignoring the arrival where its low amplitude suggested it was a headwave. Figure 3.5 shows an example of a shot record where headwaves were identified. This is a somewhat subjective process, particularly where the shot and receiver are at the depth of a coal seam, and the direct arrival is considerably later than the first arrival headwave. The direct arrival can then be difficult to identify amongst other later arrivals, and picking the first break can be inaccurate.

The section resulting from inverting the repicked data with the SIRT algorithm is shown in figure 3.6. The image shows a definite improvement with the coal seam at 42m showing a fairly sharp image. There is an indication of the deeper seam at 57m depth.

The section of figure 3.6 is about the best that has been achieved, using traveltime tomography, with the given field geometry. A comparison to the crosshole reflection method is made in section 6.1.1.

3.3 Uphole velocities

Uphole surveys (section 4.3.6) were acquired in boreholes which penetrated both solid and worked seams at Tinsley Park and Gawber, and at Highthorn, a British Coal opencast exploration site in Northumberland.

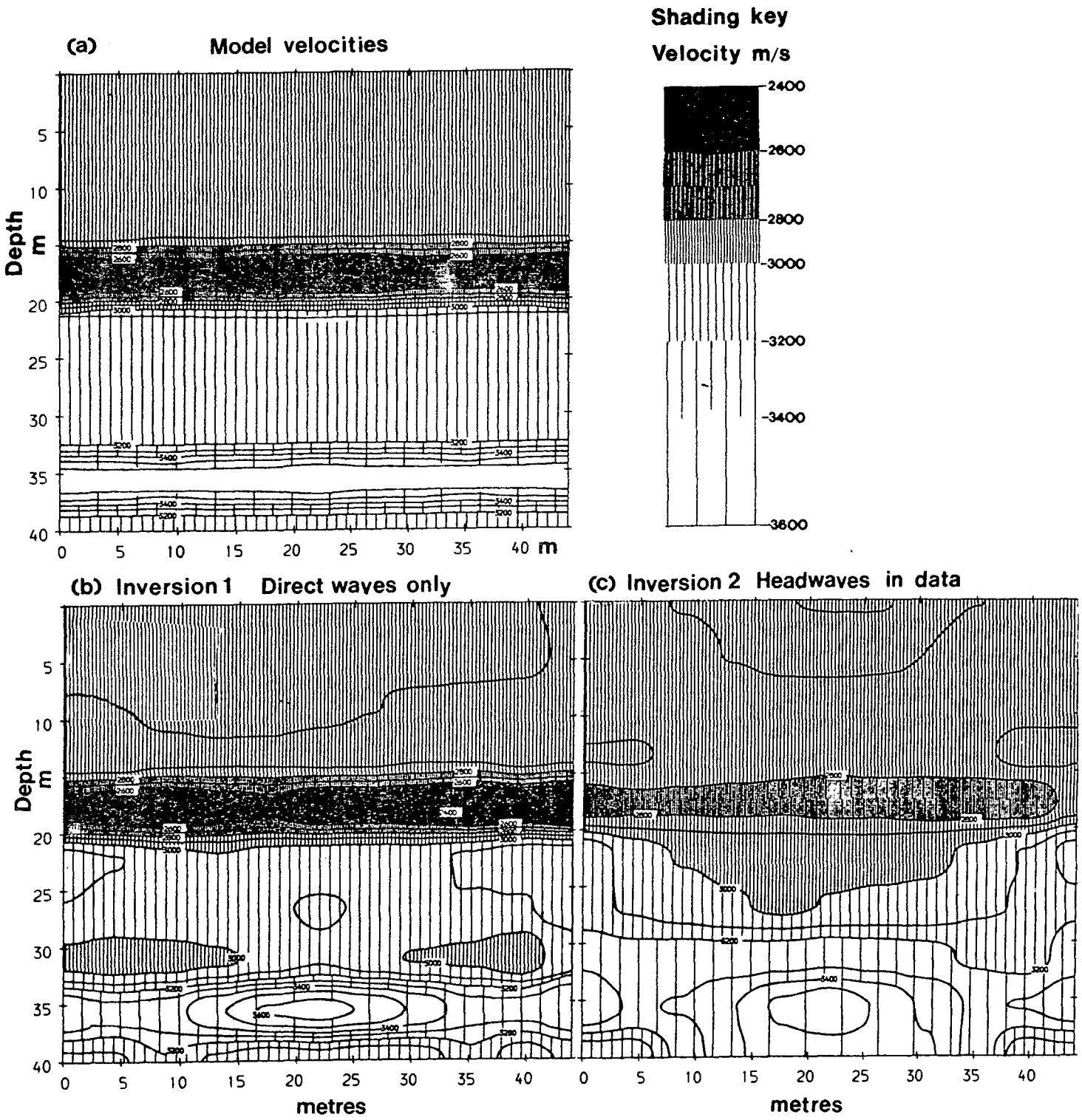

Figure 3.4 Model study. (a) Model velocities contoured using a 4m cell size. (b) Tomographic velocity field resulting from processing the direct arrival model data using the SIRT method. (c) Tomographic velocity field resulting from processing the first arrival model data with headwaves, using the SIRT method.

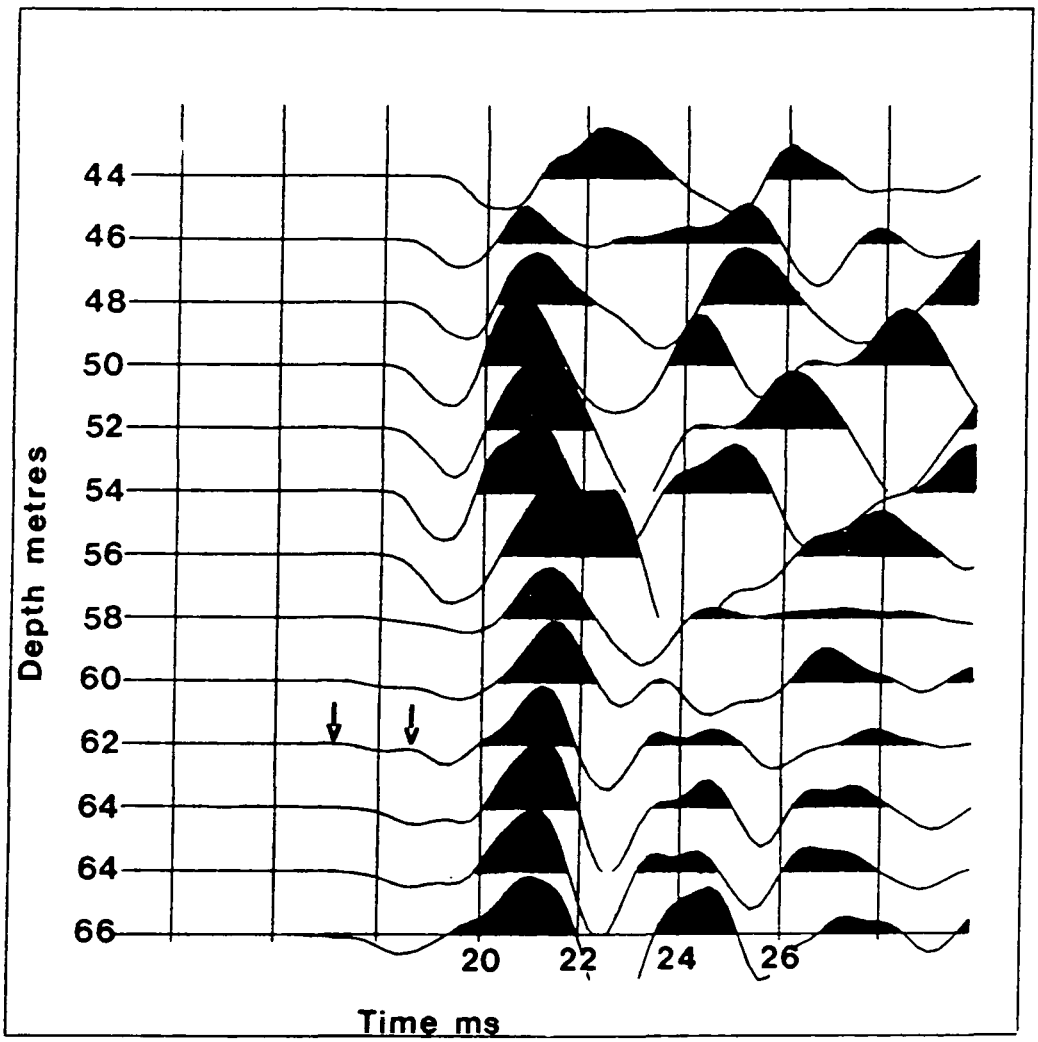

Figure 3.5 Part of a shot record record where headwaves were identified. The arrows indicate the low amplitude first arrival and the later arrival direct wave recorded on the trace at 62m depth.

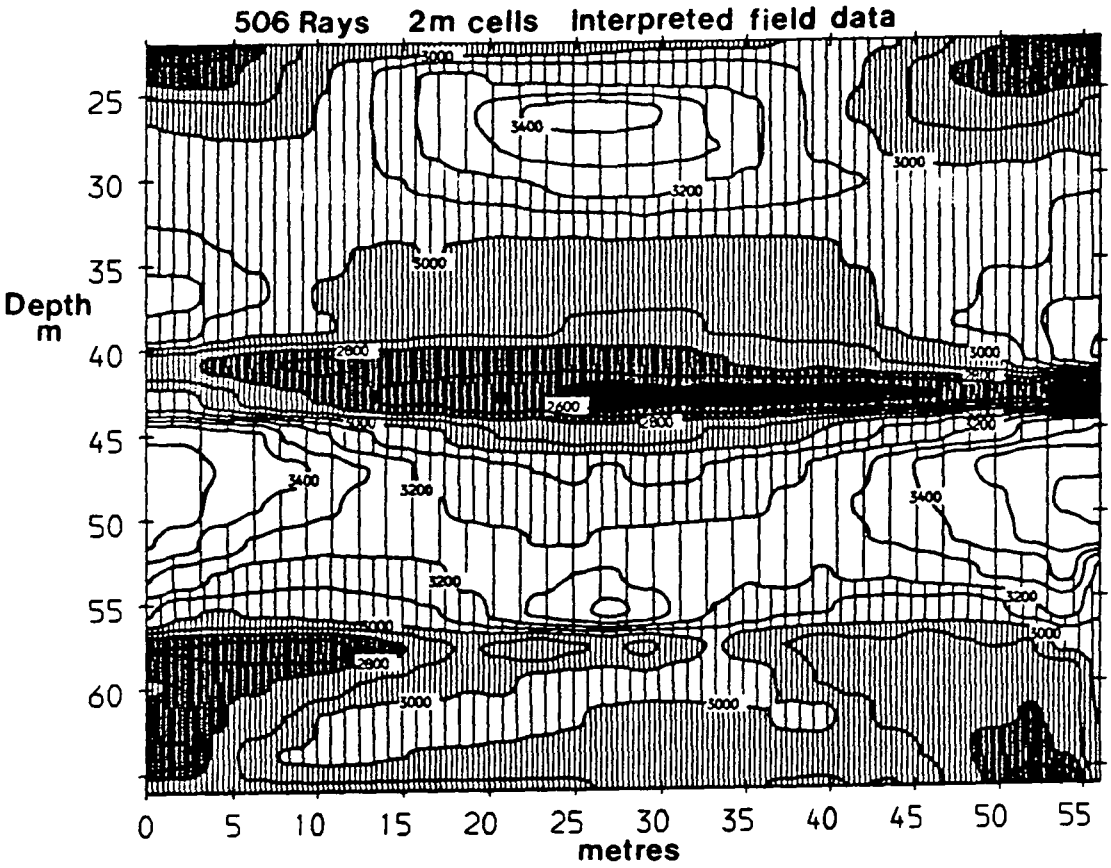

Figure 3.6 Tomographic velocity field resulting from processing the interpreted field data using the SIRT method.

The uphole surveys give a direct measurement of the seismic velocity in a vertical direction at the vicinity of the borehole. Figures 3.7 and 3.8 show the results of the uphole surveys. Traveltimes are plotted relative to an arbitrary zero position for each borehole so that the data do not overlap (Goulty et al. 1990).

At Highthorn in Northumberland (figure 3.7), shots were repeatedly fired at the level of a worked seam, which was just below the water table. A borehole geophone was used as a receiver, clamped at successive depths above the water table. The seismic velocities above the room-and-pillar type workings are generally up to 20% less than the seismic velocities above the solid seam. This is presumably due to the collapse of the strata above the old workings. Two of the uphole surveys in strata above old workings show velocities comparable to those above the solid seam. This may be due to these boreholes being immediately adjacent to pillars in the old workings.

At Gawber (figure 3.8) the worked coal seam was well below the water table. A 12-channel hydrophone string was used for the receiver, and a single shot was fired in each borehole, at the level of the seam. The seismic velocities above solid and worked coal are similar. This cannot be explained by the boreholes, which penetrated the worked seam, being adjacent to solid pillars because at Gawber the pillars in the old workings have been robbed.

It was not expected that subsidence effects in strata below the water table would cause as great a velocity reduction as subsidence effects in strata above the water table. This is simply due to the velocity of water being greater than that of air. Even so, if 1m of coal was removed, being replaced by 1m of water, and the subsidence occurred over a depth of 10m, a velocity reduction of about 10% would be expected for an undisturbed velocity of 3000m/s. If the subsidence occurred over a depth range of 20m, the velocity reduction would be about 5%.

The uphole surveys acquired at Tinsley Park in Yorkshire also showed no velocity reduction in strata above old workings and below the water table.

It is just possible that at both sites the subsidence effects associated with deep seams worked by Longwall extraction have obscured the subsidence effects associated with the shallow worked seam.

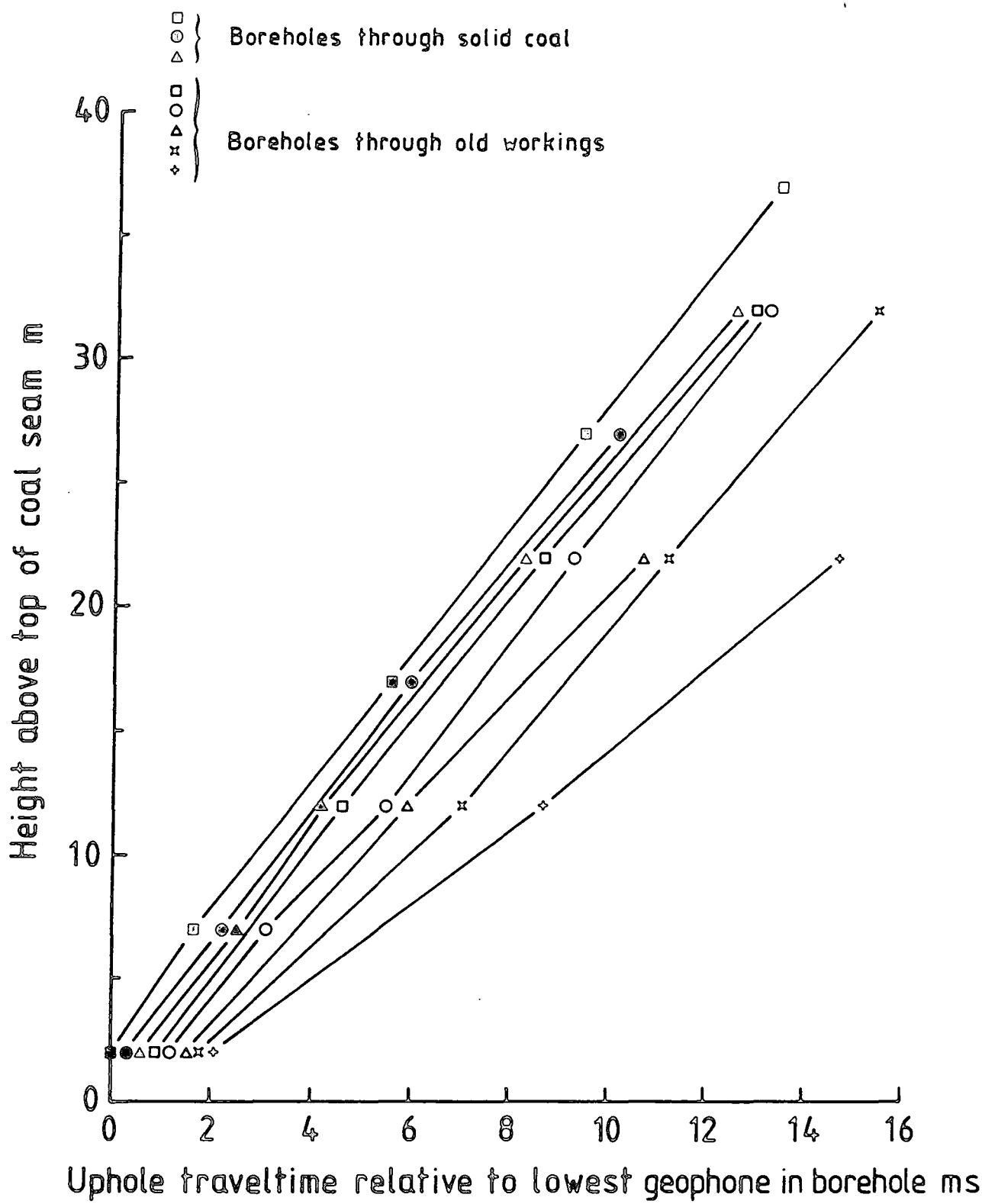

Figure 3.7 Uphole survey results at Highthorn in boreholes above solid and worked seams.

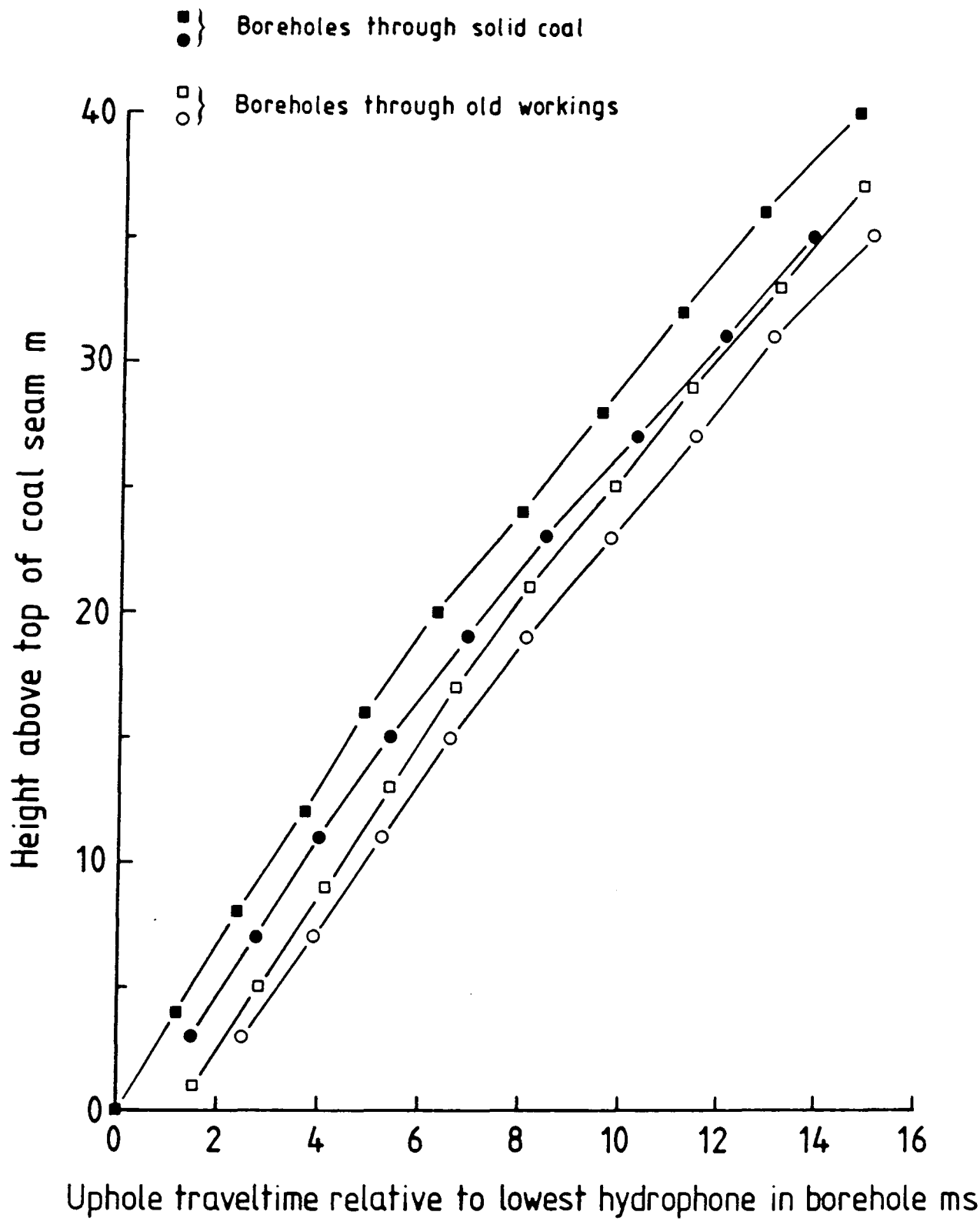

Figure 3.8 Uphole survey results at Gawber in boreholes above solid and worked seams.

3.4 Discussion

There are various areas of work which may lead to an improvement in the tomographic inversions. Poor angular ray distribution is a problem with geophysical tomography, but with source and receiver positions restricted to lie below the water table and shallow hole depths, this cannot be improved. It has been demonstrated that increasing the density of raypaths by reducing the source and receiver spacing from 4m to 2m does not improve the inversion of the real dataset.

3.4.1 Anisotropy

A comparison of the crosshole velocities with the uphole velocities showed, on average, a 15% lower seismic velocity in the vertical direction than in the horizontal direction (for raypaths through strata unaffected by subsidence). Thus, anisotropy appears to be present in the Coal Measures strata.

The assumption that seismic properties of rocks are independent of direction is a poor one. This has been known for some time (e.g. Cholet and Richards 1954). There are many deviations from isotropy, the simplest and probably the most applicable to sedimentary strata being transverse isotropy (Love 1944). In this case the physical properties are the same in all planes perpendicular to one axis of symmetry. An earth section made from homogeneous isotropic beds separated by plane parallel interfaces will appear transversely isotropic to seismic waves with wavelengths long in comparison to bed thickness. For the layered sedimentary strata of the Coal Measures, anisotropy is likely to exist within individual rock units as well as being a function of the wavelength and bed thickness. A laboratory study of anisotropy in shallow Coal Measures strata from Yorkshire was carried out by Auckland (1988). Under laboratory conditions, a figure of 10% anisotropy was suggested. Work carried out on Coal Measures rocks by Roberts (1987) suggested significant anisotropy, and Muftuoglu and Scoble (1984) found velocity anisotropy of 9 - 23 % in Coal Measures rocks.

For transversely isotropic media, velocity plotted as a function of direction of travel does not define an ellipse for P-waves or for SV-waves. The wavefront and the phase velocity curve are not congruent, circular or elliptical. However, deviations from an elliptical velocity function have been shown to be small (Uhrig

and VanMelle 1955) and the assumption of an elliptical velocity function to model anisotropy has been used by Chiu and Stewart (1987) and Levin (1978). This assumption shall be made here.

If θ is the angle of the ray to the vertical the phase velocity can then be written

$$v(\theta)^2 = {v_v}^2 \cos^2\theta + {v_h}^2 \sin^2\theta$$

where v_v is the phase velocity in the vertical direction and v_h is the phase velocity in the horizontal direction.

Since the phase velocity curves and the wavefront are not congruent, a second velocity, the ray velocity, $v(\phi)$, (or wavesurface or group velocity) arises (Kerner et al. 1989, Levin 1978, Berryman 1979, Federov 1968). This is simply defined by the vector from the origin to some point on the wavesurface (figure 3.9) and is given by

$$v(\phi)^2 = \frac{{v_v}^2 {v_h}^2}{v_v^2 \sin^2\phi + {v_h}^2 \cos^2\phi}$$

where

$$\tan(\theta) = (\frac{{v_v}^2}{{v_h}^2}) \tan(\phi)$$

and ϕ is the ray angle from the vertical.

Refraction at interfaces no longer obeys the simple Snell's law. This is now modified to include the effects of anisotropy. From Levin (1978) a generalized form of Snell's law is

$$\frac{{v_{h1}}^2}{v(\phi_1)\sin(\phi_1)} = \frac{{v_{h2}}^2}{v(\phi_2)\sin(\phi_2)}$$

where the subscripts 1 and 2 refer to the two adjacent media separated by a plane boundary.

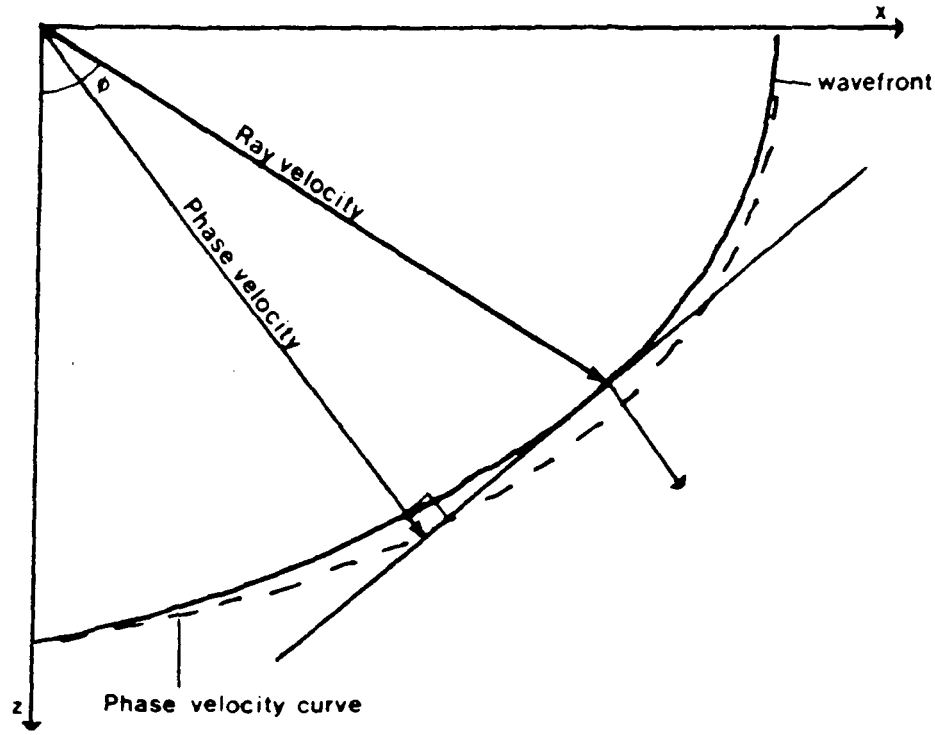

Figure 3.9 Wavefront and phase velocity curves in an anisotropic medium.

If anisotropy is present, the steeper raypaths will travel with a slower velocity. It follows that by using an isotropic raytracing method, the traveltime errors calculated for steeper raypaths will be greater than those calculated for shallow raypaths (equation 2.2). The slowness corrections will be too large (for the steeper dipping raypaths), and hence the calculated velocities too small. Thus, where there are a majority of steeper raypaths (in the corners of the raypath coverage), the tomographic velocities are expected to be too small, and conversely, where there are a majority of shallow raypaths (in the centre of the edges of the raypath coverage), the tomographic velocities are expected to be too large. This is exactly what is observed on the real dataset inversions.

The raytracing code was modified to handle anisotropy, assuming an elliptical velocity model for transverse isotropy. The SIRT algorithm was modified to use the anisotropic raytracing code, and produce a separate velocity field for the horizontal and vertical directions. This is implemented within the SIRT algorithm by modifying equation (2.3) to give a separate slowness update for the horizontal field ($\Delta g_{i(h)}$), and for the vertical field ($\Delta g_{i(v)}$),

$$\Delta g_{i(h)} = \Delta g_i \sin^2 \phi_i$$

$$\Delta g_{i(v)} = \Delta g_i \cos^2 \phi_i$$

where ϕ_i is the raypath angle from the vertical in cell i.

The resulting anisotropic inversions showed little improvement, with the vertical velocity field changing little from the initial estimate. This may be explained by the greater number of horizontal raypaths than steeper raypaths, with most of the raypaths in a typical tomography survey less than 45 degrees from the horizontal.

A further modification to the raytracing code was to enable the tracing of headwaves along defined boundaries. Again little improvement to the final inversions was seen, and this method suffered from the need for an accurate velocity model before inversion of the data.

The tomographic method has produced poor resolution images of shallow Coal Measures strata, and reduced velocities in the collapsed strata above old workings and below the water table were not seen in the uphole surveys. The tomographic method was abandoned in favour of higher resolution techniques making use of reflected arrivals in the recorded wavefield.

Chapter IV

Hole-to-surface seismic surveys

4.1 Introduction

Vertical seismic profiles (VSP's) have been used in the seismic industry for many years (Balch et al. 1982, Hardage 1983, Fitch 1984). They were developed from the well velocity survey where a (near-)surface source is fired into a downhole receiver. This gives a measurement of the traveltime of the direct seismic wave. By positioning the receiver at a succession of depths, the seismic velocity in a vertical direction as a function of depth can be found at the borehole. The VSP technique extended this idea by recording the whole wavefield, not just the first arrival times. The band-limited primary reflection response at the borehole may be obtained by processing the VSP data, which generally have broader bandwidth than surface seismic data. Correlation of the VSP with the surface seismic is an important interpretation tool. The extension of the VSP to use sources at fixed offsets from the borehole (OVSP's) gives lateral coverage on reflecting horizons. Multi-offset VSP's (MOVSP's) use many source positions to give multi-fold subsurface coverage and produce high-resolution sections around the borehole position. Offset and multi-offset VSP's are now commonplace in the seismic industry, using three-component geophones as receivers, and are being extended to give three-dimensional subsurface coverage (e.g. Ahmed et al. 1986, Noble et al. 1988).

The hole-to-surface method is a variation on the MOVSP in that the method reverses the positions of the sources and receivers. The practical advantage in shooting such surveys hole-to-surface is that it is much easier to deploy large receiver arrays on the surface than downhole. However, this is not yet common practice as suitable downhole sources have not been available. On land there is an additional advantage of having the source downhole: the coupling is better and hence the signal bandwidth is higher, even though the seismic waves still have to pass once through the attenuating near-surface layers on their way up to the receivers.

Hole-to-surface seismic surveys have previously been called inverse, inverted, reverse or reciprocal vertical seismic profiles (see Jackson et al. 1989, Laurent and Mari 1988, Lintker et al. 1990, Layotte et al. 1990). The term **hole-to-surface** seems a more concise and easily understood name.

This chapter describes the acquisition and processing of hole-to-surface data specifically for the shallow exploration of the top 150m or so of the Earth's surface.

4.2 Data acquisition

4.2.1 Field geometry

Figure 4.1 shows the typical field geometry used for a hole-to-surface survey. Small explosive charges of approximately 25g were used as sources, and these were fired at successive depths in the borehole at 2m intervals. The 2m shot spacing is necessary to prevent aliasing of the data during the wavefield separation stage of the data processing. The source apparatus is shown in figure 4.2. This consists of a length of steel tubing to which the detonator and explosive charge are fixed. The steel tubing is suspended from the trigger line, an electric cable which is marked for depth positioning and carries the trigger signal up to the recording system. The firing line is lashed to the trigger line but does not bear weight because it readily stretches plastically under tension. The source apparatus was lowered into the borehole and retrieved by hand, and charges were positioned to a relative accuracy of $\pm$ 5cm. The zero time break for recording was obtained by wrapping a wire around the detonator which is connected to the recording system by the trigger line. When the charge is fired, the wire blows to open circuit and the change in resistance causes the required trigger signal. This method gives an accurate time break which is particularly important since record lengths are short (only 100 to 150ms of data are used during processing) and the sample interval is small, typically 0.5ms. This method also allows the use of standard electrical detonators rather than the more expensive seismic detonators.

The receivers used were single geophones (natural frequency 30Hz) and were deployed at the surface along a line intersecting the top of the borehole. A 4m geophone spacing was used to prevent aliasing of the data during the migration

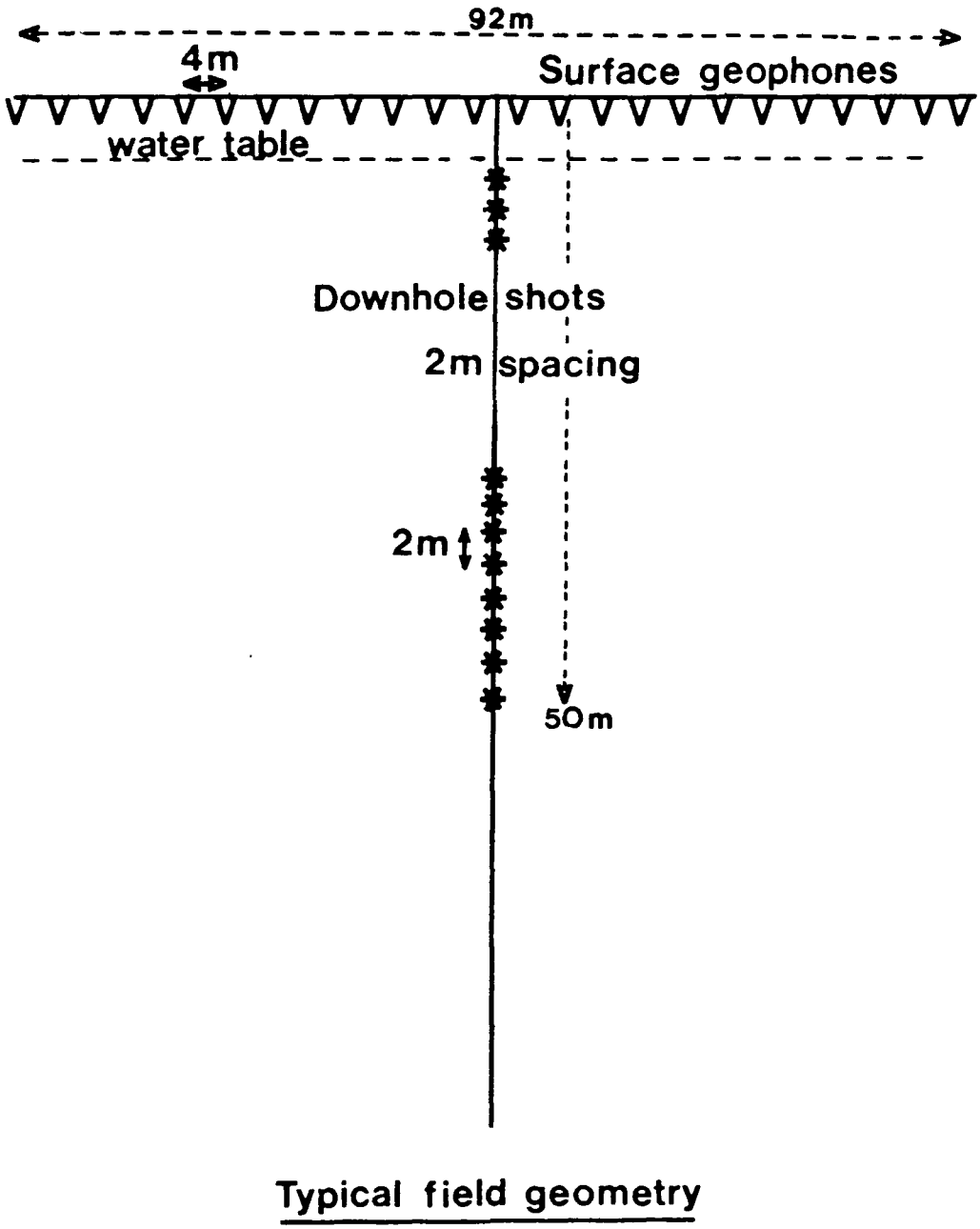

Figure 4.1 Typical field geometry used for a hole-to-surface survey.

Figure 4.2 Downhole source apparatus used for hole-to-surface and tomography surveys.

stage of the processing. This was confirmed by examining shot records and their f-k spectra. With a 24-channel seismograph this gives a geophone spread of 92m.

4.2.2 Survey design

Subsurface coverage depends upon the shot and receiver spacing and the subsurface velocity structure. With the 92m geophone spread placed symmetrically about the borehole, the maximum geophone offset is 46m. For horizontal reflectors the subsurface coverage tends to half this value at depth, and the shallowest shot gives the greatest lateral coverage for a given receiver offset. Coverage may be adjusted to be asymmetric about the borehole position by appropriately shifting the geophone spread. The deeper shots are required firstly for separation of upward and downward travelling waves and secondly to give the necessary energy penetration to image the deeper reflectors. With a symmetrical geophone spread and shots from 10m to 50m depth, good coverage is obtained from approximately 30m to 100m, or more, in depth with lateral coverage of some 40m at 50m depth. The concept of reflection point coverage loci is discussed in section 4.3.7.

4.2.3 Field technique

Once the geophones have been deployed and the seismograph set up, shots are fired at successive depths in the borehole starting with the deepest position. This is to ensure that if there is any damage to the borehole, with a risk of blockage, the survey may be completed with the shallower shot positions. Boreholes are often blocked before shooting starts, and sometimes become blocked during shooting, at levels of old workings in coal seams or faults. This limits the depth range available for shooting and can thereby reduce the data quality, especially for deeper horizons. The time to fire each shot is dependent upon shot depth. Over a depth range from 10m to 50m, a time of about 5 minutes for each shot can be expected. Thus, at least two such surveys can be acquired in one day. Misfires and triggering problems account for most wasted time.

4.3 Data processing

4.3.1 Introduction

The data were recorded with an EG&G Geometrics 24-channel enhancement seismograph, ES2401, on to a 3.5 inch floppy disc in SEG DOS standard format. The data were transferred to the Durham University NUMAC (Northumbrian Universities Multiple Access Computer) Amdahl 5860 mainframe computer, where they were reformatted for processing. Data were recorded as individual shot records with 24 channels, one for each surface geophone, and 1024 samples. The data were normally recorded with a sample rate of 0.5ms. This gives a Nyquist frequency of 1000Hz.

Figure 4.3 shows a raw shot record acquired with the geometry previously described. The record is dominated by the direct arrivals and shows large static shifts on some geophones. Little else apart from some noise is seen on the shot record. Data processing requires the extraction of the P-wave primary reflected energy and then imaging this energy to a depth section. Figure 4.4 shows a flow chart of the basic processing sequence for the hole-to-surface data. A suite of programs has been written to process the hole-to-surface data, and is detailed in appendix A of this thesis.

Each step in the processing sequence will be examined in detail and an example of each step shown from a real dataset.

4.3.2 The common-receiver gather and the principle of reciprocity

The first step in the processing sequence is sorting the data to common-receiver gathers. A common-receiver gather from a hole-to-surface survey consists of a set of independent seismic experiments, each trace resulting from a separate shot. Assuming that the source is repeatable, the common-receiver gather may be treated as a single experiment by invoking the principle of reciprocity: the traveltime along a seismic raypath is independent upon the direction of travel (e.g. Aki and Richards 1980). The raypath geometry for a common-receiver gather is exactly that of a fixed offset VSP, except that the rays are reversed in direction. Each

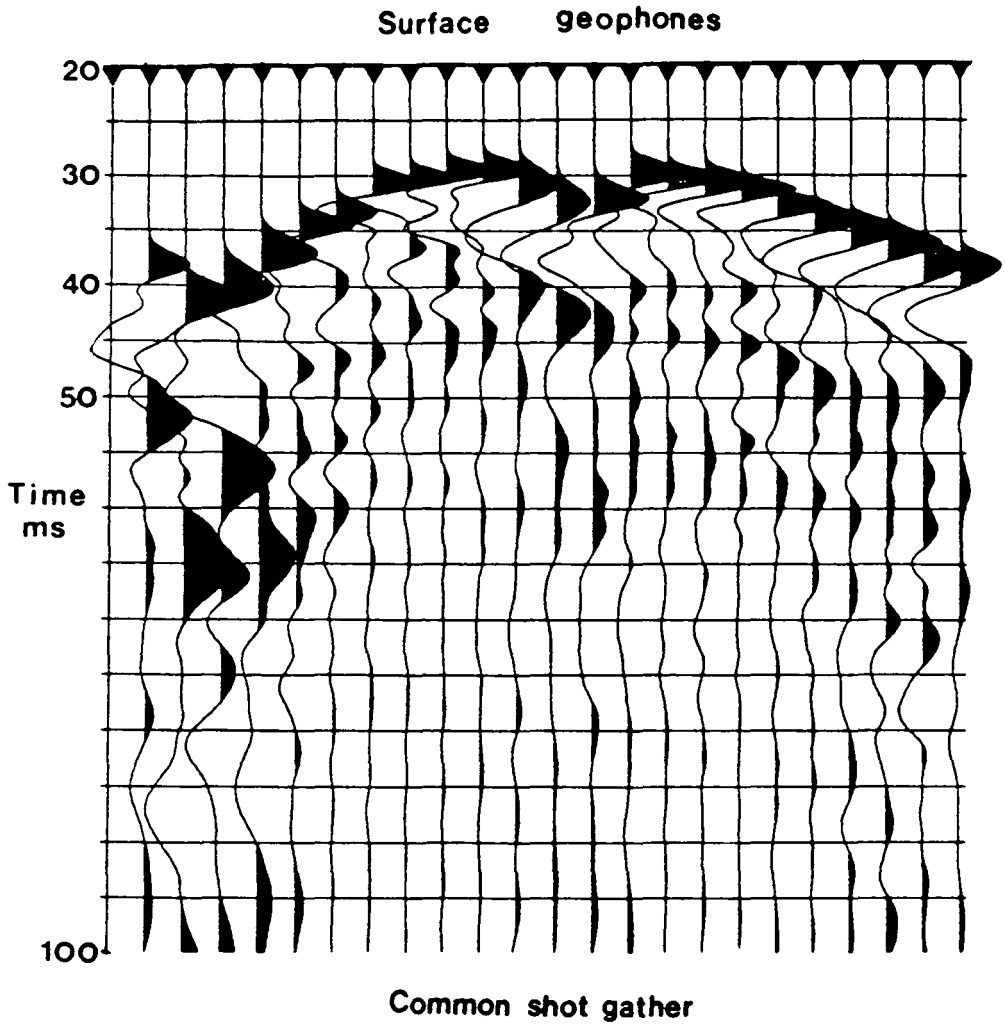

Figure 4.3 Raw shot record from a hole-to-surface survey acquired with the field geometry of figure 4.1. The surface geophone spacing was 4m and the shot depth 40m.

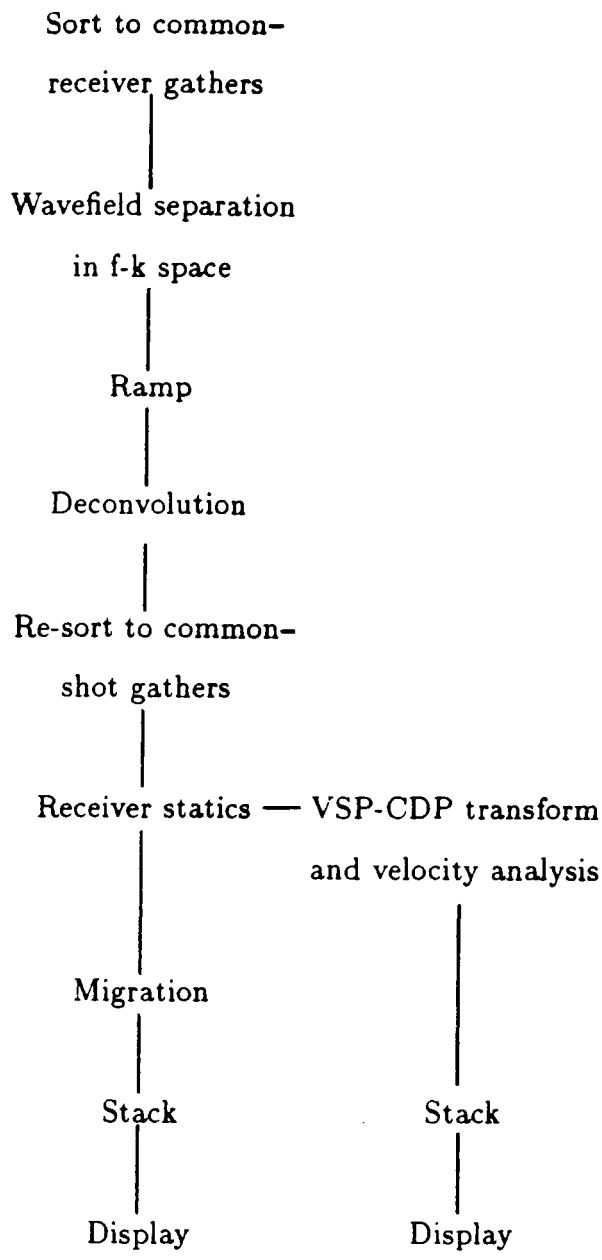

Figure 4.4 Flow chart of the basic processing sequence for the hole-to-surface data.

common-receiver gather is treated as a fixed offset VSP. The usual terms 'downward travelling' and 'upward travelling' for waves recorded on the gather will be adopted here. A wave is described as downward travelling if its traveltime increases with increasing depth (of shot), as seen on the common-receiver gather.

First break arrival times are picked automatically, and are stored in the trace headers. A sample is picked as the first break if it satisfies the following two criteria:

- Its absolute value is at least twice the RMS energy in the preceeding 10ms of data.

- The gradients either side of the sample value are of the same sign, and are increasing in magnitude with time.

4.3.3 Wavefield separation

Figure 4.5a shows a common-receiver gather from an offset of 30m. There are 20 shots from 12-50m depth. The direct arrival dominates the gather, apparently travelling in a downward direction as just described. No upward travelling energy is apparent on these raw data. The apparent velocity of the direct arrival (the velocity at which the wave appears to move across the gather) is approximately -3600m/s and this increases with increasing receiver offset. Downward travelling energy is defined to have a negative apparent velocity. Energy reaching the surface geophone after a single reflection from a near-horizontal interface appears to travel in the opposite direction across the common-receiver gather. This is the so-called upward travelling energy and is defined to have a positive apparent velocity. The downward and upward travelling energy may be separated by filtering in the frequency-wavenumber (f-k) domain (Embree et al. 1963). This is a standard technique for VSP processing (Hardage 1983), and is made computationally possible by the fast Fourier transform (FFT) (Cooley and Tukey 1965). The computation of the f-k spectrum of the data requires a constant shot spacing. This means that care must be taken not to miss any shot positions. The small shot spacing of 2m prevents aliasing when the data in each common-receiver gather are transformed into the f-k domain.

Before transforming the data to the f-k domain, each trace in the common-receiver gather is normalised to equal energy since the energy radiated by each shot is different. This is principally due to different source coupling factors. Anomalous trace amplitudes in the input data cause ringing in the f-k spectra and this degrades the wavefield separation. For the same reason a spatial taper is applied to the data to smooth the step in amplitude at the edge traces and no time ramp is applied to the data until after the wavefield separation. The spatial taper may be removed after the wavefield separation. For a review of two-dimensional filters, see March and Bailey (1983).

Figure 4.5b shows the common-receiver gather after wavefield separation. A ramp proportional to time squared has been applied to the data. Upcoming reflected energy is clearly visible on the gather with an apparent velocity of approximately 2300m/s. This is less than that of the direct arrivals due to the upcoming reflected energy following raypaths which are nearer to the vertical. The greater the geophone offset, the higher is this apparent velocity.

Figure 4.6a shows another common-receiver gather from an offset of 20m. These data are from a different survey with 34 shots over a depth range of 16-82m depth. There is some upward travelling energy visible before wavefield separation, originating from a depth of about 74m. The apparent velocity of this energy is approximately 1200m/s. This is particularly slow. Figure 4.6b shows this common-receiver gather after wavefield separation. A ramp proportional to time squared has been applied to the data, and the arrows mark the position of the first breaks. Upcoming energy is visible with two distinct apparent velocities. The events with the higher apparent velocity are P-wave reflections. The events with the lower apparent velocity are interpreted as upcoming S-wave events. These may have originated by mode conversion on reflection, and particularly strong S-wave reflections originate from a depth of about 74m which is the depth the borehole cuts a large fault. Careful selection of the dips for the f-k filter can leave only the required P-wave events on the gather (figure 4.6c).

4.3.4 Deconvolution

Deconvolution serves two purposes: it is used to make the amplitude spectra uniform for all receivers and to remove multiples from the data. Before the de-

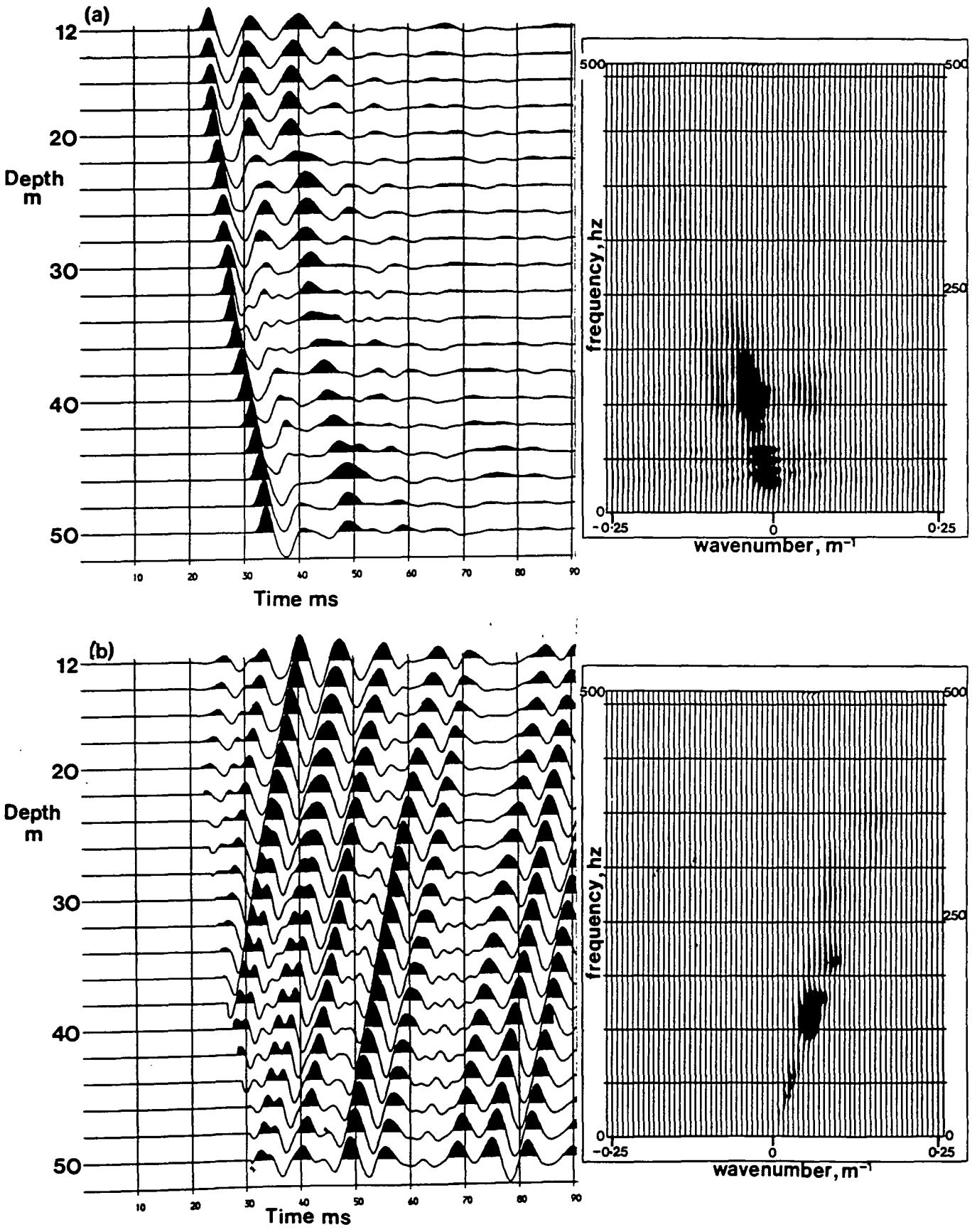

Figure 4.5 Wavefield separation showing f-k spectra. (a) A common-receiver gather from an offset of 30m. (b) The common-receiver gather after wavefield separation. A ramp proportional to time squared has been applied to the t-x display only.

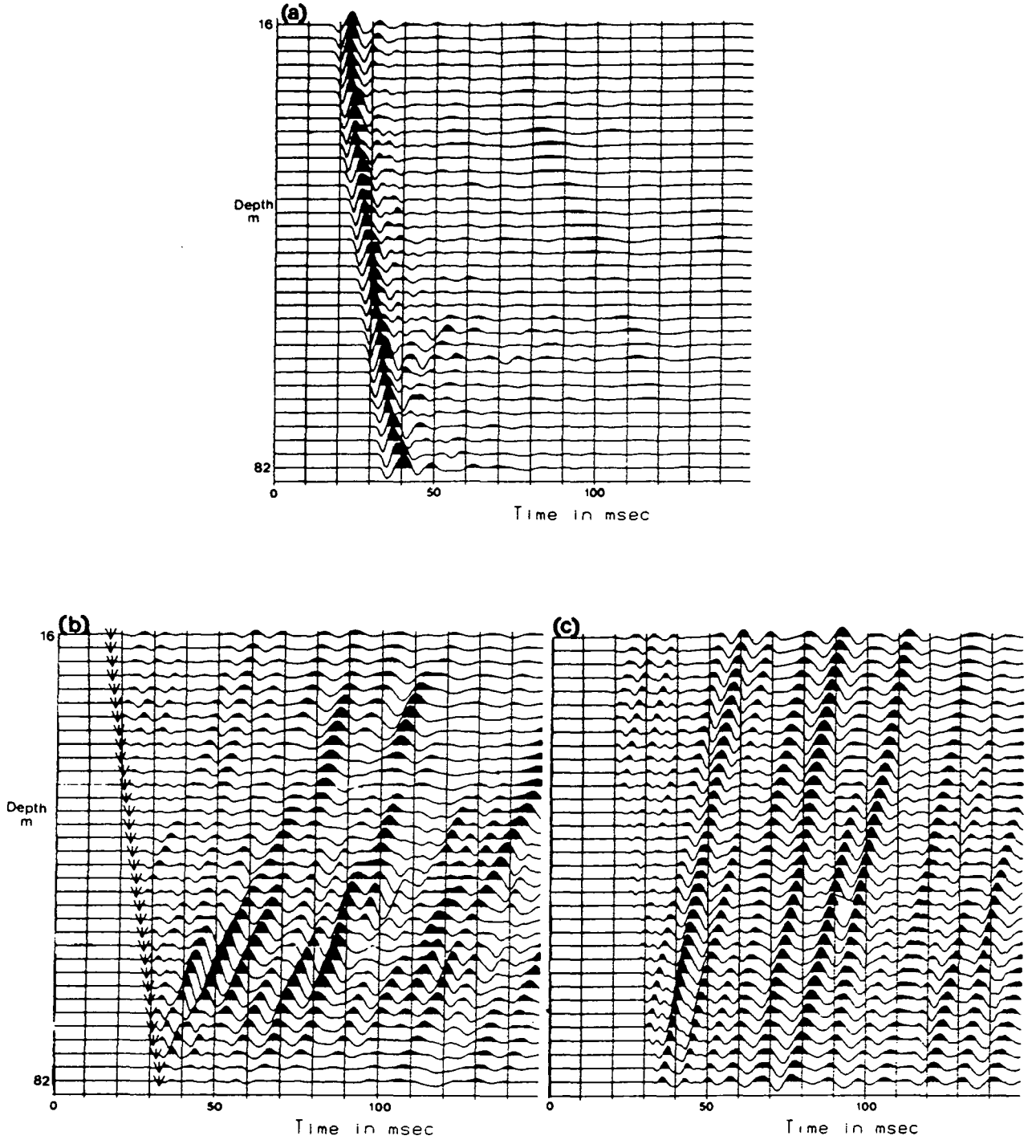

Figure 4.6 Wavefield separation demonstrating the need for selection of f-k filter slopes. (a) A common-receiver gather from an offset of 20m. (b) The common-receiver gather after wavefield separation containing both S- and P-wave energy. A ramp proportional to time squared has been applied. (c) Selection of the correct filter slopes leaves only the required P-wave energy.

convolution is performed, a time ramp is applied to the data. This attempts to correct for geometric spreading and absorbtion effects. A ramp proportional to time squared is used (Claerbout 1985).

The transmission characteristics of the near-surface not only produce static time shifts, but are also highly frequency-dependent between geophone locations. This means the seismic character is very inconsistent across a common-shot gather compared to a common-receiver gather (figures 4.3 and 4.5a). Figure 4.7 shows a comparison of the amplitude spectra from a common-shot gather and a common-receiver gather. Only eleven traces are plotted for clarity. The consistency across the common-receiver gather is quite apparent compared to the common-shot gather. The assumption that the source has a repeatable signature seems to be valid. The amplitude spectra (plotted with a linear scale) have been normalised to peak values and are taken from the raw data. Thus the majority of energy contributing to the spectra is from the direct arrivals.

Deconvolution is performed on each common-receiver gather. For a zero-offset common-receiver gather, the downward travelling wavefield at a given depth may be used to design a deconvolution operator for the upgoing wavefield at the same depth. The deconvolution operator suppresses the multiples and compresses the primary wavelets in the upward travelling wavefield. With increasing offset, the deconvolution becomes less effective as the multiple periodicities in the up- and downward travelling wavefields differ for non-normal incidence (Ahmed et al. 1986). A single downward travelling wave is extracted from each gather by aligning the downward travelling energy and summing the traces in the gather. Ideally the deconvolution would be performed tracewise, but consistency across a common-receiver gather shows this to be an unnecessary waste of computing recources. A Wiener-shaping deconvolution filter (Robinson and Treitel 1980) is designed interactively using a zero-phase Butterworth wavelet (e.g. Sheriff and Geldart 1983) as a desired output. This output wavelet is specified in the frequency domain to correspond to the useful signal bandwidth. Typically, desired output bandwidths are 80-300 Hz and this is specified to be the same for all common-receiver gathers.

Figure 4.8 shows an example of the deconvolution design. Trace 1 (figure 4.8a) is the estimated downward travelling energy and trace 2 is the zero-phase Butter-

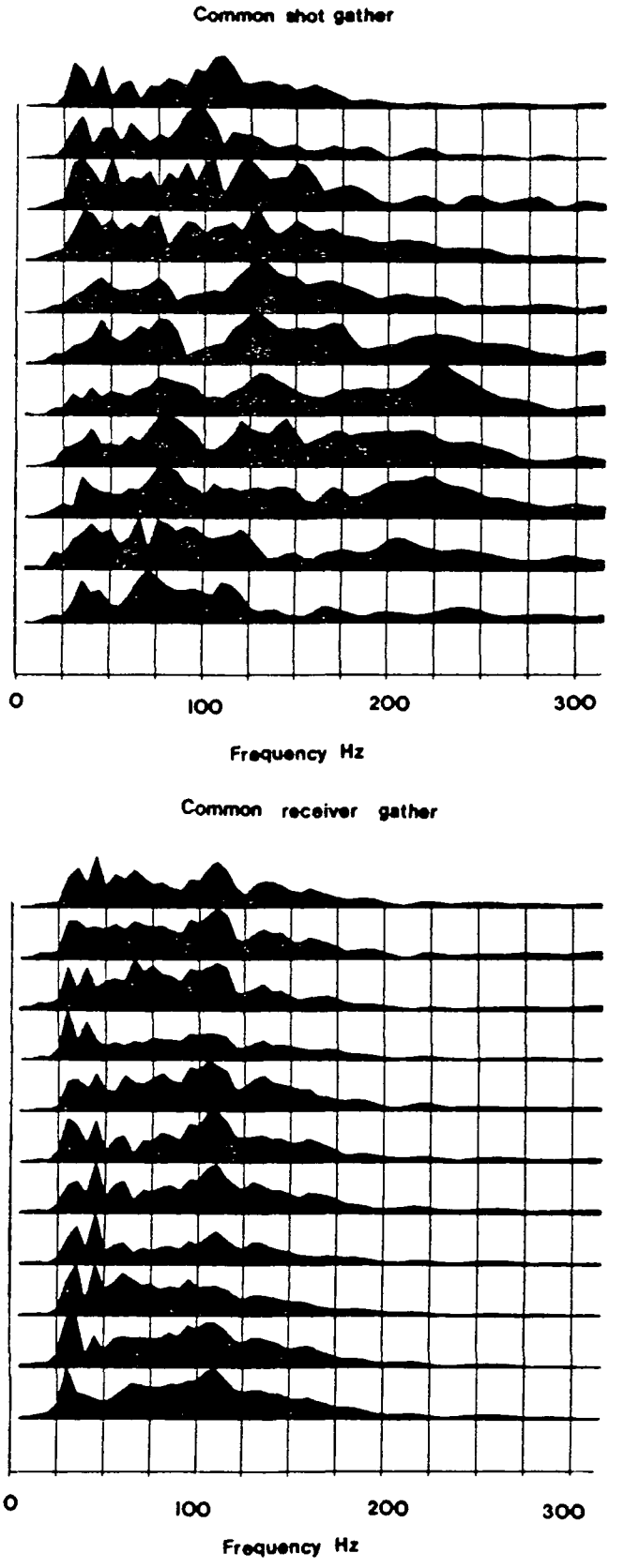

Figure 4.7 Comparison of amplitude spectra from a common-receiver gather and a common-shot gather. The spectra are plotted to a linear scale and are normalised to peak values.

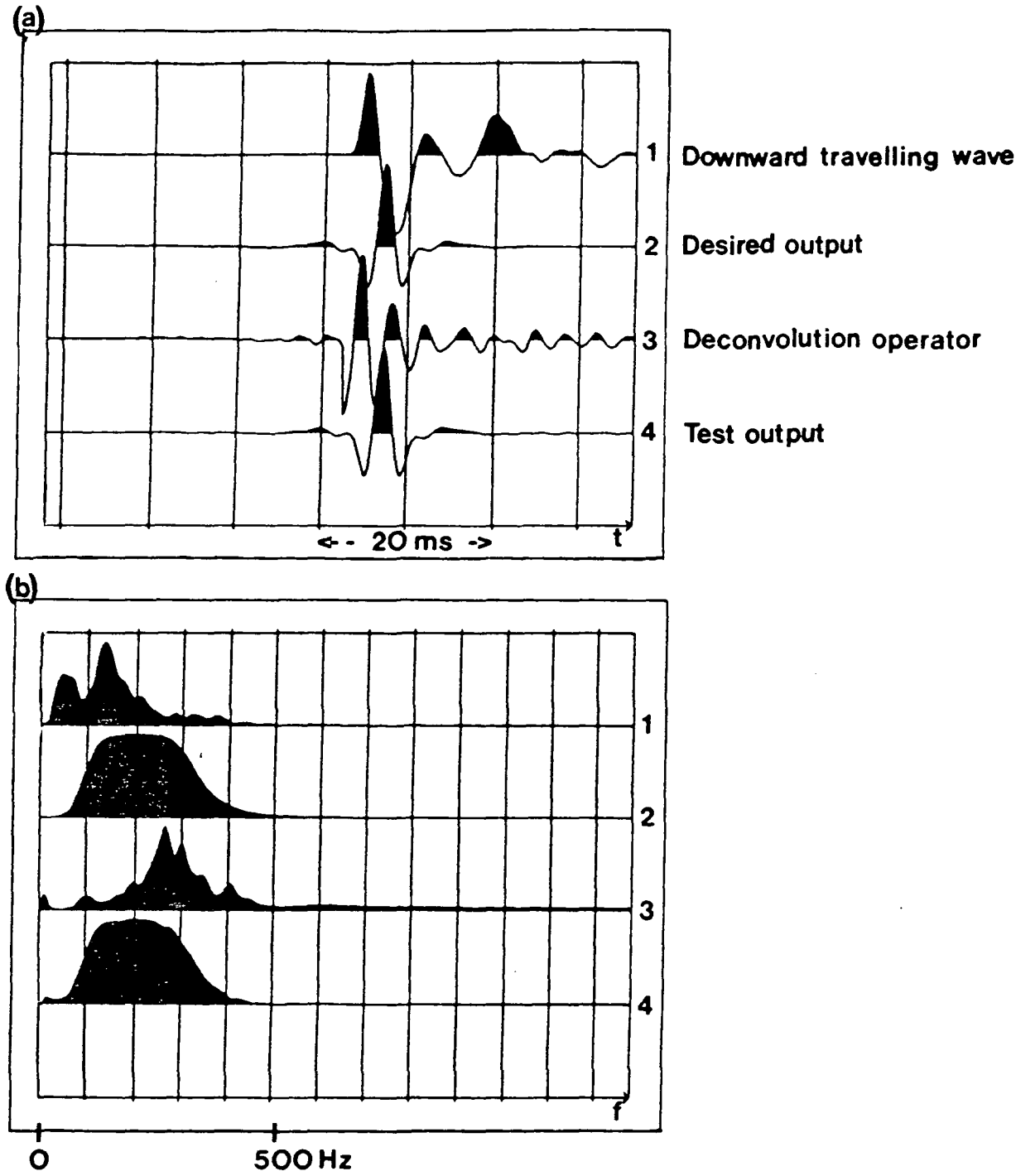

Figure 4.8 Example of the deconvolution design. (a) Time domain traces. The test output (trace 4) is formed by convolving trace 1 with trace 3. (b) Amplitude spectra of the traces in (a) plotted to a linear scale.

worth desired output. This is specified at a time lag to optimize the performance of the deconvolution filter which is plotted on trace 3. Trace 4 is a test output formed from convolving trace 1 with trace 3. Figure 4.8b shows the amplitude spectra of the traces in figure 4.8a, plotted with a linear scale.

Figure 4.9 shows a common-receiver gather containing upward travelling energy only, before and after deconvolution. The temporal resolution is improved and the data should now be zero-phase. Conversion to zero-phase, rather than minimum phase, is chosen so as to make the depth interpretations on the final sections simpler. It is easier to pick the maximum peak of a symmetric wavelet immersed in random noise than it is to pick the onset of a minimum phase wavelet.

An alternative approach to the deconvolution is to extract a wavelet from each common-receiver gather independently, and not use the measurement of the downward travelling energy as a wavelet estimate. This does not rely on the assumption that we can apply zero-offset theory to fixed-offset data but it depends upon two other assumptions. The autocorrelation function of the wavelet is taken to be the sum of the autocorrelation functions of all the traces in the upward travelling wavefield. This is equivalent to assuming that the reflectivity is white and stationary. The minimum phase assumption is then used to obtain a minimum phase wavelet (Robinson and Treitel, 1980). The deconvolution can then be applied as before. This method appears to work quite well, but it cannot be expected to suppress longer period multiples due to the shorter length of the wavelet extracted. The former method gives more consistent results when comparing final sections from neighbouring surveys and has been adopted in processing the final sections presented in this thesis.

4.3.5 Static corrections

After deconvolution, the data are resorted to common-shot gathers. Before they can be imaged to a depth section, static corrections must be applied to the receivers. Receiver statics can be large. Geophones planted close to the boreholes commonly exhibit particularly large static effects (e.g. figure 4.3). These are always time delays, corresponding to velocity reductions, and are due to ground disturbance by the air flush drilling of the boreholes. The first breaks used for the static corrections are picked manually to an accuracy of one sample.

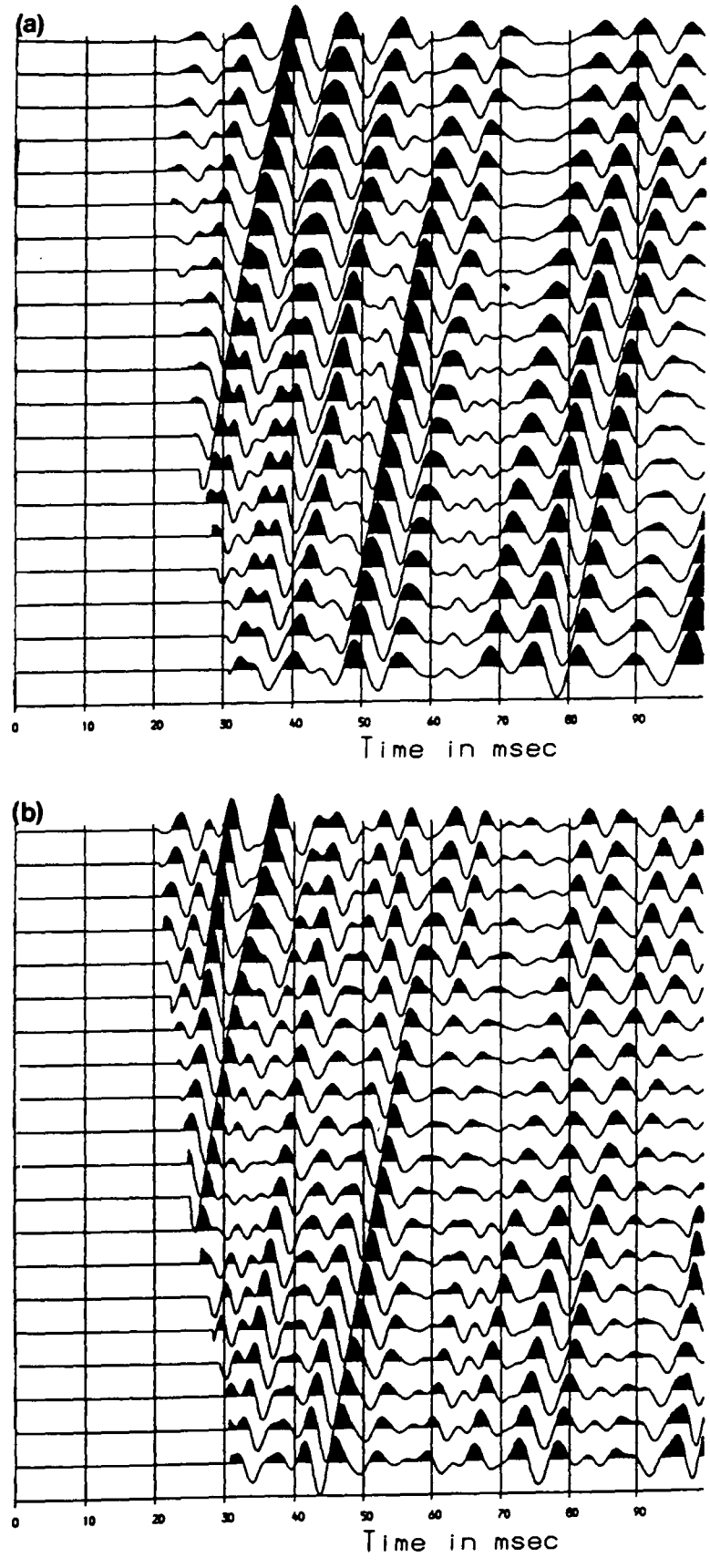

Figure 4.9 Deconvolution. (a) Common-receiver gather containing upward travelling energy only. (b) After deconvolution. The data has been muted from the start of the record to 3ms (approximately half the dominant wavelength) before the first arrival times.

The most accurate way of applying the static corrections would be to make use of a shot at a depth significantly greater than the offset of the farthest receiver from the borehole. Raypaths may then be accurately approximated as vertical, and the data adjusted accordingly. Unfortunately, this is not usually possible with the data obtained from the British Coal opencast sites, either because the boreholes are not drilled to such depths in the first place, or because they get blocked at shallower depths soon after drilling.

Instead, the static corrections are calculated by modelling the first arrival traveltimes by raytracing from the deepest shot and comparing them to the observed first breaks. To do this a velocity model is required. Sonic logs are not run in British Coal's opencast boreholes so an initial velocity model is obtained directly from an uphole survey, and then refined using the VSP-CDP transform, as explained below.

4.3.6 Uphole surveys

An uphole survey is a form of well velocity survey. It consists of shooting detonators at the bottom of the borehole into a hydrophone array, which is suspended below the water table in the borehole, spanning the depth of interest. The first break pick of the direct wave as it passes across the hydrophone array gives an estimate of the vertical velocity at the borehole.

Although the uphole survey is in effect similar to the zero-offset common-receiver gather, the downhole source and receivers give higher frequency content and a better signal-to-noise ratio in the direct wave. The data are recorded with the finer sampling interval of 0.1ms. This allows for more accurate picking of the first breaks and hence a more accurate estimate of velocity. First breaks can be picked to an accuracy of one sample and the hydrophone spacing is 2m. Over a 10m spacing with a velocity of 2500m/s the error on the velocity is less than 5%. Initial velocity models obtained from the uphole surveys are specified as plane parallel layers with a dip representing the average dip of the geology. This is apparent from the borehole log information. The model is layered to coincide with the major reflecting horizons, which are invariably the coal seams. A single layer, the base of which parallels the deeper interfaces, is used from the the depth of the top shot to the surface. The velocity for this layer can be estimated from the

small offset receivers, noting that large statics may be present on these particular receivers, and then refined using the velocity analysis technique descibed below.

4.3.7 The VSP-CDP transform and velocity analysis

Velocity analysis is carried out using the VSP-CDP transform (Dillon and Thomson 1984). This is most easily explained referring to figure 4.10. Consider one source and receiver pair. For a given velocity model there will be a locus of primary reflection points. In a surface seismic survey (figure 4.10a) this locus would be a vertical straight line at the CMP position, but when source and receiver are at different depths (figure 4.10b), the locus is curved, even for a constant velocity model. For each shot and receiver pair there is a reflection point locus. Figure 4.10c shows a complete set of loci for a hole-to-surface shot record. The loci are found by raytracing through a given velocity model, and this also yields a traveltime associated with each point on the loci. Each seismic trace can therefore be mapped on to the corresponding reflection point locus. After this has been done for all traces in a common-shot gather, the data are binned on to evenly spaced vertical traces. The output depth sample interval is 1m and the horizontal trace spacing is 2m.

The velocity analysis is summarised by the following steps:

- Choose an initial velocity model.
- Apply the VSP-CDP transform to the complete data set.
- Bin the data on to evenly spaced vertical traces.
- Sort the data to common depth point (CDP) gathers.
- Estimate velocity corrections from the residual moveout on the CDP gathers.

Consider a single reflector in a constant velocity medium at a depth Z_r. The source depth is Z_s and the receiver offset is x. The offset of the reflection point (CDP offset) is X_r (figure 4.10b).

We wish to see how the reflection point, (X_r, Z_r), will be mispositioned with an error in the velocity, v.

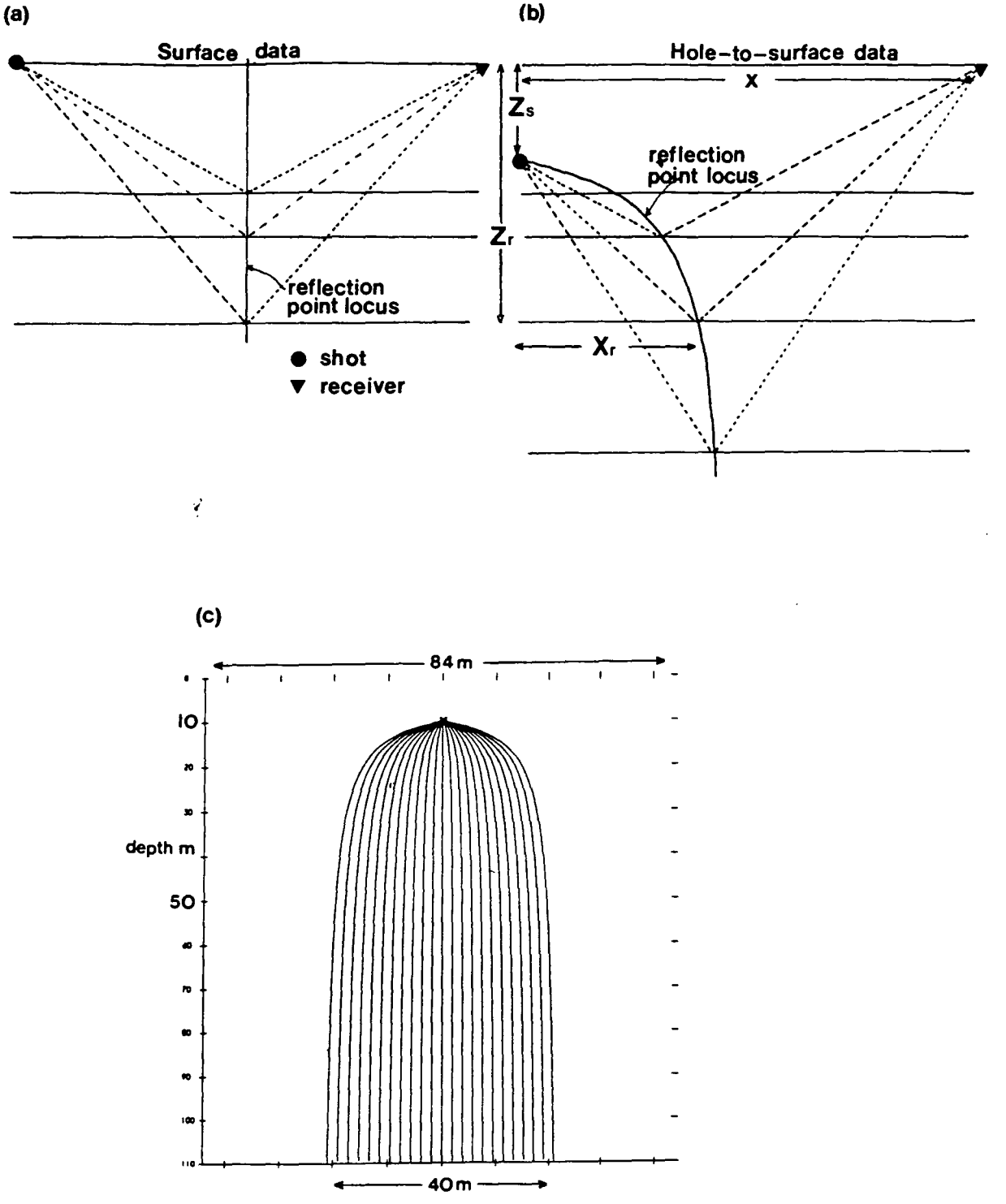

Figure 4.10 The reflection point locus. (a) For surface seismic data the reflection point locus is a vertical straight line at the CMP position. (b) For hole-to-surface data the reflection point locus is curved, even for a constant velocity model. (c) A complete set of relection point loci for a hole-to-surface shot record.

$$Z_r = \frac{Z_s + \sqrt{v^2t^2 - x^2}}{2}$$

where t is the traveltime from source to receiver.

$$\frac{\partial Z_r}{\partial v} = \frac{vt^2}{2\sqrt{v^2t^2 - x^2}}$$

Define $A = (2Z_r - Z_s) = \sqrt{v^2t^2 - x^2}$, the total vertical distance travelled by the ray.

$$\frac{\partial Z_r}{\partial v} = \frac{A^2 + x^2}{2vA} \tag{4.1}$$

From similar triangles:

$$x = \frac{AX_r}{Z_r - Z_s} \tag{4.2}$$

Figure 4.11a plots equation 4.1 using 4.2 for a reflector depth of 50m, a velocity of 2500m/s and a velocity error of 5%, for various CDP offsets. This shows the expected moveout of an event across a CDP gather. With this knowledge an estimate of the velocity error can be made and the velocity model updated. The velocity error is not computed exactly as the equations are only true for a constant velocity, but the method enables an accurate stack of the data to be obtained.

The error in the lateral positioning of the reflection point can also be examined.

$$X_r = \frac{(Z_r - Z_s)x}{2Z_r - Z_s}$$

$$\frac{\partial X_r}{\partial v} = \frac{A^2 + x^2}{A^2 v}\left(\frac{x}{2} - X_r\right) \tag{4.3}$$

where

$$x = \frac{AX_r}{(Z_r - Z_s)} \tag{4.4}$$

Figure 4.11b plots equation 1.3 using 1.4 for a reflector depth of 50m, a velocity of 2500m/s and a velocity error of 5%. With a horizontal trace spacing of 2m this is only significant for shots within 10m of the reflector, though the effect worsens with inreasing CDP offset.

When a velocity has been derived it may be necessary to recompute the receiver statics using the new velocity model, if this new model is significantly different to the initial model. Again, the first arrival traveltimes are modelled by raytracing from the deepest shot to the receiver positions and comparing them to the observed first breaks. Since any changes to the velocity field in the shallow part of the section affect the raypaths to all deeper events, it may then necessary to repeat the velocity analysis and iterate on the whole procedure until a final model is obtained. From experience to date, it should not be necessary to iterate round this loop more than twice.

Since no sonic logs have been available, it remains to be seen whether the more detailed velocity information available from the sonic log will improve the quality of the final sections.

4.3.8 Real data velocity analysis example

Figure 4.12a shows a CDP gather after VSP-CDP transformation. The trace on the left is the stack of all traces in the gather. The reflected energy at 50m depth stacks to give a strong event, but the reflected energy at 25m depth stacks destructively. The slight downward dip of this energy implies that the velocity is too small above 25m depth. Thus the velocity model can be updated and the process repeated. Changing the velocity above 25m depth will also affect the moveout of the deeper reflected energy. Figure 4.12b shows the same CDP gather after the model has been changed. The energy at 25m now stacks to give a strong event.

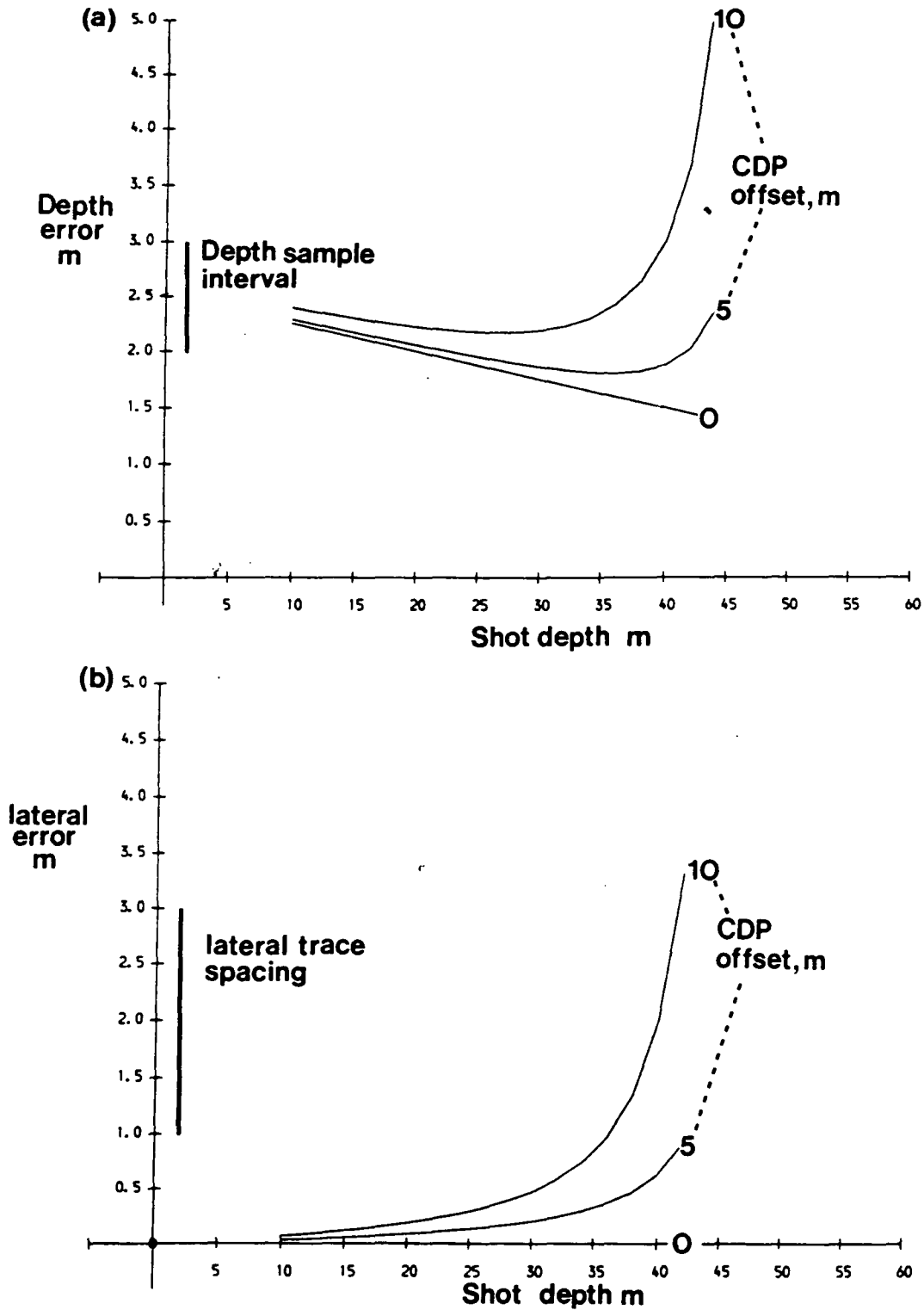

Figure 4.11 Position error curves for the VSP-CDP transform for various CDP offsets. The velocity error is 5% and the reflector depth is 50m in a constant 2500m/s velocity model. (a) Depth error curves. (b) Lateral error curves.

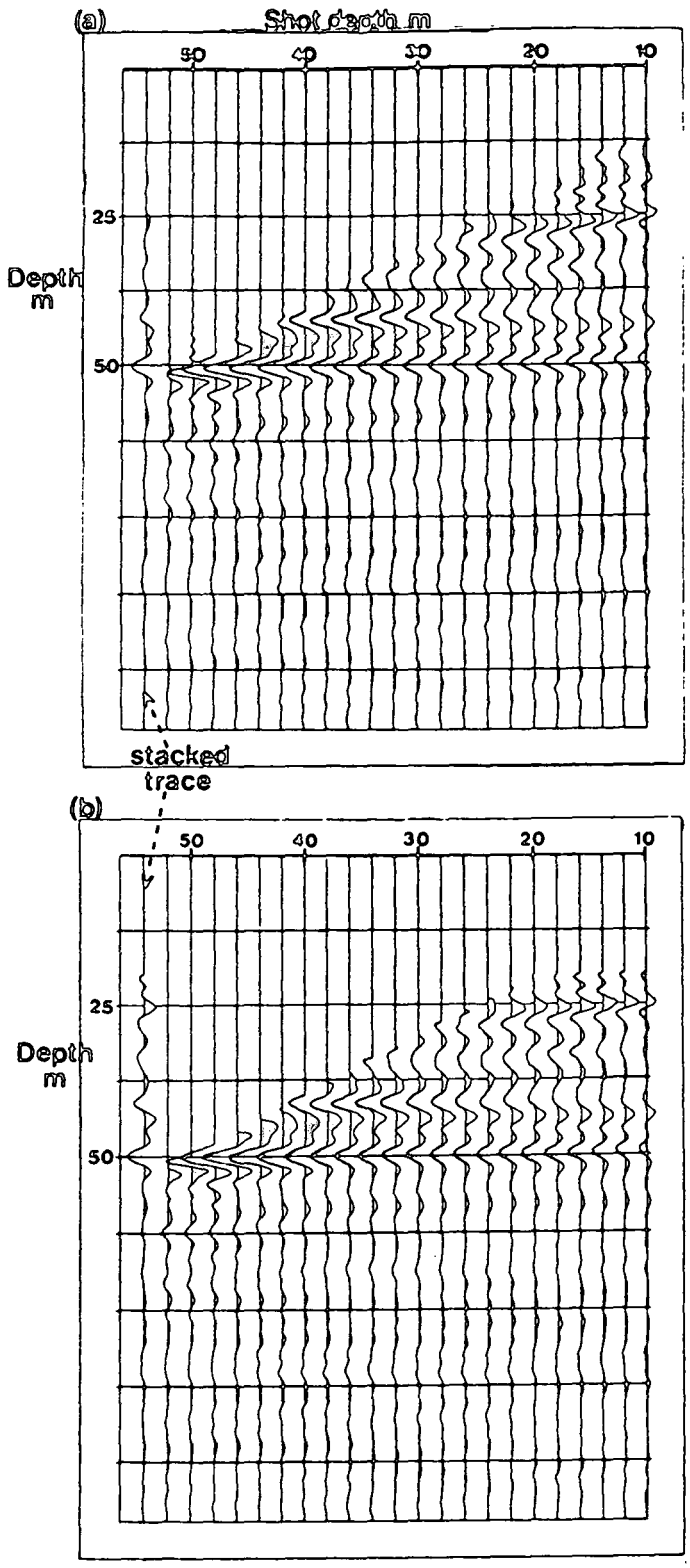

Figure 4.12 CDP gather after VSP-CDP transformation. (a) Incorrect velocity model giving destructive stack at 25m depth. (b) Corrected velocity model improving stack.

4.3.9 The VSP-CDP stack

When the final velocity model has been obtained, the VSP-CDP stack of the data may be examined. This depth section will show structure much the same as a conventional surface seismic stack will. The structure will be mispositioned and diffraction energy is not handled. However, this proves a useful part of the processing. Reflector depths can be correlated with borehole information and polarity of events examined. Also a first glance of the structure can indicate where stacking problems will arise, such as at faults, and the section shows the approximate subsurface coverage obtained.

4.3.10 Anisotropy

As the receiver offset increases and the shots become closer to reflectors, the raypath angles become further away from the vertical. This raises the question of whether the isotropic velocity approximation is good enough. The tomography work showed that anisotropy is present within the Coal Measures strata, and this was discussed in detail in section 3.4.1.

Elliptical anisotropy was coded into the velocity analysis. No improvement was made to the stack of the data. If a value of 10% is used on a 'final' velocity model then the velocity values become too great and the stack is degraded. Reducing the velocities by, say, 5% and then using 10% anisotropy shows no improvement and only makes the velocity analysis more complicated. If anisotropy is expected to be significant, then it should be detectable by examining the CDP gathers. As the offset is increased, the model velocities should be underestimated by successively larger amounts, and hence events should be overcorrected to erroneously shallow depths with increasing offset. This is not observed, and is not altogether surprising since, even with a geophone offset of 50m, a reflector depth of 30m and a shot 6m above the reflector, the raypath angle is only 55 degrees from the vertical. At greater depths the angle is less. Shots closer to reflectors than 6m will have shallower raypaths, but these shots do not provide useful information. Data wavelengths are of the order of 6-8m and a mute is applied to the data to remove such energy. This also suggests a simpler but cruder method of dealing with small amounts of anisotropy. Data that are imaged from raypaths with less

than a specified takeoff angle can be muted, either before or after the VSP-CDP transform, though such a mute must be applied before migration of the data.

The code to perform the VSP-CDP transform was written by Findlay (1990). This code was modified to handle the hole-to-surface geometry, carry out the CDP sorting for the velocity analysis, and to handle elliptical anisotropy in the velocity model.

The hole-to-surface shot records have now had the receiver static corrections applied and a velocity model of the subsurface has been derived. The data should contain only primary reflected energy.

4.3.11 Migration

The aim of migration is to relocate reflection events to their true subsurface positions. Most surface seismic data are migrated post-stack where the stacked seismic section is assumed to be equivalent to a zero-offset section (coincident source and receiver positions). Where the subsurface is not simple (i.e. not homogenous layers with horizontal interfaces), this assumption will be incorrect, the stacked data will be smeared and post-stack migration will not be able to correct for it. Pre-stack migration, on the other hand, will correctly migrate the data providing that the velocity field is known. The problem of knowing the velocity field, combined with the relative expense and the possible computer storage problems of large amounts of data, means that pre-stack migration is not commonly used in surface seismic data processing. It is more common to use 'partial pre-stack migration' in which each (single-fold) constant-offset section is migrated to zero offset before stack. This enables the post-stack migration to achieve better results. Since the data volumes of the hole-to-surface surveys are small and we have derived a velocity model, pre-stack migration can be performed.

Migration of the hole-to-surface data is carried out on individual shot records. The principle can easily be understood from geometrical considerations. Consider a shot record with a single receiver showing a single impulsive arrival (figure 4.13a). If a constant velocity is assumed, the reflector configuration must be the depth ellipse shown in figure 4.13b. Conceptually, migration is performed by taking the

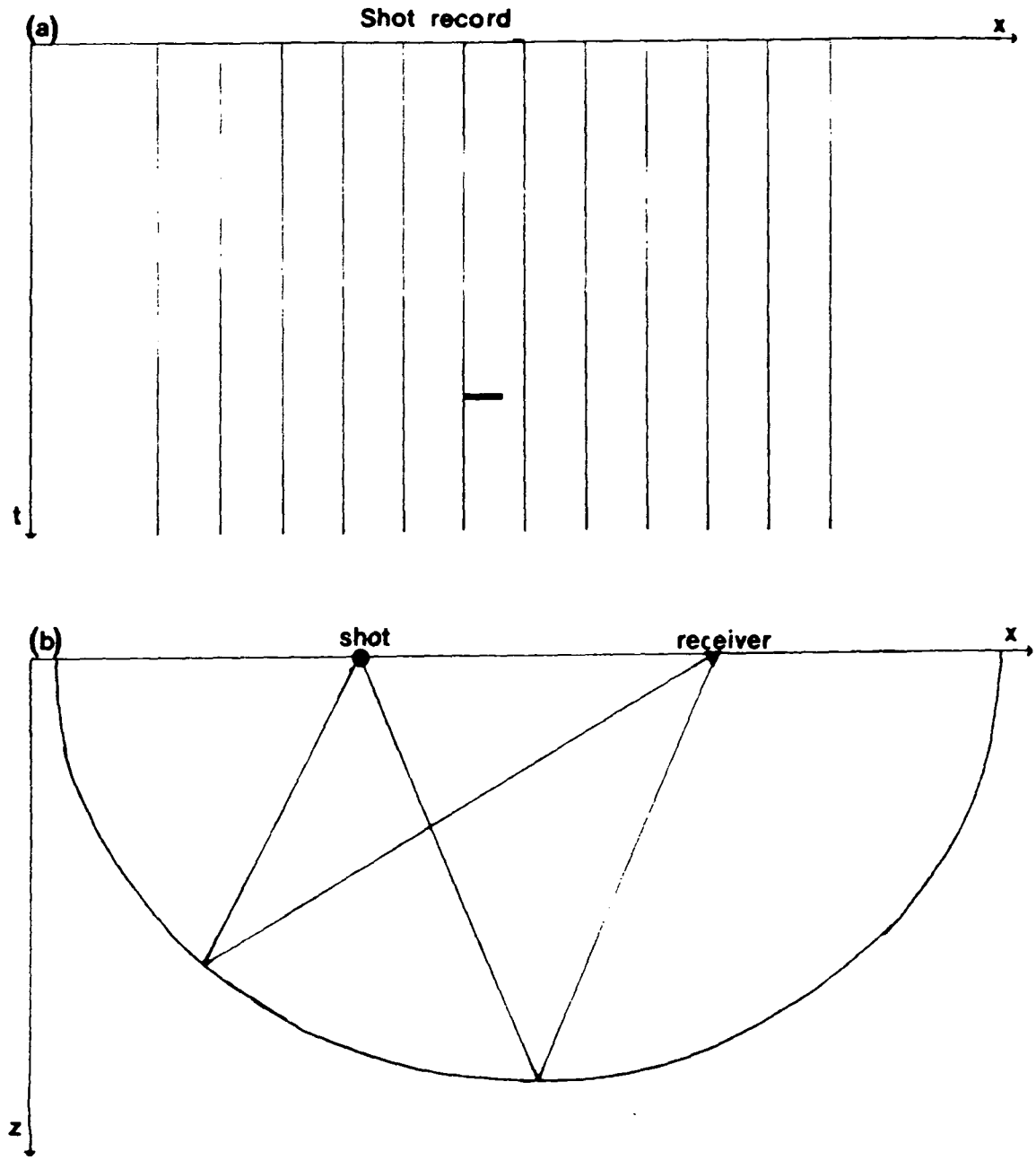

Figure 4.13 The principle of pre-stack migration. (a) A shot record with a single receiver showing an impulsive arrival. (b) Depth ellipse of reflector configuration required to produce the impulsive arrival in (a). A constant velocity is assumed.

event from the shot record and distributing it around the appropriate ellipse. This must be done for all samples in the shot record.

Migration can be performed in many ways (Yilmaz 1987). Migration of the hole-to-surface data is carried out using the shot record migration method of Berkhout (1984), and may be summarised as follows:

o The detected wavefield is inversely extrapolated to an image depth, z.

o The source wavefield is forward extrapolated to the same depth.

o At the image depth, both wavefields must occupy the same lateral space. The wavefields are correlated at depth z.

Imaging is then carried out by extracting the zero time component of the correlated data as the two wavefields must be time-coincident at reflectors and diffractors (Claerbout 1971).

Since the migration algorithm is two-dimensional, structure will be accurately imaged only if it can be approximated as this and the data is acquired perpendicular to its strike.

4.3.12 Wavefield extrapolation

Wavefield extrapolation is based upon the one-way (in depth) scalar wave equation. This means that the migration will not handle multiples, mode conversions, surface waves or noise etc, and these are assumed to have been removed from the data by the pre-migration processing. If such data are input to the migration, they are simply treated as primary reflected energy. The wavefield extrapolation is performed in the f-k domain.

For a fixed source a recorded wavefield is described by the scalar wave equation. If the wavefield is denoted by $P(x, z, t)$ with a propagation velocity of v, then in two dimensions the scalar wave equation may be written

$$\frac{\partial^2 P}{\partial t^2} = v^2 (\frac{\partial^2}{\partial x^2} + \frac{\partial^2}{\partial z^2}) P$$

A plane wave may be described by the general solution, $P = e^{-i\omega t + ik_x x + ik_z z}$ where k_x and k_z are the lateral and vertical wavenumbers ($k_x = \frac{2\pi}{\lambda_x}$). Substituting the general solution into the scalar wave equation gives the dipersion relation of the scalar wave equation:

$$k_x{}^2 + k_z{}^2 = \frac{\omega^2}{v^2}$$

Differentiating P with respect to z gives $\frac{\partial P}{\partial z} = ik_z P$. This can be solved analytically to give the wavefield extrapolation equation:

$$P(z + dz) = P(z)e^{ik_z dz}$$

The dispersion relation gives k_z in terms of known quantities and the wavefield extrapolation equation can be simply and accurately implemented in the f-k domain. The choice of the sign of k_z implies the direction of the wavefield.

$$P(\omega, k_x, z) = P(\omega, k_x, z = 0)e^{i\sqrt{\frac{\omega^2}{v^2} - k_x{}^2}.z}$$

The f-k implementation of the wavefield extrapolation equation is inherently stable and handles steep dips, phase angle and obliquity corrections exactly (Claerbout 1985). The migration may be described as a phase-shift depth migration as wavefield extrapolation is performed in equal depth steps by simply shifting the phase by specified amounts.

Figure 4.14 shows the migration impulse response for a coincident source and receiver pair at the surface. A single impulsive event was modelled on the receiver at a two-way traveltime of 50 ms. The model velocity is 2000m/s. The impulse response should be a circular 'smile' originating from a depth of 50m. The amplitude on each trace should be proportional to the cosine of the angle of incidence to the vertical. This is the obliquity function which arises from Huygens principle of secondary sources (Sheriff and Geldart 1982). The original impulse has been broadened into a wavelet. This is due to the limited aperture in f-k space of the

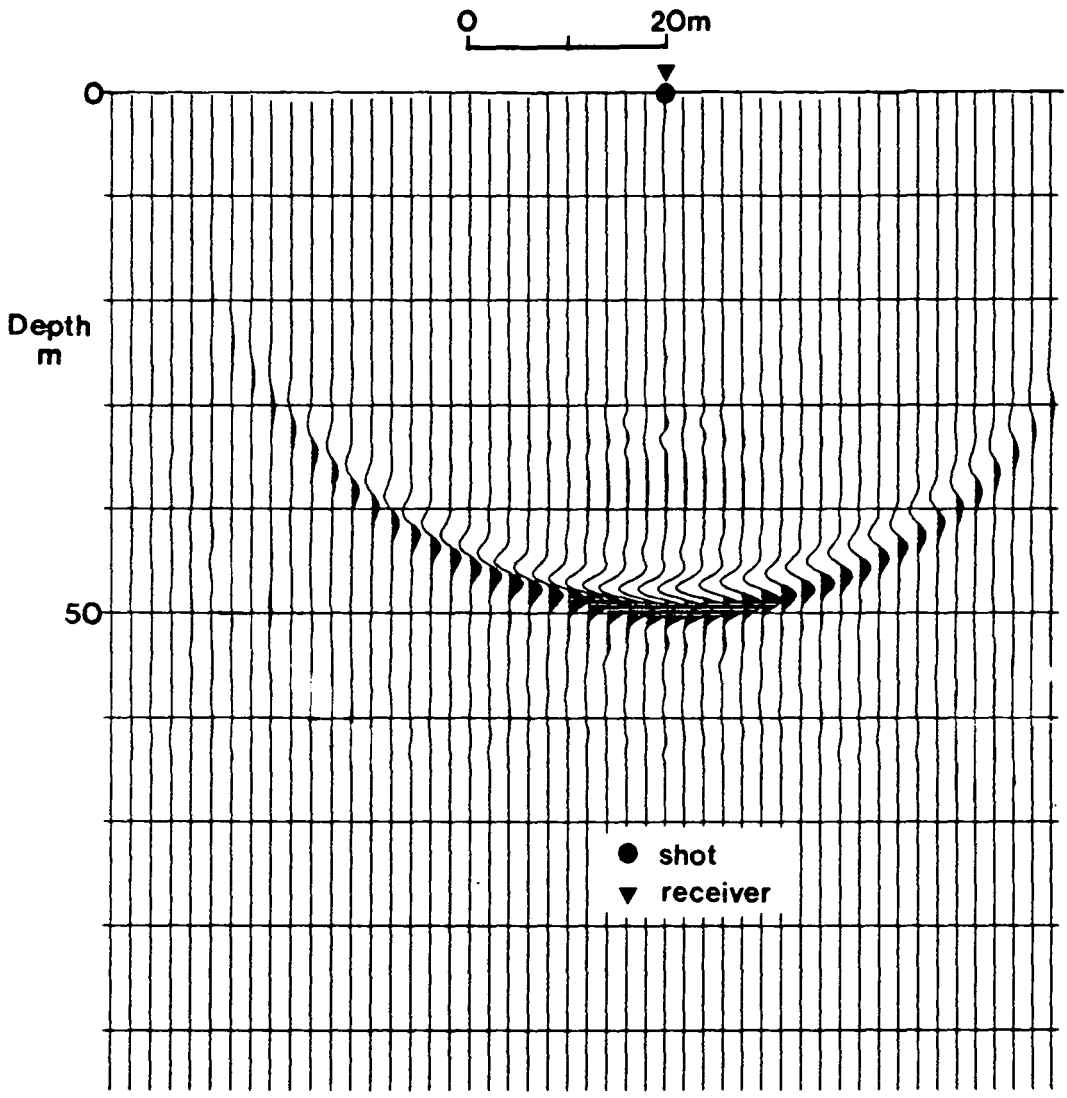

Figure 4.14 Migration impulse response for a coincident source and receiver pair at the surface. A single impulsive event was modelled on the receiver at a two-way traveltime of 50ms. The model velocity is 2000m/s and the trace spacing is 2m.

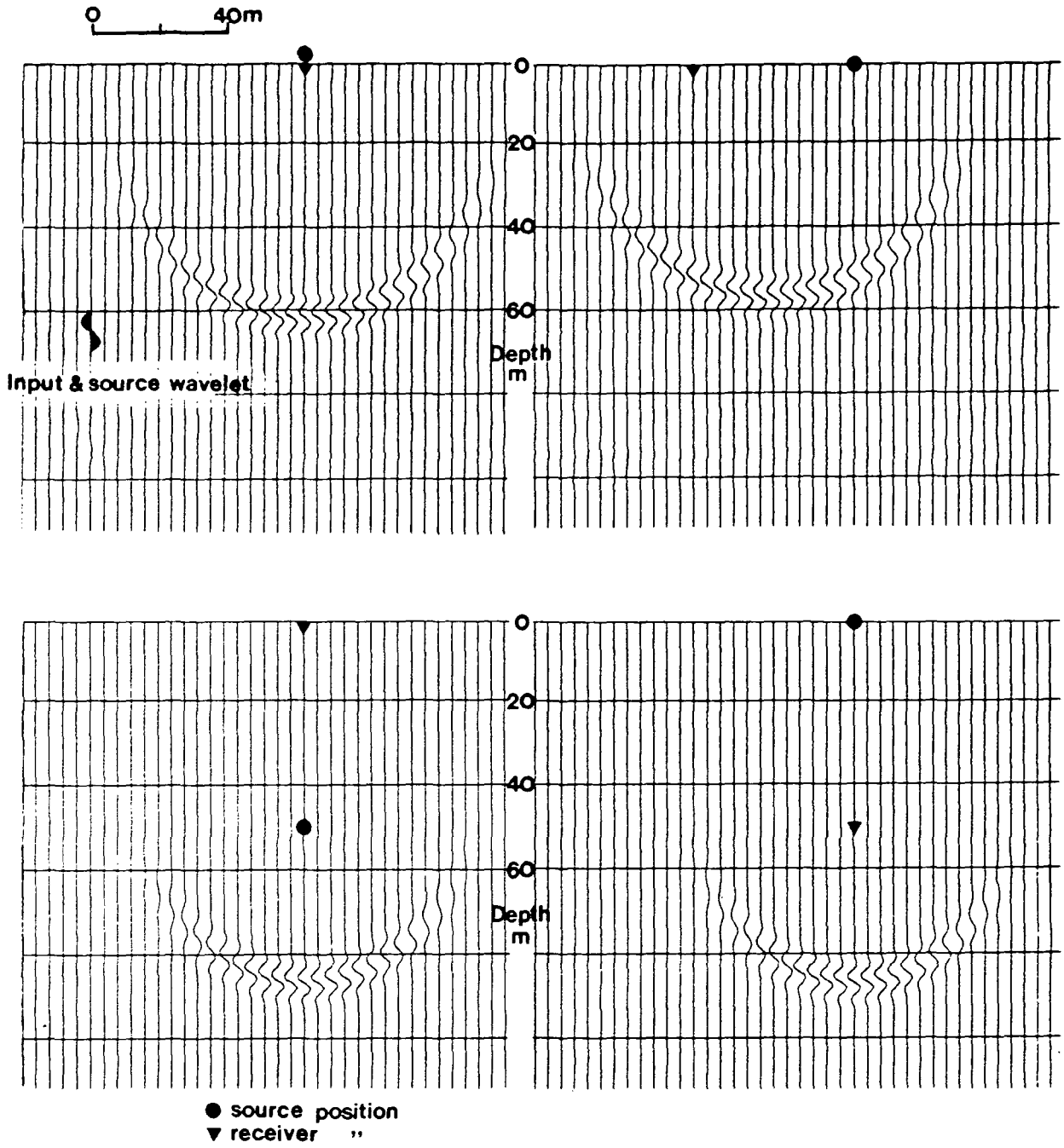

Figure 4.15 Migration impulse responses for various shot and receiver configurations. A 200Hz sine wave was modelled on the receiver at a two-way traveltime of 50ms, and a 200Hz sine wave was specified as the source. The model velocity is 2500m/s and the trace spacing is 4m.

phase-shift operator, which is discussed below, and is due to the wavelet shaping or phase angle of the operator which has a constant 45 degree phase spectrum and an amplitude proportional to the square root of the frequency for a 2-dimensional migration (Yilmaz 1987). Figure 4.15 shows further impulse responses for various shot and receiver configurations. A single 200Hz sine wave was modelled on the receiver, at a two-way traveltime of 50ms. A similar source wavelet was specified (section 4.3.15), and a constant velocity of 2500 m/s was used for the model.

4.3.13 Evanescent energy

The heart of the wavefield extrapolation process is the phase-shift operator, $e^{i\sqrt{\frac{\omega^2}{v^2}-{k_x}^2}.z}$. The square root in this equation is only real for certain values of k_x and ω. When vk_x exceeds ω, the exponential becomes real so that depth dependence is a growing or damped exponential. These solutions are termed evanescent waves (Claerbout 1985) and need to be muted. In the migration algorithm the offending part of the f-k spectrum is simply zeroed, and this amounts to velocity filtering of the data as the migration proceeds. If the velocity varies with depth the velocity filter will be different at each depth step. Since velocity normally increases with depth the velocity filter normally becomes more severe at greater depths. This explains the distortion of the wavelets after migration (figures 4.14 and 4.15).

4.3.14 Spectral shaping within the migration algorithm

As the source and receiver wavefields are extrapolated to each depth step, they are correlated to obtain the common lateral coverage to be imaged. At this stage the amplitude spectra of the correlated wavefield is shaped to a specified bandwidth whilst retaining the phase information. Correlation of the wavefields is performed in the f-x domain, and each spectral value is multiplied by an appropriate amount to give a Butterworth amplitude spectrum over the specified bandwidth. The migration impulse response of figure 4.14 has been shaped to a Butterworth spectrum of 80-300Hz.

4.3.15 Specification of a source wavelet

The migration algorithm requires a source wavelet. This can most simply be

specified as a spike. The hole-to-surface data have had a deconvolution applied and the wavelet in the data has been shaped to a zero-phase Butterworth wavelet. The least distortion of the input data occurs if the specified source wavelet matches the wavelet in the data. For the hole-to-surface data the source wavelet is specified as a zero-phase Butterworth impulse with the appropriate bandwidth.

4.3.16 Imaging

Imaging is carried out at each depth step using the imaging principle of Claerbout (1971): at reflectors and diffractors the source and receiver wavefields must be time coincident. In the migration algorithm this is carried out by extracting the zero-time component from the correlated source and receiver wavefields after the spectral shaping has been carried out. This wavefield is stored in the f-x domain and the zero-time component is obtained by summing all the frequency components at each depth step. This can be understood from the inverse Fourier integral.

$$p(t,x) = \int_{\infty}^{\infty} \int_{\infty}^{\infty} P(\omega, k_x) e^{-i\omega t + ik_x x} dk_x d\omega$$

with the usual notation.

Substituting t=0

$$p(t=0,x) = \int_{\infty}^{\infty} \int_{\infty}^{\infty} P(\omega, k_x) e^{ik_x x} dk_x d\omega$$

$$p(t=0,x) = \int_{\infty}^{\infty} P(\omega, x) d\omega$$

and this can be computed by a summation.

4.3.17 Stacking of the data after migration

Each common-shot gather is migrated separately, and produces an image in depth of the subsurface. The depth sample interval (the wavefield extrapolation step) is 1m and the horizontal trace spacing is 2m. The separate images are

combined by stacking. Stacking of the data improves the signal-to-noise ratio in the data. Maximum reflector coverage is obtained from the shallowest shot, so ideally only the shallowest shot need be migrated. In practice the poor signal-to-noise ratio requires shots to be stacked. The correct normalisation should be applied to the data when stacking. If there are N contributions to a particular point, then the stacked output should be normalised by N at that point. To do this it is necessary to mute the data, in order to zero the noise (migration smiles) outside the expected coverage for each shot. It is not possible to distinguish signal from noise during the stacking process. The mute can be calculated by raytracing through the velocity model. The mute can only be as accurate as the velocity model and it is realised that some data may be lost in this way. For this reason, it is important to examine the migrated shots, and carefully check the mute. The eye is by far the best way to distinguish signal from noise.

Further mutes can be applied to the data to improve the stack quality. It is normal to mute the first few metres below each shot, and a maximum depth mute can improve the signal-to-noise ratio deeper in the section. This excludes the deeper parts of the shallow shot images from the stack.

The fold of coverage on a final section will depend upon the number of shots in a survey. At the very edges of the section the fold of coverage is unity, as only the shallowest shot images this region. The fold of coverage builds up towards the centre of the section and within the coverage of the deepest shot the fold is equal to the number of shots. A minimum fold of coverage can be specified but this is very subjective. If the outer traces are consistent with the rest of the data then it is normal to include them in the final display. If they look noisy and inconsistent with the rest of the data a minimum fold of coverage is specified.

4.3.18 Maximum receiver offset

Increasing the receiver offset affects the processing at various stages:

- Wavefield separation becomes increasingly difficult with the direct wave energy moving closer to, and even overlapping with, the primary reflected energy, in f-k space.

- The deconvolution becomes less effective.
- Anisotropy becomes more significant with the shallower raypath angles.

Data have been successfully processed with receiver offsets up to 94m. The limiting factor on the maximum offset is the difficulty in specifying a velocity field to accurately stack the individually migrated shot records. Although these data were successfully processed, the deconvolution was more difficult to apply, and a deterioration of the stack quality was evident. It is suggested that for the shallow depths up to 100m or so, that this is the maximum receiver offset that can be handled.

Chapter V

Hole-to-surface data in shallow Coal Measures strata

5.1 Introduction

A total of eight hole-to-surface surveys are presented in this chapter. These surveys were acquired from two British Coal opencast exploration sites, Lowther South in Yorkshire, and Lostrigg in Cumbria. The data were acquired and processed as described in chapter 4.

5.2 Lowther South, Yorkshire

5.2.1 Survey A; test survey showing edge of washout

Four hole-to-surface surveys were acquired from Lowther South Yorkshire. The first survey, shot in borehole A, was a test to see the quality of data obtainable. As it turned out, not only were strong reflections recorded, but the edge of a washout was detected due to the associated disruption in reflector continuity.

Figure 5.1 shows the shot and receiver positions for survey A with the subsurface coverage, calculated assuming a constant velocity field. Twenty shots were fired from 12m to 50m depth. The water table was at 10m depth, and the borehole was blocked below 50m. Figure 5.2 shows the interpreted stratigraphic logs for borehole A, and the two neighbouring boreholes to either side in the plane of the survey. There is a 1.0m thick coal seam with its base at 37m which appears flat and continuous between the three boreholes. This is the Barnsley Top Softs (Warren House) Seam. A 70cm thick coal seam with its base at 68m, the Dunsil, also appears flat and continuous between the three holes. The boreholes to either side of borehole A show 46cm of coal present at about 62m depth. This is the lower leaf of the Low Barnsley Seam which is completely washed out in borehole A. The edges of the washout of the lower leaf lie somewhere between borehole A and the two neighbouring boreholes. A sandstone layer at 50m depth is missing from the borehole to the left of borehole A, which is seen in the other two holes.

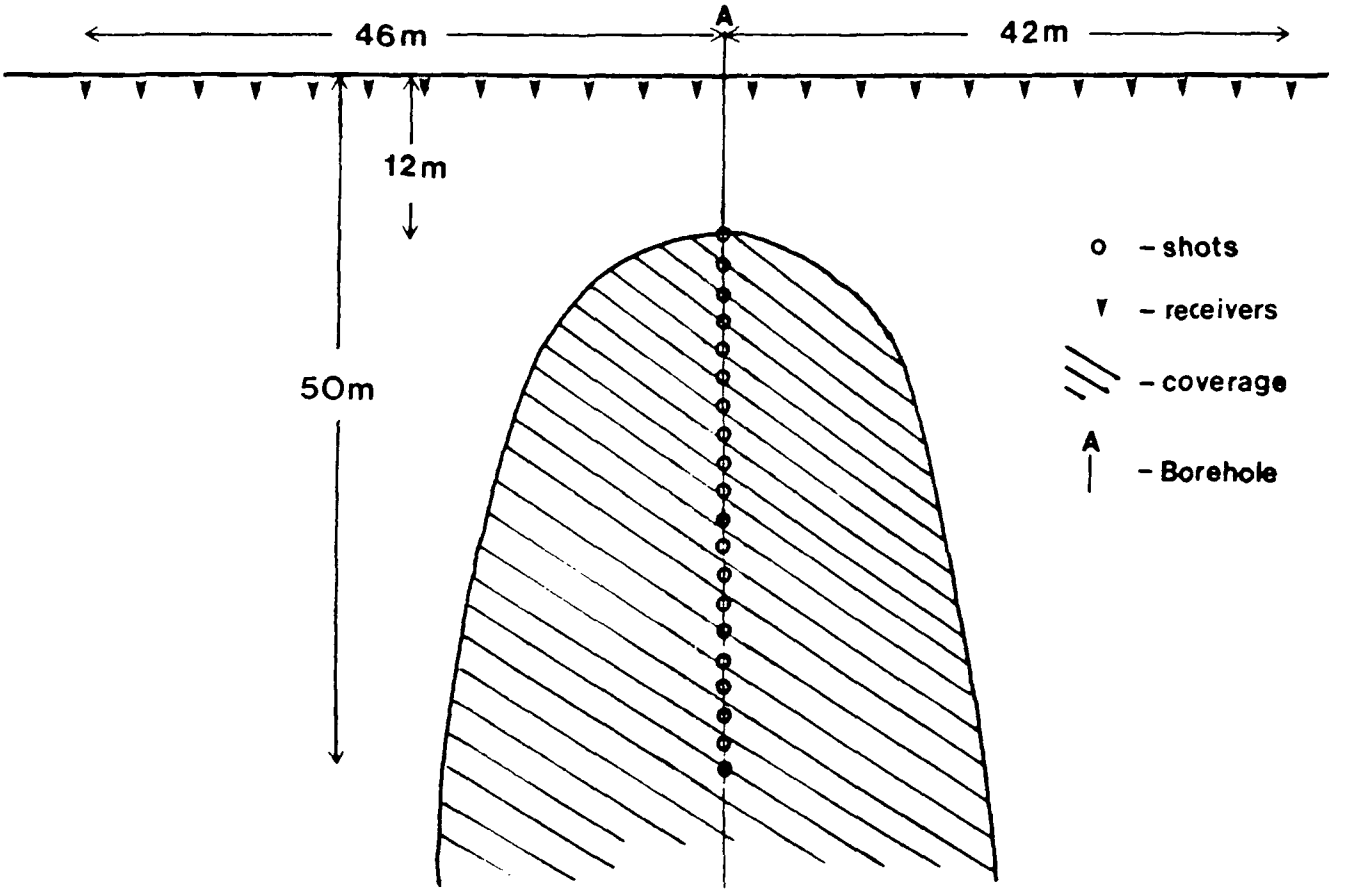

Figure 5.1 Shot and receiver positions for survey A at Lowther South. The receiver spacing was 4m and the shot spacing 2m. Subsurface coverage has been calculated assuming a constant velocity field.

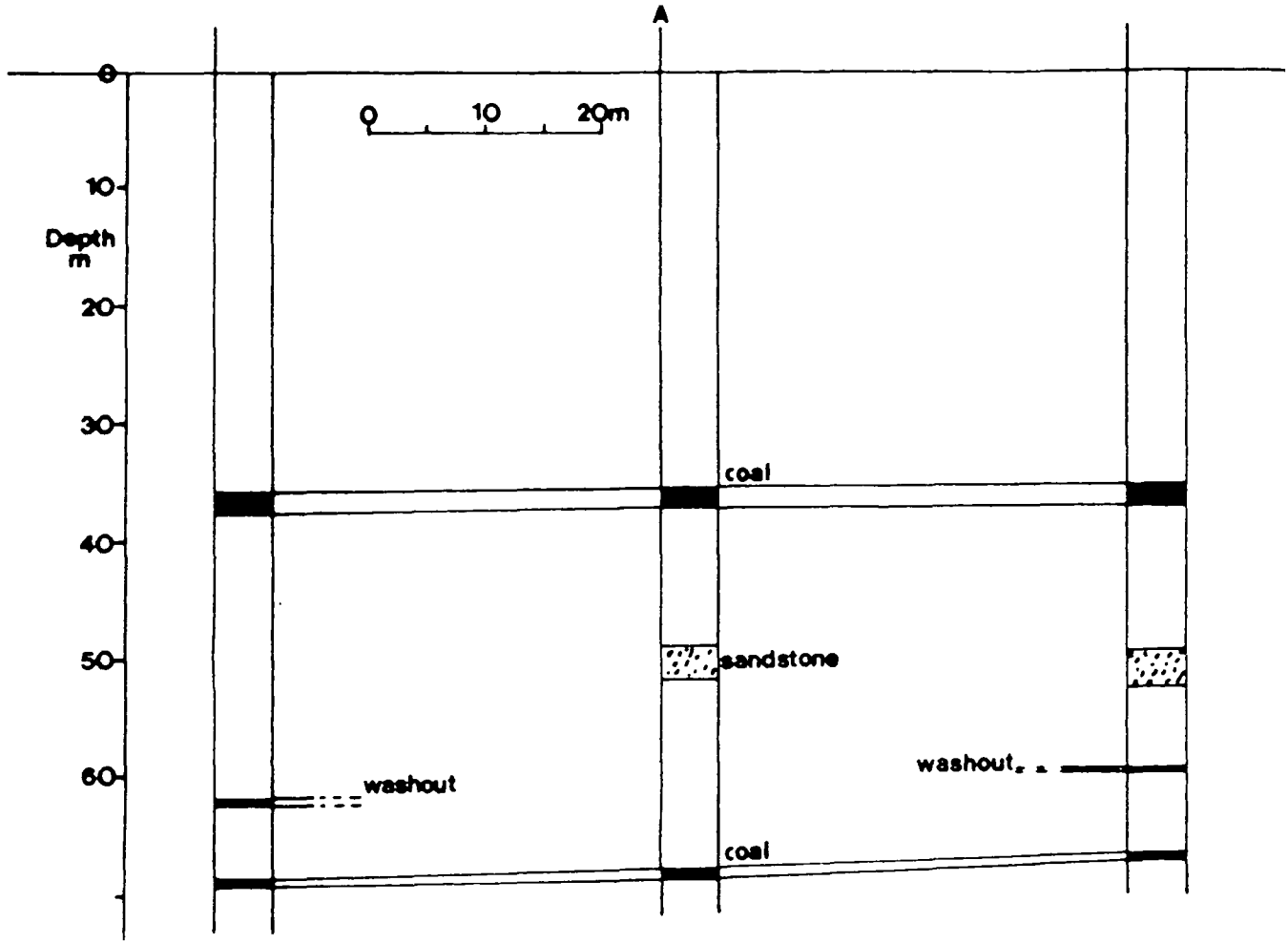

Figure 5.2 Interpreted stratigraphic logs for borehole A and the two neighbouring boreholes at Lowther South.

The beds in the rest of the sequence are logged as undifferentiated sandstone and mudstone.

Figure 5.3 shows the depth section resulting from this survey. A simplified borehole log is shown to the right of the section. The section is true-scale and is plotted with normal polarity (a compression is plotted as a white trough). The section is zero-phase and an automatic gain control (AGC) of length 30m has been applied to balance up the amplitudes throughout the section. The trace spacing is 2m.

Two strong reflections are seen, at depths corresponding to the two coal seams. The shallow reflector at 37m depth is expected to show a flat and continuous reflection. The small discontinuity just to left of the borehole could not be removed by careful reprocessing and is not explained as a geological feature. This is possibly caused by small static errors on the geophones, and is discussed further in section 5.3. The deeper reflector appears faulted upwards towards the left of the section. This apparent fault is interpreted as the edge of the washout, as indicated by the borehole logs. The disruption in the reflection from the lower seam is thought to be an interference effect caused by the overlapping reflections from the two seams, which are 6m or less apart in depth. The other edge of the washout, to the right of borehole A, is not apparent on the section, and must lie further to the right than the 18m of lateral coverage obtained at this depth.

There are no other strong coherent events on the section, though a weak reflection at 80m depth is seen. This reflection cannot be tied to the stratigraphy as the borehole logs stop at 70m depth. The energy at the very top and bottom of the section is migration noise which has been amplified by the AGC.

This survey has demonstrated that high resolution data may be obtained from Coal Measures strata with strong reflections originating from very thin coal seams. Wavelengths of the coal seam reflections are approximately 6m on the final sections, and the lateral resolution appears to be about one trace spacing, or 2m. This is very encouraging for the detection of small faults where they cut coal seams, with throws too small to be evident from borehole log information.

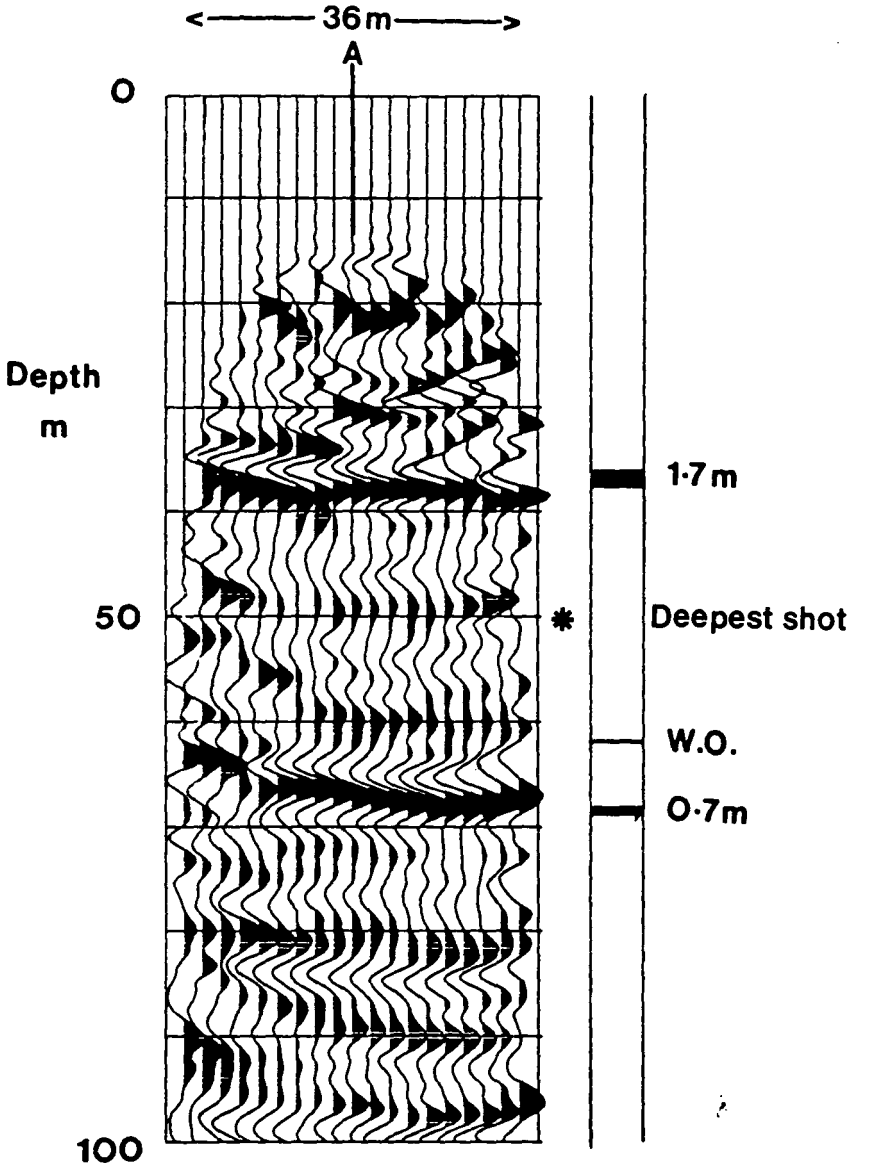

Figure 5.3 Depth section resulting from processing the hole-to-surface survey in borehole A. The section is zero-phase and an automatic gain control of length 30m has been applied. The trace spacing is 2m.

5.2.2 Surveys B,C and D; small fault adjacent to major fault zone

Figure 5.4 shows the shot and receiver positions for the surveys shot in the three collinear boreholes B,C and D. Subsurface coverage has been calculated assuming a constant velocity field. Surveys B and C share the same geophone positions and have some common subsurface coverage. Stacking the overlapping data will increase the fold of coverage and hence reduce any edge effects. The water table was again at 10m depth and the boreholes were blocked at approximately 50m, which corresponds to the depth of a worked seam. Figure 5.5 is a cross section showing the interpreted stratigraphic logs for the three boreholes. The main features of interest are the worked Barnsley Top Softs Seam at 50m depth, and the presence of a fault intersecting borehole B between 70m and 80m depth, which is readily inferred from the seam levels. This fault appears not to cut the sandstone unit at 70m depth, and hence it probably cuts the underlying 70cm Dunsil Seam close to borehole B. The 1.6m coal seam with its base at 21m is the Kents Thick Seam.

Figure 5.6 shows the resulting depth sections from boreholes B,C and D. The sections are true scale and are zero-phase. An AGC of 30m length has been applied and the lateral trace spacing is 2m. Final velocity models for all three surveys were similar and one single velocity field was used to migrate all three surveys (figure 5.7).

Since these surveys are collinear and there is common subsurface coverage, they may be combined to give a single section. The combined depth section is shown in figure 5.7. An AGC of 30m length has again been applied to the data. This is applied after the combined stacking of the individual migrated shot records. The velocity field used to migrate the data is shown to the right of the section.

The shallow seam at 21m depth is expected to be flat and continuous. The seam shows a strong reflection, but there are small discontinuities which are probably due to the low fold of cover in the shallow part of the section. There are only five shots above this seam, and after muting (see section 4.3.17) the fold of coverage is reduced to a maximum of four around the borehole, and less at increasing offset.

The seam at 50m depth has been worked right across the section, though borehole B passed through the edge of a solid pillar of coal. The seam shows a

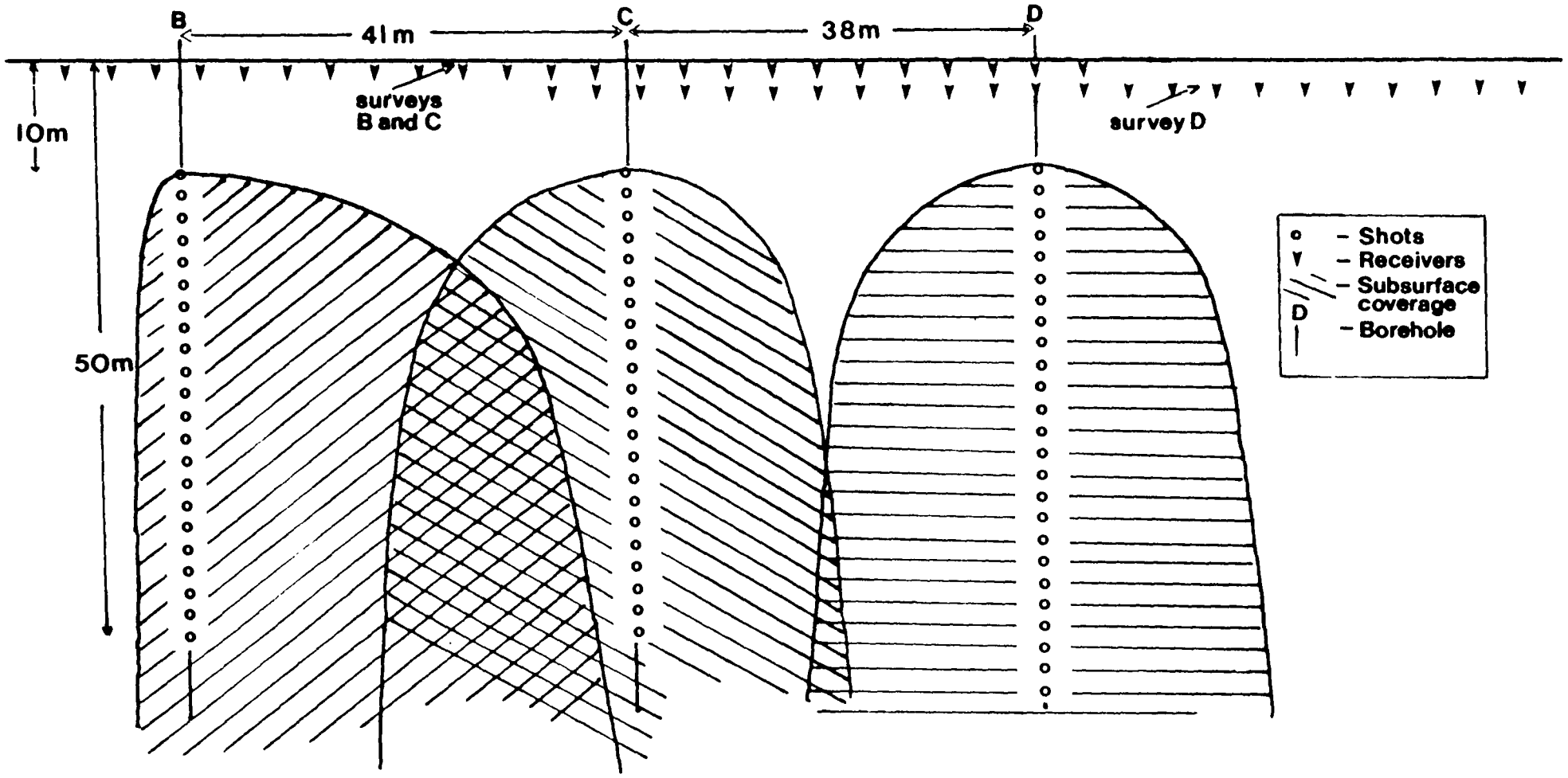

Figure 5.4 Shot and receiver positions for the surveys shot in the three collinear boreholes B, C, and D at Lowther South. The receiver spacing was 4m and the shot spacing 2m. Subsurface coverage has been calculated assuming a constant velocity field.

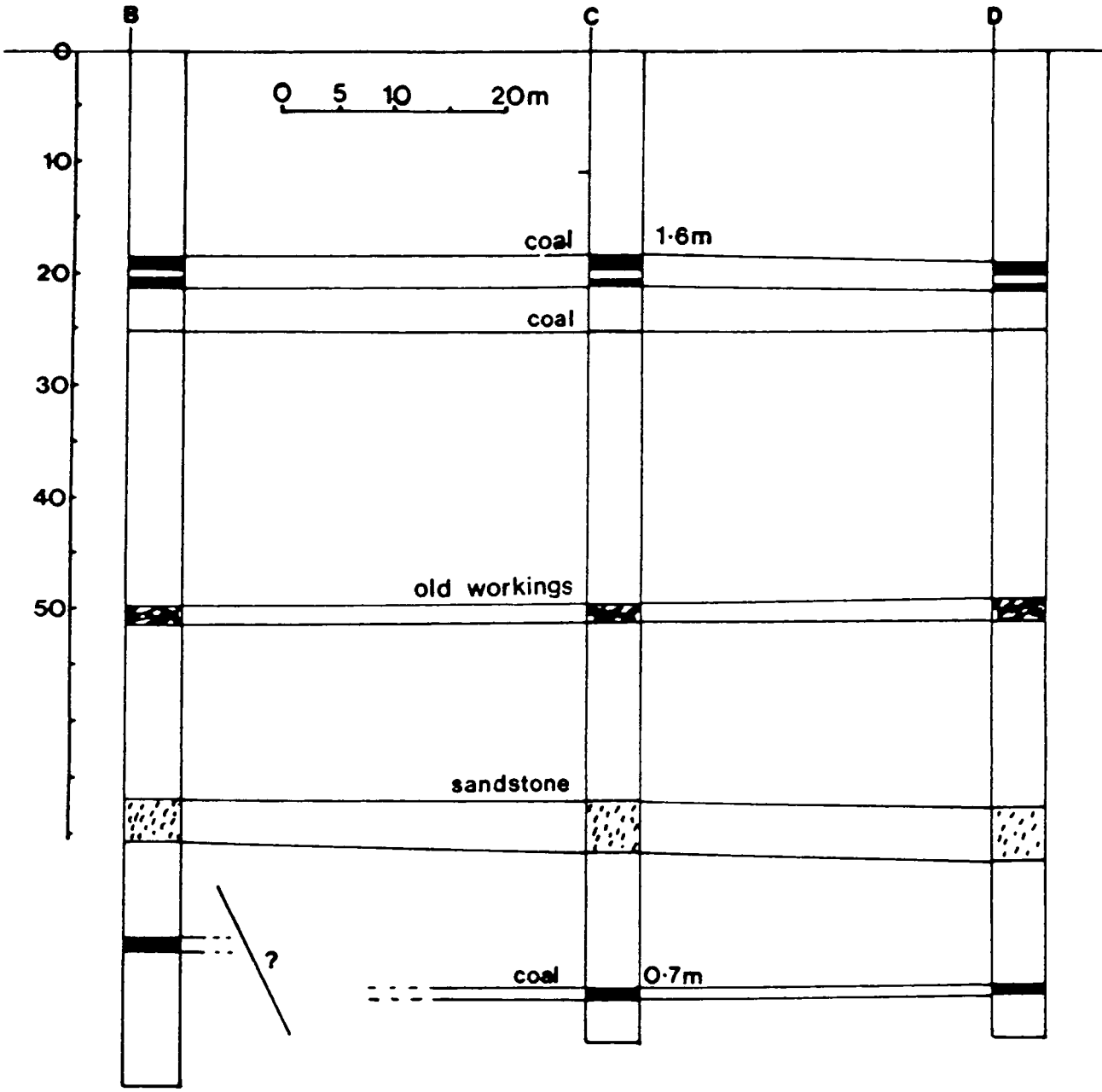

Figure 5.5 Interpreted stratigraphic logs for the three collinear boreholes B, C and D at Lowther South.

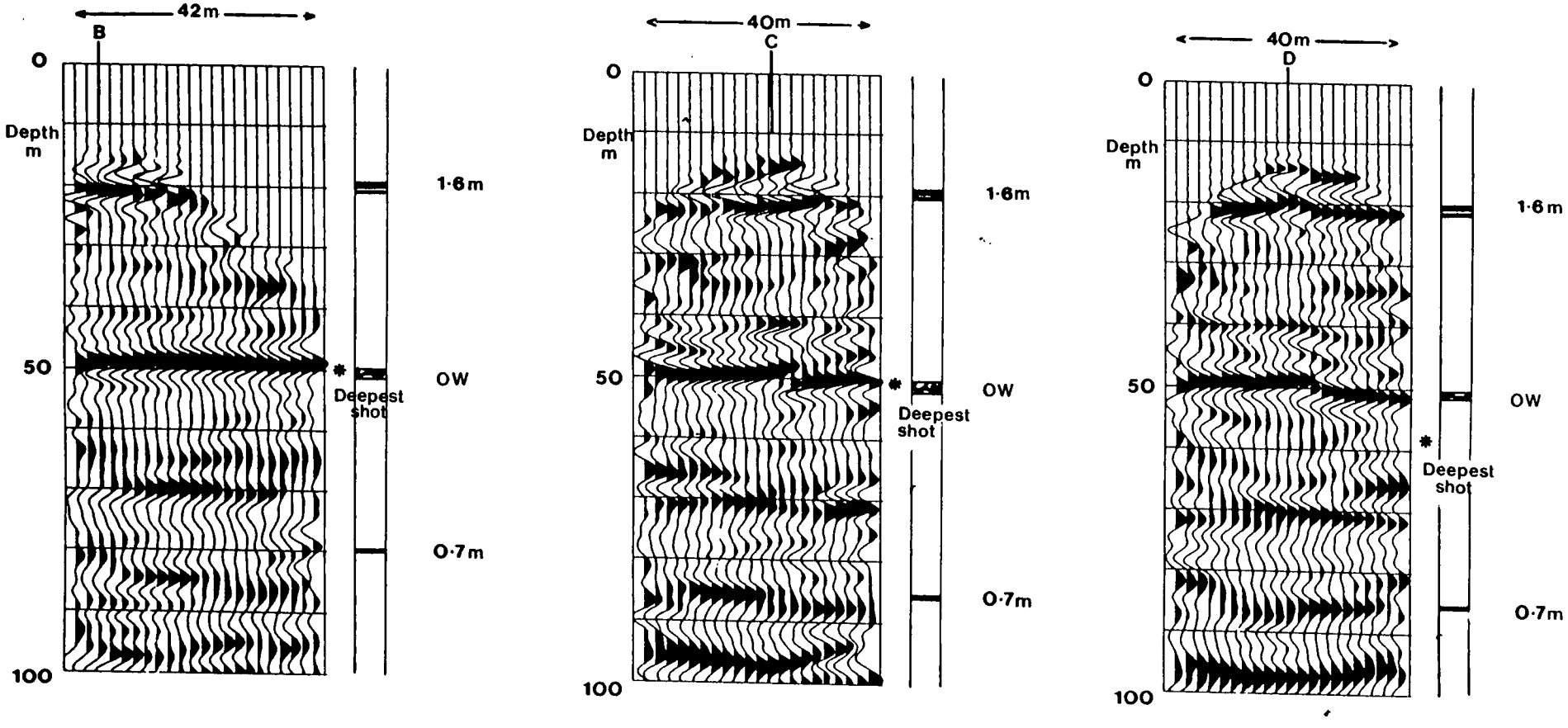

Figure 5.6 Depth sections resulting from processing the hole-to-surface surveys in boreholes B, C and D. The sections are zero-phase and an automatic gain control of length 30m has been applied. The trace spacing is 2m.

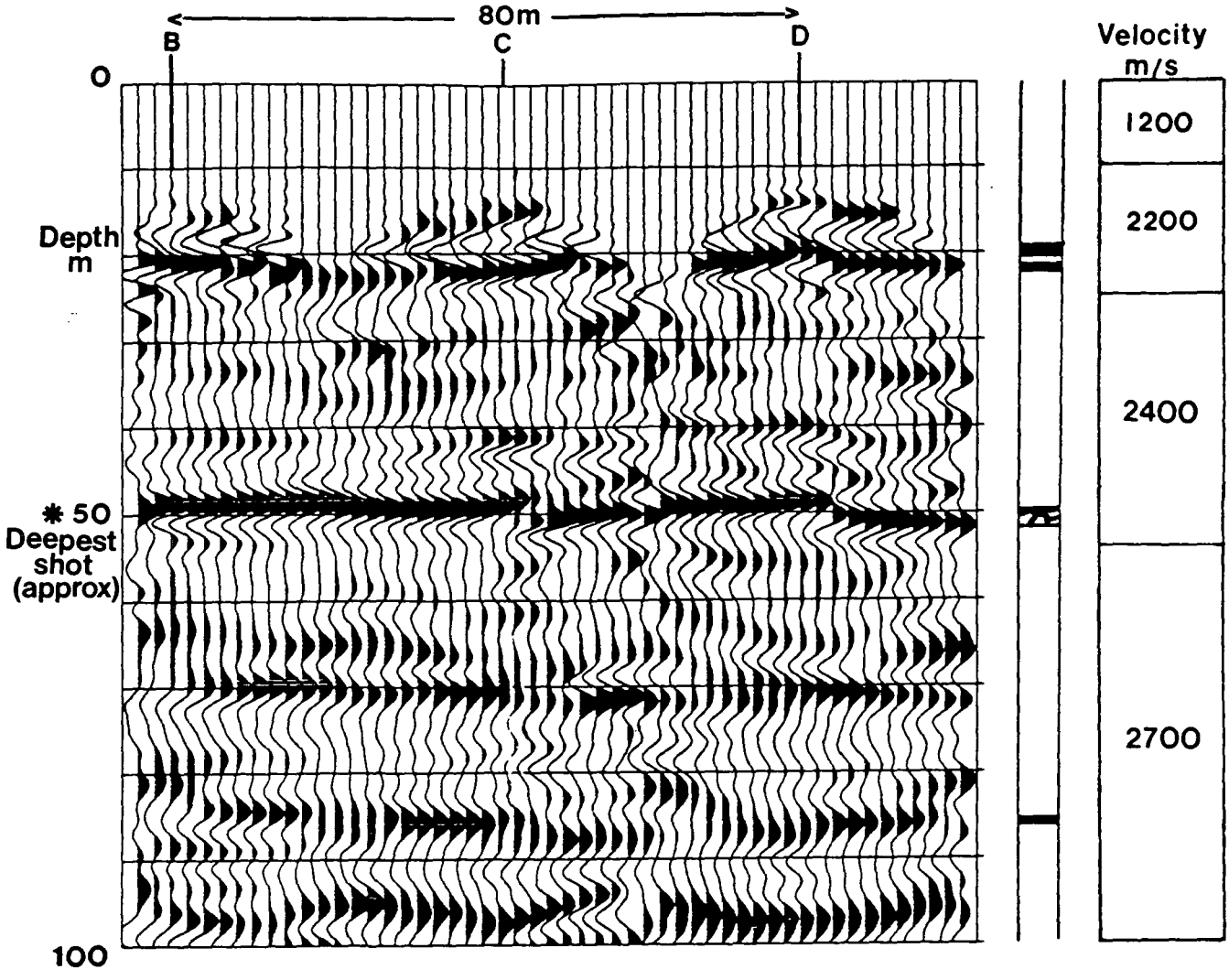

Figure 5.7 Single combined depth section of the hole-to-surface surveys in boreholes B, C and D. The section is zero-phase and an automatic gain control of length 30m has been applied. The trace spacing is 2m. The complete set of shot and receiver positions is shown in figure 5.4.

strong and continuous reflection with no sign of a change in reflection character across the worked seam, and the reflection character is no different to where the seam is solid on survey A (figure 5.3). There are two major disturbances in the reflector. The feature just to the right of borehole D is interpreted as a fault with a vertical throw of about 2m down to the right. Interpretation of the feature just to the right of borehole C is not so clear-cut. There is a net displacement of only about 1m across the disturbed zone and there appears to be a migration smile to the right of the feature which may be a processing artifact. It is possible that such features may be caused by static problems, by anomalous amplitudes in the data, or by velocity reductions in the strata above worked seams, (something which has not been observed by the uphole surveys). Careful reprocessing could not eliminate the feature. It may be structural, sedimentological, or in some way related to the old workings. Neither of these features was suspected, and neither can be confirmed from the existing borehole information.

The slight discontinuity midway between borehole C and D is simply due to where the two surveys meet and do not match exactly. There is little overlap between the two surveys and no geological significance is attributed to this feature. The mismatch may be caused by a lateral velocity change or change in the near-surface, or a combination of these.

There are two weaker deep reflectors seen on the section. The reflection at 70m depth appears to be associated with a sandstone unit. The signal-to-noise ratio is very poor for this reflector, and it does not appear continuous across the whole section. It is notably discontinuous near the edges of the individual surveys. A second, deeper reflector is seen at 85m depth, and is associated with the Dunsil Seam, only 70cm thick. The fault identified from the borehole information cannot be pinpointed on the section due to the low signal-to-noise ratio of the reflector. It appears that there is an energy penetration problem below the worked seam at 50m depth. The uncased boreholes were blocked by the broken ground at this depth and no shots could be fired below the worked seam. The 70cm Dunsil Seam has shown a strong reflection on the test survey A, and was expected to show a similar reflection strength on these data.

5.3 Geophone statics and small faults

Static errors on surface geophones are known to produce apparent faults in seismic data (e.g. Ziolkowski 1979). Static errors are more significant with high frequency data, such as the hole-to-surface data. The method of applying the static corrections is discussed in section 4.3.5.

The fault with 2m throw at 50m depth just to the right of borehole D (figure 5.7) was not suspected and cannot be confirmed by any other data. The seam at 20m depth shows a disruption at the borehole location. This could be interpreted as the the fault cutting this reflector, and the image is poor due to the low fold of coverage. This makes the dip of the fault plane nearly vertical. The fault should then cut the deeper reflectors in the section. This is not seen but may be explained by the poor signal-to-noise ratio and lower frequency of the deeper reflectors. A second possibility might have been that the fault plane has a greater dip, cuts the shallower reflector midway between boreholes C and D, and hence is not seen on these data. If this were the case, the fault might be seen at shallow depths on the crosshole seismic reflection survey shot between boreholes C and D (section 6.2); Such a fault was not detected, but it should be noted that such small faults may not cut a great thickness of strata.

To produce an apparent fault with 2m throw requires a static error of 1-2ms (depending on velocity) on a number on consecutive geophones. This can easily be demonstrated. Figure 5.8 shows two migrated shot records from survey B. The shot depth is 18m, an AGC of 30m has been applied, and the data have been muted according to reflection point coverage. The lateral trace spacing is 2m.

The migrated shot record on the left (figure 5.8a) has had static corrections applied as calculated from the migration velocity field. The reflector at 50m appears continuous and is flat to within 1m. The migrated shot on the right (figure 5.8b) has had static errors added before migration. A static error of 2ms (four samples) was applied to the eleven farthest offset geophones (figure 5.4 shows the geophone positions). The reflector at 50m depth now contains a 'fault' with a throw of 3m. There are also strong migration smiles originating from the fault in both directions. The reflector to the left of the 'fault' is disrupted by the migration

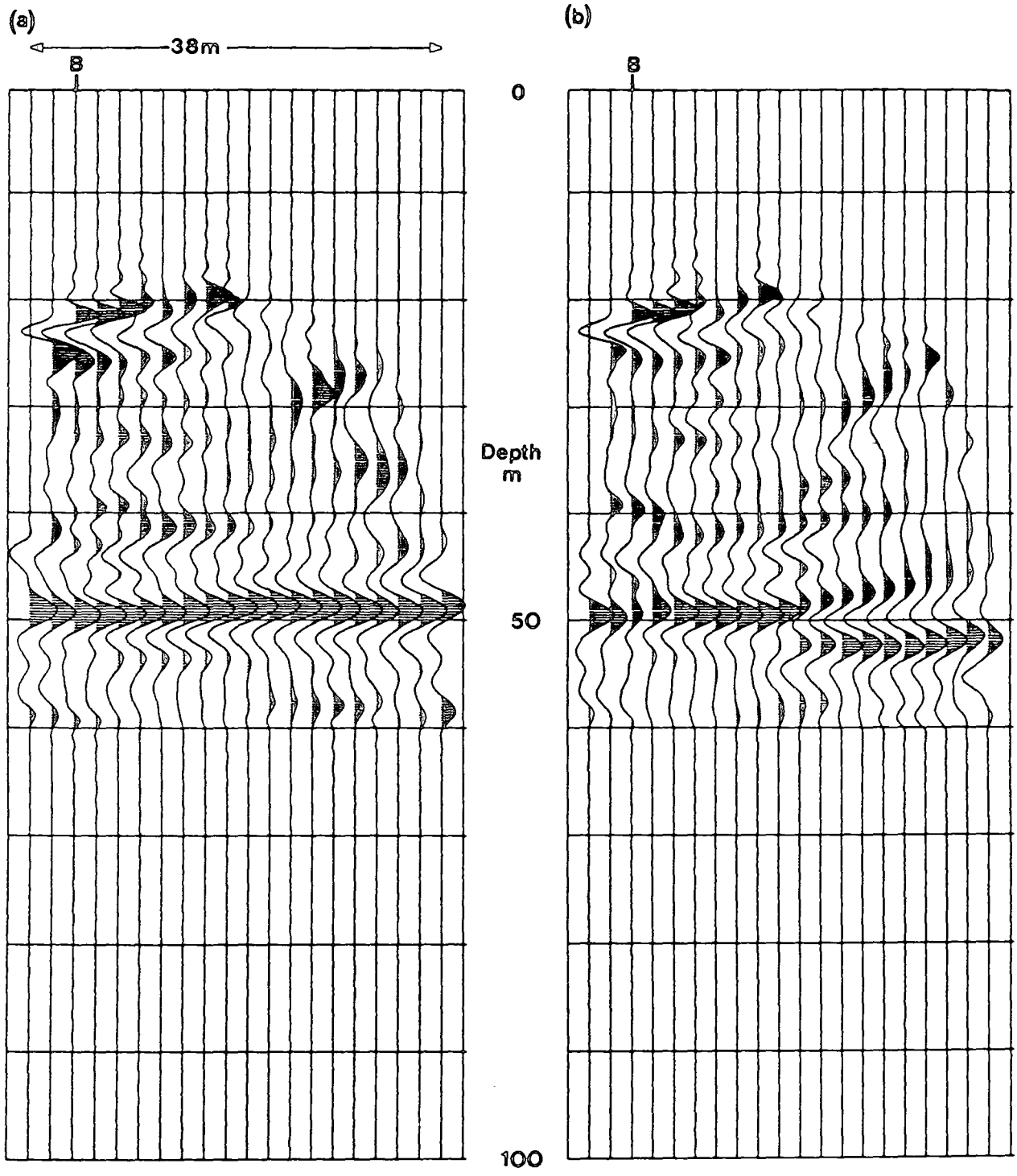

Figure 5.8 Migrated shot record from 18m depth from survey B. (a) Geophone statics calculated using the migration velocity field. (b) A static error of 2ms was applied to the eleven farthest offset geophones before migration.

smile. This synthetic fault does not appear like the 2m fault seen next to borehole D.

The 2ms shift applied to obtain the apparent fault is noticeable on the input data to the migration. This 2ms static error is the size of the largest static errors on these data, and it would difficult to obtain this size of consistent error in computing the geophone statics.

Figure 5.9 shows two more migrations of the same shot record. Display parameters are the same. The section on the left (figure 5.9a) was produced after a 1ms (two sample) static was applied to the eleven farthest offset geophones, and the section on the right (figure 5.9b) was produced after a 0.5ms (one sample) static was applied to the same geophones.

The section on the left again shows an apparent fault, but the migration smiles are less apparent than on figure 5.8b. This now looks very similar to the feature seen just to the right of borehole D. The section on the right does not show any fault, but the reflector is no longer as flat in depth as it was originally, and has a curved appearance.

The synthetic fault in figure 5.9a has one major difference to the feature seen just to the right of borehole D. It is only one single migrated shot, and not a stack of many shots. Static errors on geophones will always be associated with the same input traces which will have given offsets. Even if the the shifts are too small to be seen on the input data (because signal-to-noise ratio is poor), each migrated shot will show the apparent fault at a different offset. A real fault will be seen at different offsets on the input data, but at the same offset on the migrated data. Figure 5.10 illustrates this point. The section on the left (figure 5.10a) shows a second migrated shot record from survey B. The shot depth is 34m, and the strong reflector is imaged to just above 50m depth. The section on the right (figure 5.10b) has had a static error of 1ms (two samples) added to the eleven farthest offset geophones before migration. This is an identical static error to that which produced the apparent fault of figure 5.9a. Again a fault is seen on the reflector but now at an offset of 14m from the borehole, rather than at 20m offset as is in figure 5.9a.

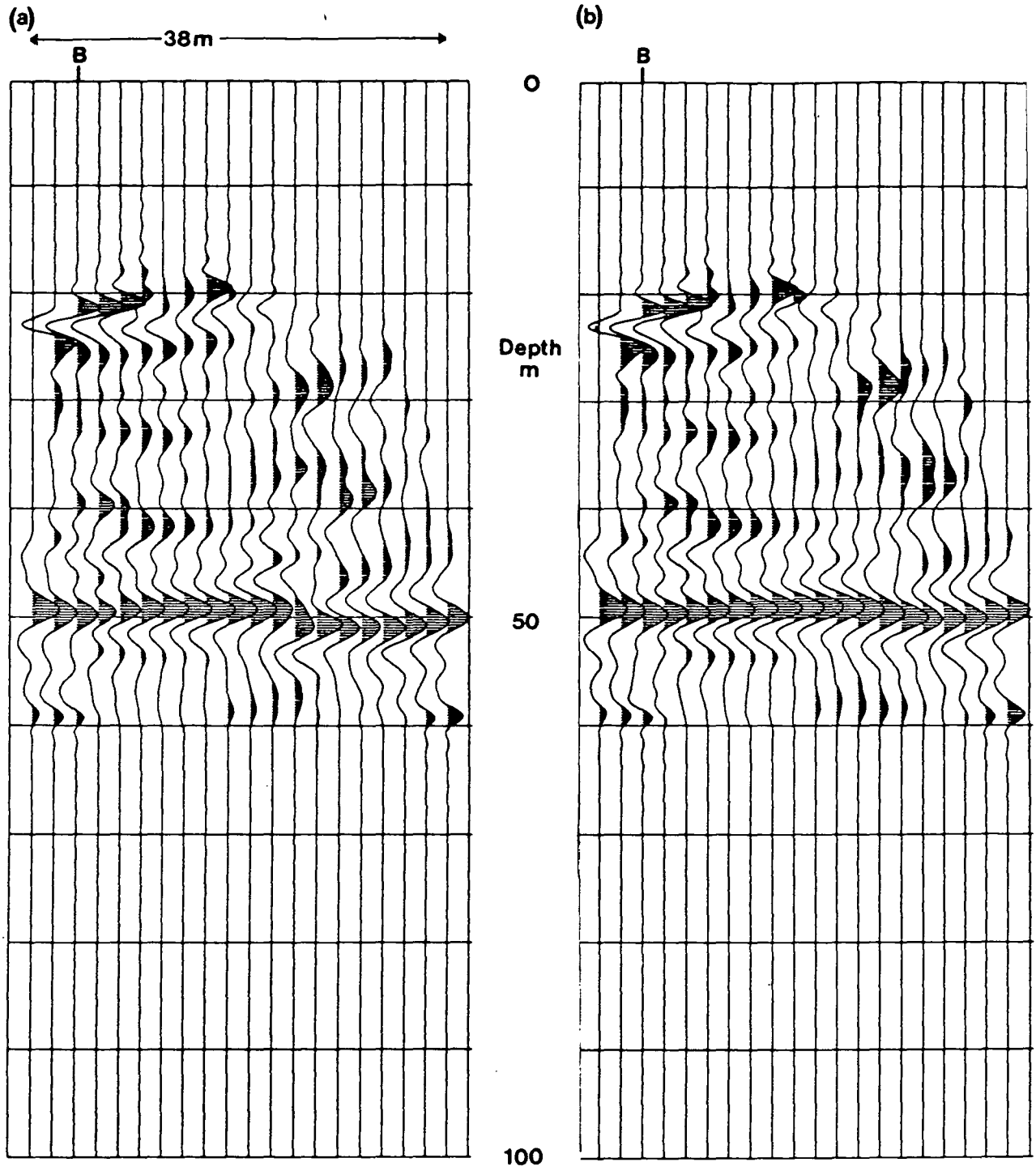

Figure 5.9 Migrated shot record from 18m depth from survey B. (a) A static error of 1ms was applied to the eleven farthest offset geophones before migration. (b) A static error of 0.5ms was applied to the eleven farthest offset geophones before migration.

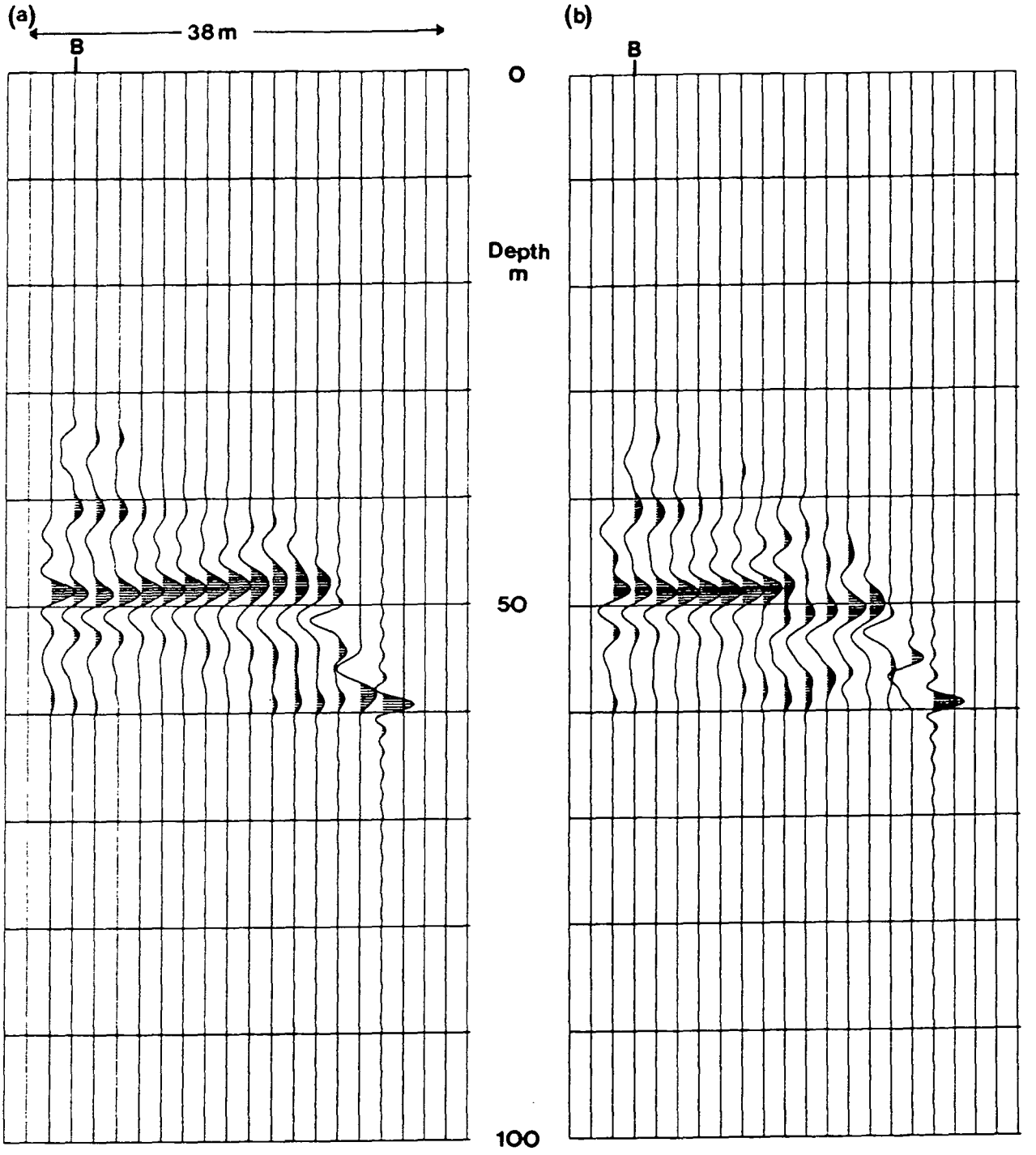

Figure 5.10 Migrated shot record from 34m depth from survey B. (a) Geophone statics calculated using the migration velocity field. (b) A static error of 1ms was applied to the eleven farthest offset geophones before migration.

By looking at the real data before and after migration, it should be now possible to tell if the fault just to the right of borehole D is real.

Figure 5.11 shows three shot records from 18m, 28m and 34m depth, before migration, taken from survey D. The shot records are fully processed with static corrections applied. The coherent energy which appears approximately hyperbolic, and has its peak on trace 12 at 40ms (figure 5.11a), is that which images to the reflector at 50m depth. There is a suggestion of an amplitude loss just to the right of the borehole, and spurious amplitudes are seen on various traces in the shot gather. Figures 5.11b and 3.11c also show some amplitude loss to the right of the borehole location, and no static errors are evident.

Figure 5.12 shows the three shot records of figure 3.11 after migration. Figure 5.12a shows the shot record from 18m depth. The fault is imaged at an offset of 2m from the borehole, although the image is poor. The disruption in the shallower reflector is also apparent. Figure 5.12b shows the shot record from 28m depth. The fault is imaged clearly at an offset of 4m from the borehole. Figure 5.12c shows the shot record from 34m depth, and again the fault is imaged at 4m offset from the borehole.

These observations are not consistent with the synthetic fault where the imaged offset decreases with increasing shot depth, and this suggests the fault to be real.

Static errors of two samples may occur on the data, but are not likely to be consistent across a range of consecutive geophones. Static errors of one sample are caused by first break picking errors and rounding errors. The static corrections are considered to be accurate to the nearest sample for the given velocity model, and table 5.1 shows the static corrections for the three surveys, B, C and D, for the geophones which are common to more than one single survey (figure 5.4 shows the geophone positions for each survey). The static corrections for each geophone location generally agree to within 0.5 ms. The larger errors for geophones 22, 23, and 24 are likely to be caused by the large offsets of the geophones in survey B. The first break amplitudes are lower, making the picks less accurate, and the raypaths less vertical.

Figure 5.13 shows two further migrations of the shot record from 18m depth

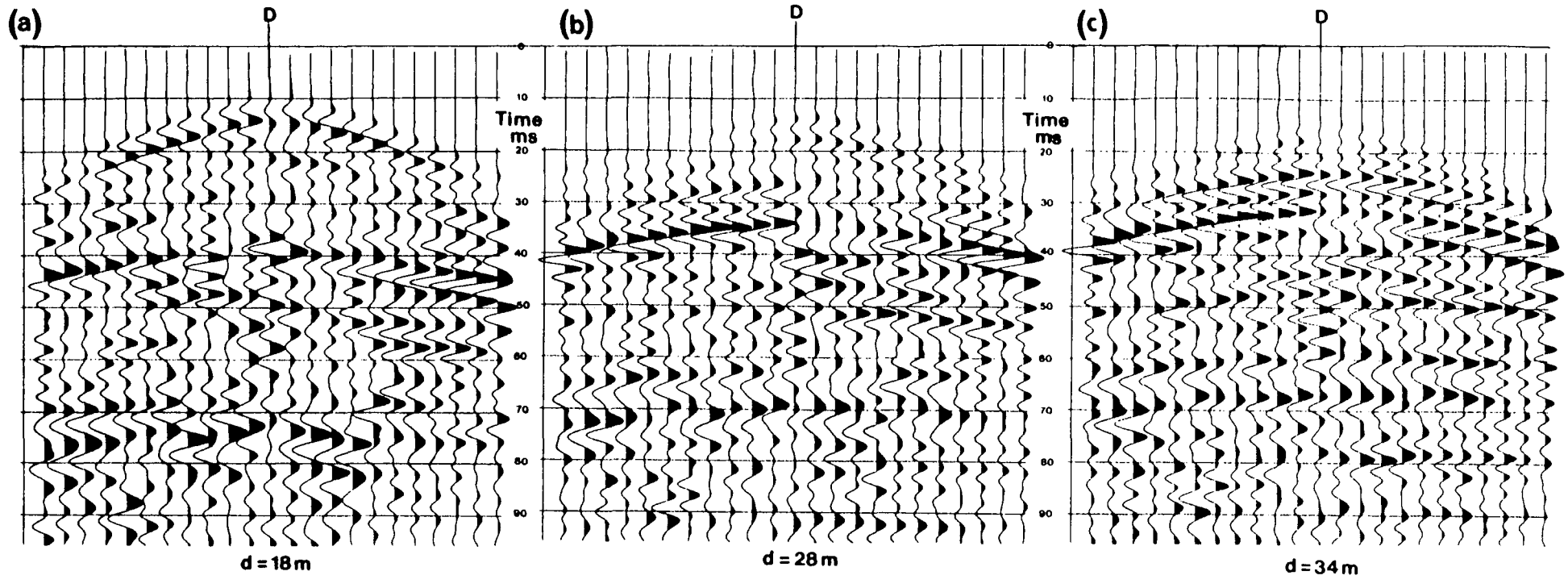

Figure 5.11 Fully processed shot records from survey D before migration. (a) From a shot depth of 18m. (b) From a shot depth of 28m. (c) From a shot depth of 34m.

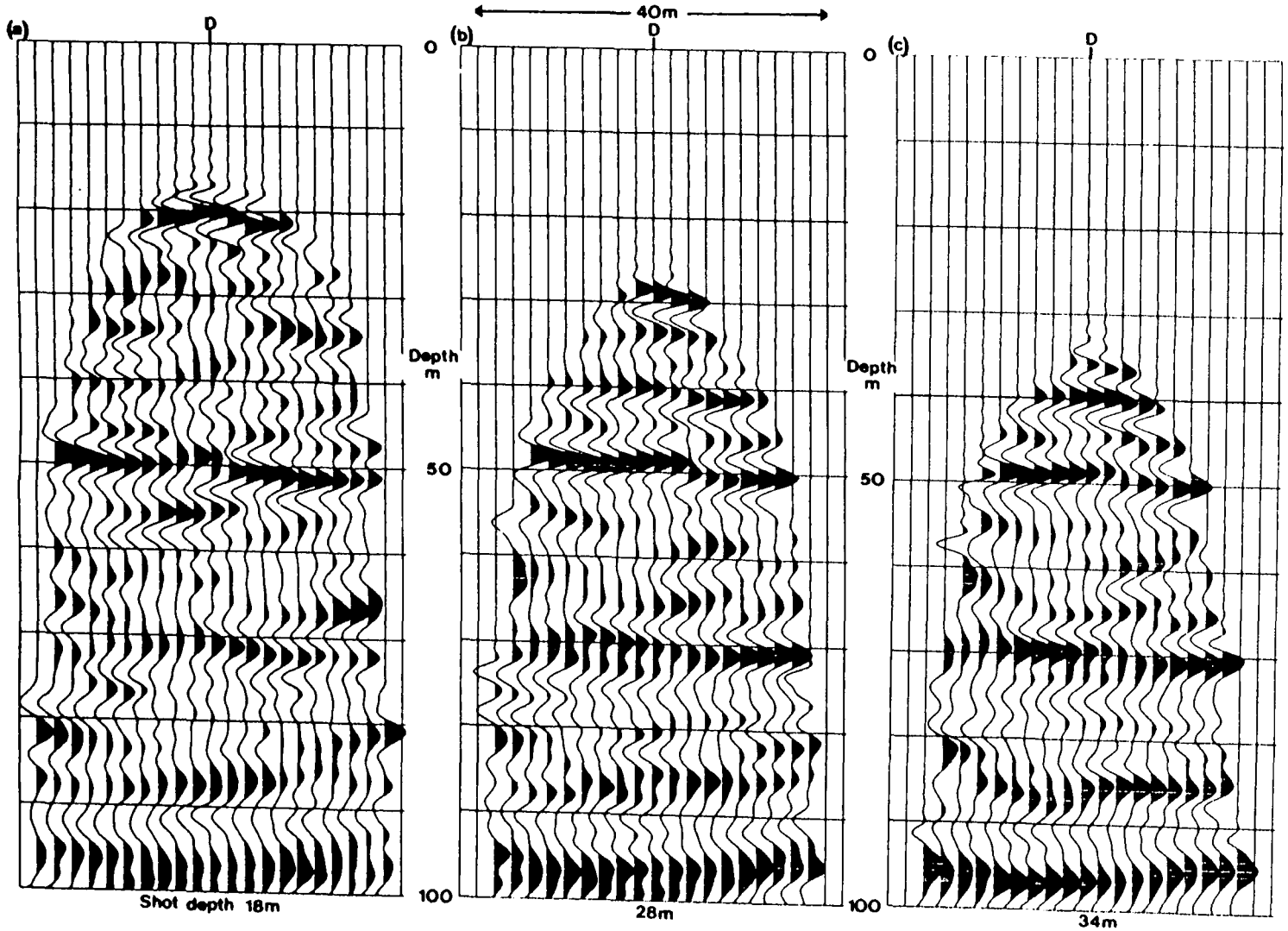

Figure 5.12 Migrated shot records of figure 5.11. (a) From a shot depth of 18m. (b) From a shot depth of 28m. (c) From a shot depth of 34m.

borehole B

Geophone no.	Static ms Survey B	Static ms Survey C	Static ms Survey D
1	0.5	1.0	
2	-0.5	0.0	
3	0.0	0.5	
4	-0.5	0.5	
5	-0.5	0.5	
6	0.0	0.0	
7	-1.0	-0.5	
8	-1.0	-0.5	
9	-0.5	0.0	
10	-0.5	0.5	
11	-1.0	0.0	
12	-1.0	-0.5	-1.0
13	-1.5	-1.5	-1.2
14	-2.0	-2.0	-2.2
15	-1.5	-1.5	-1.0
16	0.5	0.5	0.6
17	0.0	0.5	0.2
18	1.0	0.5	0.4
19	1.0	0.5	0.4
20	0.0	-0.5	0.0
21	0.5	0.0	0.4
22	1.0	-0.5	-0.2
23	0.5	-0.5	-0.2
24	0.5	0.0	-1.0

Table 5.1 Geophone static corrections derived from the surveys in boreholes B, C and D for the geophones which are common to more than one survey.

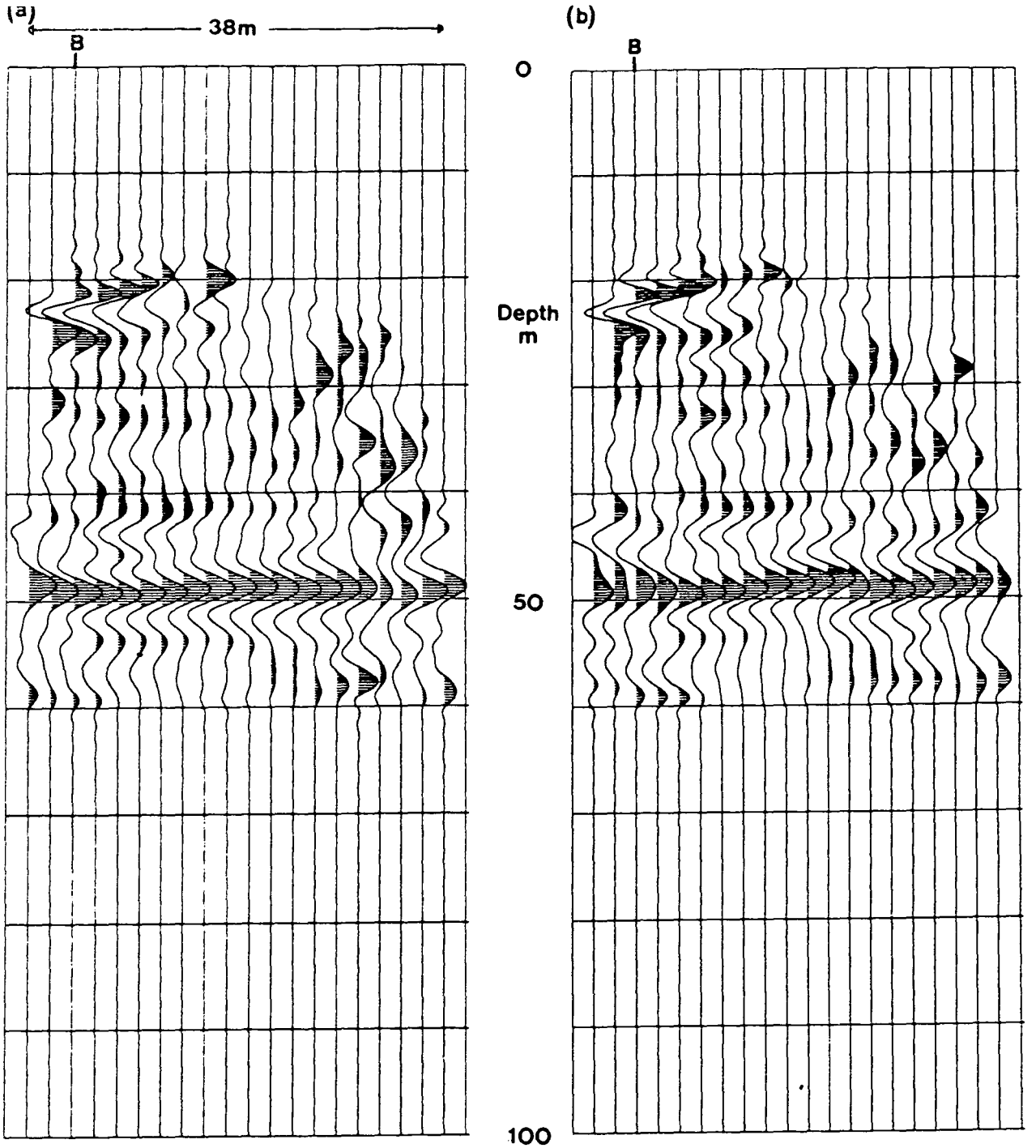

Figure 5.13 Migrated shot record from 18m depth from survey B. (a) A random static of either zero, plus one, or minus one sample (0.5ms) was applied to each geophone before migration. (b) A second set of similar random statics applied before migration.

from survey B. A random static error of either zero, plus one, or minus one sample has been applied to each geophone. These random static errors were generated twice, producing the two sections in figure 5.13. The resulting change in the reflector (compare with figure 5.8a and figure 3.9b) is quite apparent. The reflector shows small changes in depth and in reflection character across the sections, and neither are as flat or continuous as the original section (figure 5.8a). This implies the original statics were correct to an accuracy of less than plus or minus one sample, and also demonstrates the need for accurate static corrections. These random one sample static errors give the reflector a curved appearance, and similar characteristics are seen on the reflectors elsewhere in the data, for example on survey A (figure 5.3) on both the shallow and deeper reflectors, and on the shallow reflector on surveys B,C and D (figure 5.7).

Statics may be applied more accurately by interpolating the data to a finer sample interval. Unfortunately, the error in picking the first breaks, particularly on the deeper shots which are used for the static calculations, does not merit this. Survey D was processed with a sample interval of 0.2 ms.

The fault near borehole D and the disruption near borehole C will only be confirmed when the site is finally excavated, unless it is felt worthwhile to drill further boreholes simply to test the validity of the seismic results.

5.4 Lostrigg, Cumbria

5.4.1 Introduction

Four hole-to-surface surveys were acquired from Lostrigg in Cumbria. These four surveys were acquired from a line of fourteen boreholes drilled at 15m separation. The boreholes were drilled to define the structure at a major fault, the Close End Fault, which will be a site boundary. Twelve such lines of boreholes were planned for this fault alone.

The boreholes for the hole-to-surface surveys were chosen so as to provide as near-continuous subsurface coverage as possible. The fourteen collinear boreholes have been labelled A through to N, and the four surveys were acquired in boreholes B, F, H and N.

5.4.2 Surveys B, F, H and N; section across site boundary fault

Figure 5.14 shows the shot and receiver positions for the four collinear surveys B, F, H and N. Only the shallowest and deepest shots are shown for the sake of clarity. The shot spacing was 2m, and subsurface coverage was calculated assuming a constant velocity field. The water table was at 12m depth, and the boreholes were blocked below 80m. Borehole logs were run in all of the fourteen holes, and an interpreted cross-section of the line using the borehole information is shown in figure 5.15. The coal seams are labelled on the cross-section.

The major feature on the cross-section is the large fault which surfaces between boreholes K and L, and cuts borehole H at 72m depth. This fault has a throw of 220m downwards to the left of the section. A small fault with 3m throw has been interpreted below the Harrington Seam, cutting the Udale Seam near borehole H at 90m depth.

On the left of the section at 50-70m depth, there appears to have been much channel activity during deposition. The Brassey Seam, and the two thin seams at 50m depth are completely washed out in places. The interpretation of the White Metal Seam in borehole G at 100m depth gives an unusual feature, and this is apparently evident in other parts of the site (G. Jackson pers. comm). On the right of the major fault the sedimentary sequence is simply layered, with numerous thin coal seams evident above the Harrington Seam.

Figure 5.16 shows the depth section resulting from surveys B, F, H and N. The section is true-scale and normal polarity. It is zero-phase and has had an AGC of length 50m applied. The overlay shows the coal seam details of figure 5.15.

A strong correlation of reflected energy and coal seams is seen. The large fault is clearly imaged on survey H, where both the Harrington Seam (at 74m depth to the right of the fault), and the two thinner seams (at 63m and 70m depth to the left of the fault), all truncate sharply. The fault can be positioned to an accuracy of $\pm$ 2m laterally at this depth. Shallower in the section the fault is not imaged due to the lack of strong reflectors in the section. Deeper in the section, the Black Metal Seam, at 80m depth, clearly truncates to the left of the fault, as does the White Metal Seam, at 100m depth. The splitting of the White Metal Seam inferred from

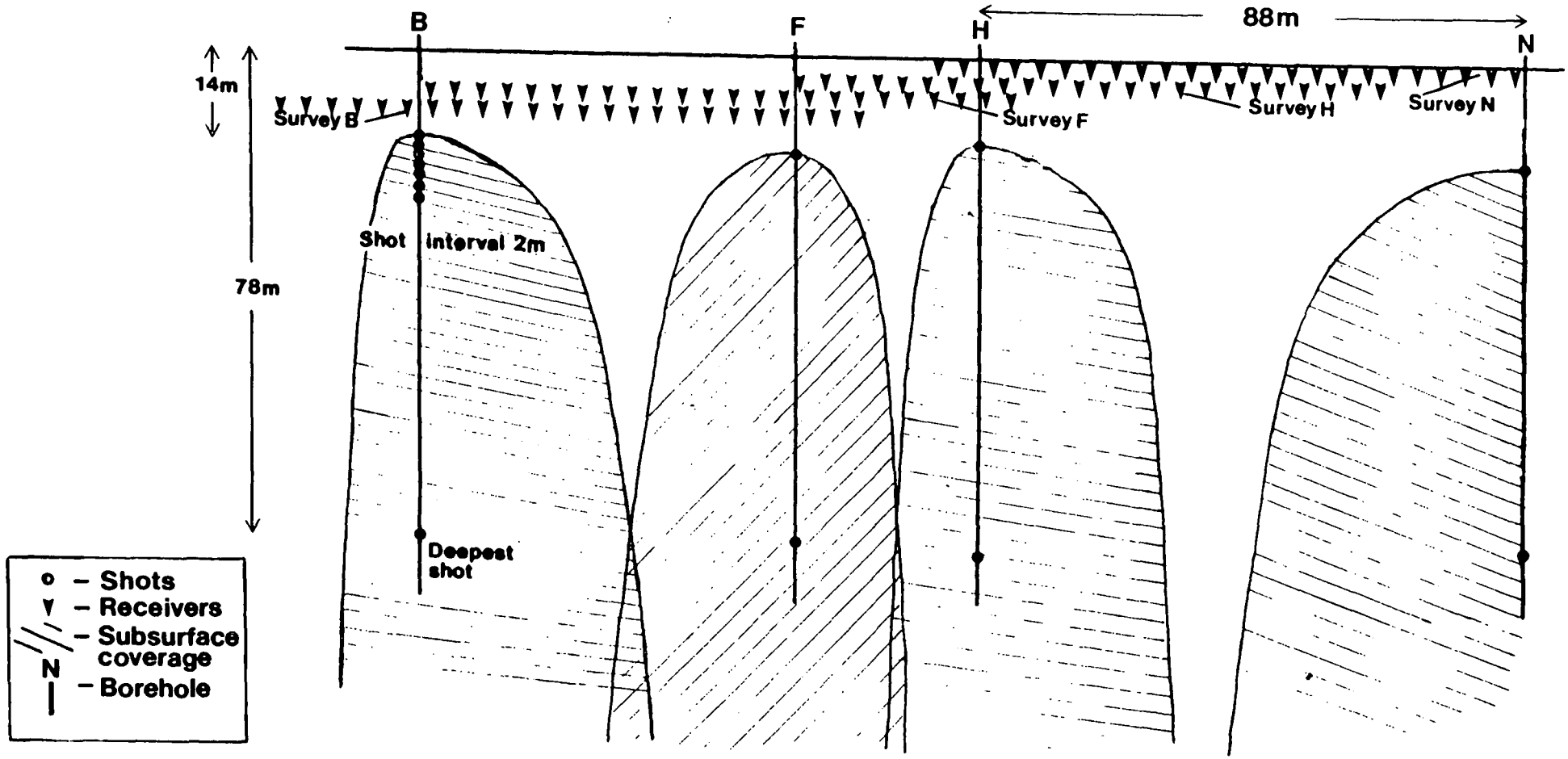

Figure 5.14 Shot and receiver positions for the hole-to-surface surveys shot in the four collinear boreholes B, F, H and N at Lostrigg. The receiver spacing was 4m and the shot spacing 2m. Only the deepest and shallowest shot positions are shown for clarity. Subsurface coverage has been calculated assuming a constant velocity field.

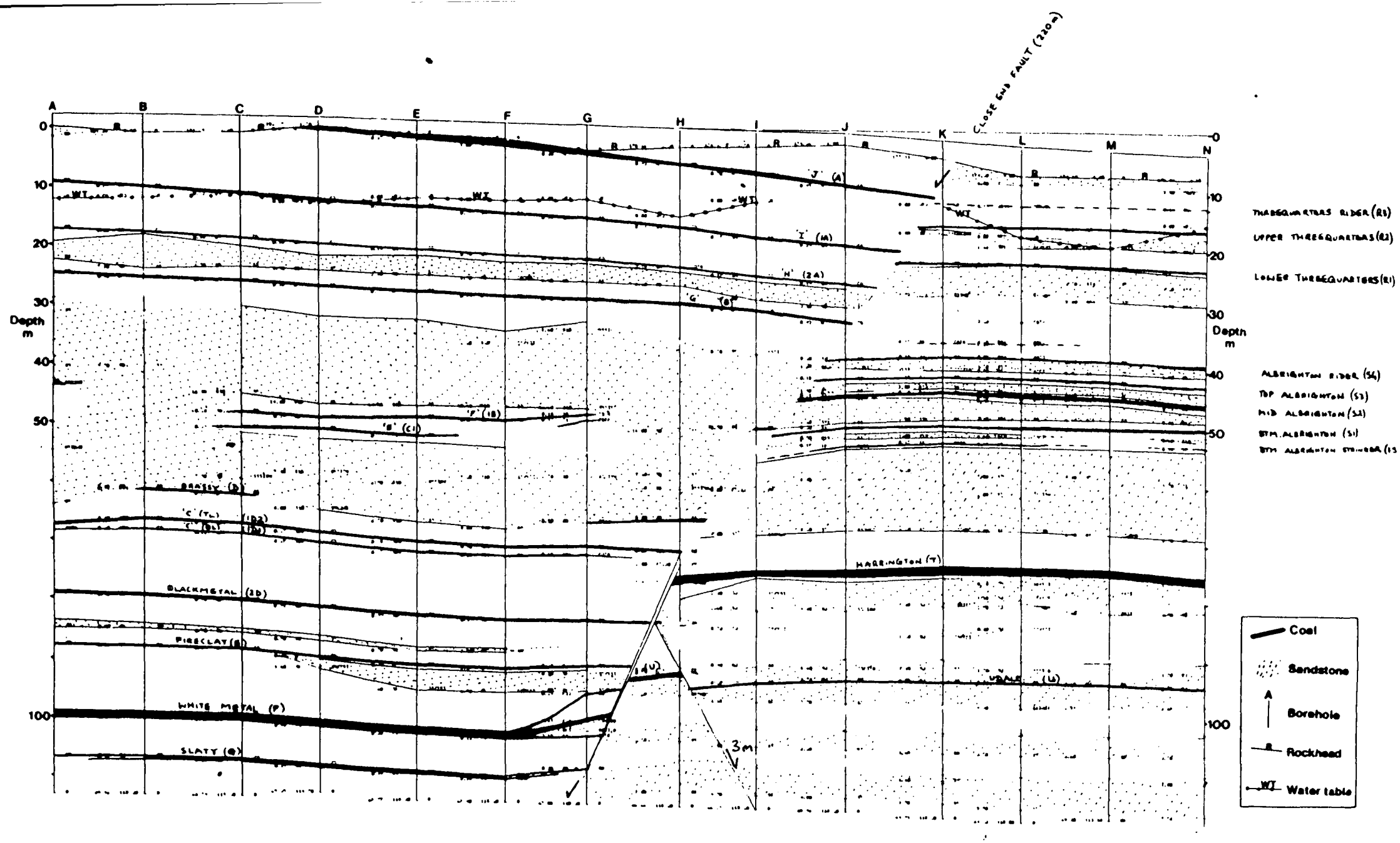

Figure 5.15 Interpreted cross-section (courtesy G. Jackson, British Coal) using the borehole information in all fourteen boreholes A through to N at Lostrigg.

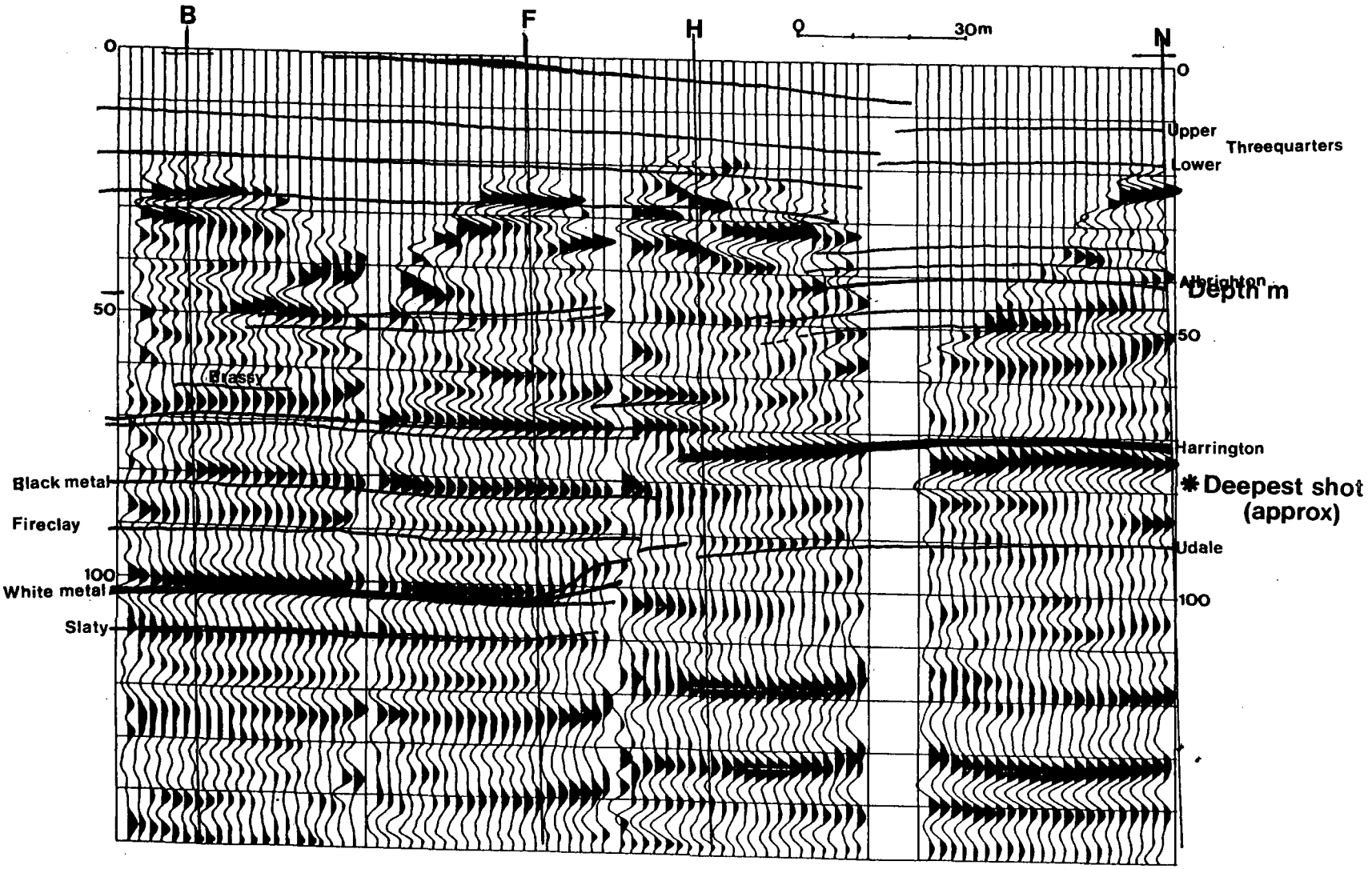

Figure 5.16 Depth section resulting from processing the hole-to-surface surveys in the four collinear boreholes B, F, H and N. The section is zero-phase and an automatic gain control of length 50m has been applied. The trace spacing is 2m. The overlay shows the coal seam details from figure 5.15. The complete set of shot and receiver positions is shown in figure 5.14

the borehole data (where it is truncated by the fault) clearly affects the hole-to-surface data, but it is not possible to interpret details of the splitting from the seismic section. Below 110m the fault is not clearly imaged. Unfortunately the interpreted position of the fault is close to the right edge of survey F at 80-100m depth.

There is no evidence of the 3m fault (interpreted to the right of the main fault and below the Harrington Seam) near borehole H. This is not helped by the virtual absence of a reflection from the Udale Seam at 91m depth on surveys H or N.

There are two strong deep reflections seen on surveys H and N which cannot be tied to the stratigraphy because they are located below borehole depths. These reflectors do not extend to the edge of survey F where they are expected to truncate against the fault. Both events are strong reflections on the input data and do not appear to be multiple energy.

The shallow seam at 28m depth in borehole H, which is continuous in all the boreholes to the left of the fault, gives a strong reflection on all three surveys B, F and H. There is no borehole evidence for the disruption of this reflector seen on survey H in the vicinity of the borehole. The thin Lower Threequarters Seam, at 22m depth to the right of the fault, shows as a strong reflection on survey N.

The two thin seams at 50m depth to the left of the fault, which are completely washed out in places, are poorly imaged. Survey B shows a strong reflection and has imaged the washout on the left edge of these two seams, though this reflection is not seen on survey F. This is difficult to explain, but is possibly due to the lower seam being washed out further to the left than is interpreted. The two seams together may be needed to give the reflection seen on survey B. There is no evidence of the Brassey Seam at 60m depth in borehole B, though this seam has been imaged near borehole F where it truncates against the fault, with the hole-to-surface data indicating the edge of the washout to be closer to borehole F than the interpreted section suggests.

The numerous thin seams, at 40-60m depth above the Harrington Seam and to the right of the fault, are poorly imaged on survey N. This is possibly due to interference effects destroying any one clear reflection.

The curved appearance of the Harrington Seam on survey N may be due to static errors on the surface geophones (see section 5.3). Geophone offsets for this survey were particularly large (up to 94m), making the static corrections less accurate.

The migration velocity fields for the four surveys are shown in figure 5.17. The uphole shots showed a fairly constant velocity of 3000m/s below about 30m. It was necessary to reduce the shallow velocities on survey B to produce a good stack of the data, and the shallow velocities on survey N, to the right of the fault, needed to be increased. These velocity field changes were confirmed by the match between the predicted and observed first arrival times.

5.5 Borehole deviation

Measurement of borehole deviation enables an accurate description of the downhole source position which is necessary for the migration of the data. Deviation measurements in the boreholes at Lowther South were carried out as described in section 2.2.1. At Lostrigg, deviation measurements were provided by British Coal and were carried out by the site logging contractor.

Borehole deviations in the plane of the surveys were small for all boreholes, and the deviations were not sufficient to cause noticeable degradation of the migrated data. The deviation was included for completeness. Borehole deviations giving rise to lateral errors of 2m in the plane of the survey and/or vertical errors of 50cm are necessary before a noticeable degradation occurs in data quality.

Figure 5.18 shows borehole track plots for the four boreholes B, F, H and N at Lostrigg. The scale bars and circles represent lateral deviation, and the tick marks on the track plots mark every 20m of logged depth.

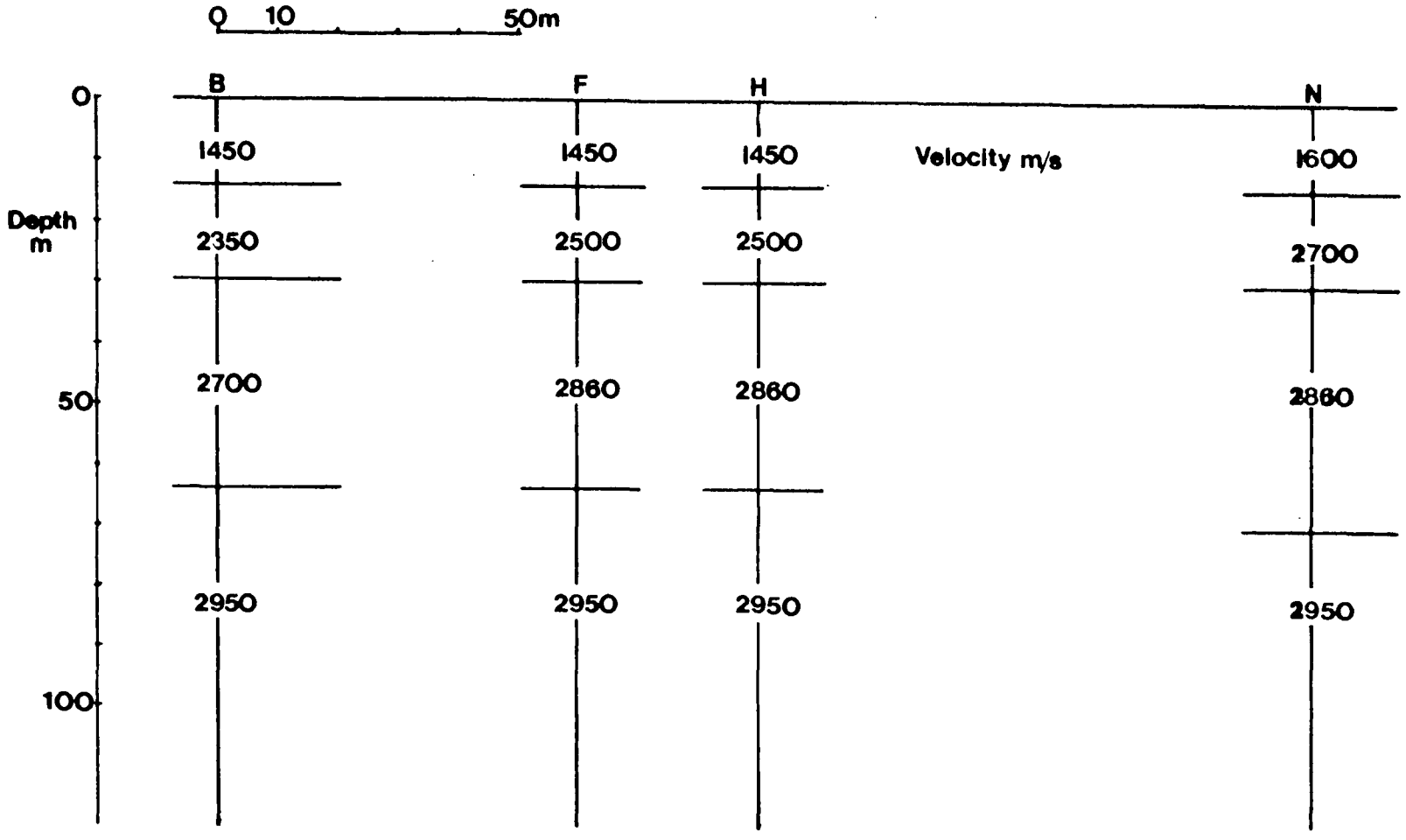

Figure 5.17 Migration velocity fields for the four collinear surveys B, F, H and N at Lostrigg.

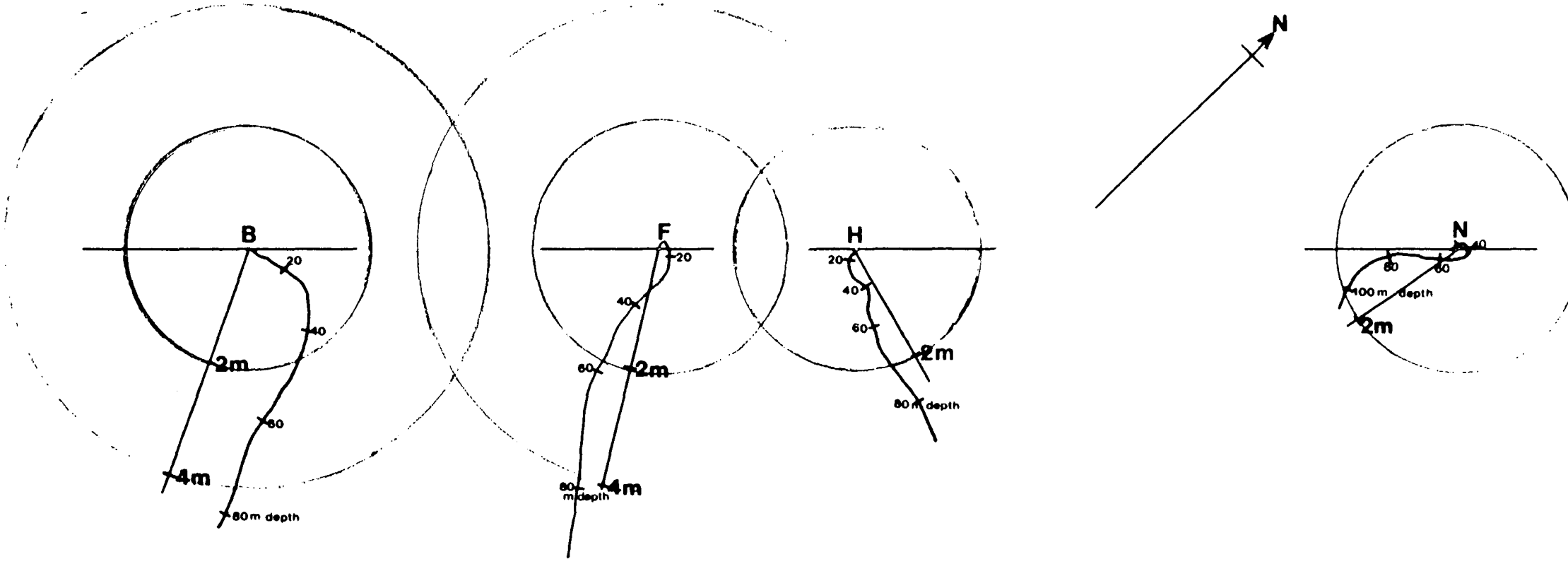

Figure 5.18 Borehole deviation tracks for the boreholes B, F, H and N at Lostrigg. The scale bars and circles represent lateral deviation and the tick marks on the track plots mark every 20m of logged depth. The borehole separations and track plots have been plotted to different scales.

Chapter VI

Comparison of hole-to-surface and crosshole methods

6.1 The crosshole seismic reflection method

The crosshole seismic reflection method uses both downhole sources and receivers. It shares the same field geometry as the tomographic method which is discussed in chapter 2. Processing of the data is similar to that of the hole-to-surface method, but there are some important differences.

o Near-surface effects are eliminated, and the data have greater bandwidth, typically twice that of hole-to-surface data.

o Separation of the upward travelling and downward travelling wavefields is more complex, since the direct wave crosses the receiver array in both directions.

o The data can be imaged using the VSP-CDP transform or by migration methods, but, due to the shallower angle of the raypaths, the velocity field must be known more accurately and anisotropy is more significant.

o Sources and receivers are placed both above and below reflectors, and hence both downward travelling and upward travelling reflections can be imaged.

o Since two boreholes are used, and the data have greater bandwidth, borehole deviation must be known more accurately.

o The final image is confined to a plane between the two boreholes, assuming moderate dips.

Findlay (1990) developed the processing software for the crosshole reflection data and gives a detailed discussion of the method.

Figure 6.1 shows the reflection point loci for upward travelling primary reflections in a common shot gather, for a crosshole survey. Figure 6.2 shows the zones

of coverage from processing a crosshole survey (both upward travelling and downward travelling wavefields) and from a hole-to-surface survey using one of the two boreholes. There is some overlap, but it is interesting to note that the coverage is complementary with the hole-to-surface survey giving coverage directly below the bottom of the borehole.

6.1.1 An example crosshole survey

The crosshole dataset discussed in chapter 3 was processed by Findlay (1990) using the crosshole reflection method. The final stacked section is shown in figure 6.3a, and the result of tomographic processing of the first breaks is shown in figure 6.3b. The section in figure 6.3a has had an A.G.C. of length 30m applied, but no deconvolution has been applied to the data. The section shows strong reflections from two coal seams at 42m and 57m depth (figure 3.1 shows details from the stratigraphic logs for these boreholes) and weaker reflections from the worked seam at 67m depth and from the seams below this. Wavelengths in the section are 3-4m (approximately half those of hole-to-surface data), with the peak of the energy in the frequency range 400-500Hz. The reflector coverage narrows below the deepest shot and receiver, and no coverage is obtained above about 40m depth since only the upward travelling reflected energy has been processed. The section shows far greater resolution than the tomographic processing of the first breaks (figure 6.3b). However, the velocity information obtained from the tomographic processing is useful for the migration of the data.

6.2 Boreholes B, C and D, Lowther South

Two crosshole datasets were acquired at Lowther South, between boreholes B and C, and boreholes C and D. These were processed by Findlay (1990).

Figure 6.4a shows the resulting depth section from these two surveys, and the comparison hole-to-surface section from figure 5.7 is shown in figure 6.4b. The section in figure 6.4a is migrated, and has had an AGC of length 25m applied (the AGC on the hole-to-surface section is of length 30m).

The vertical resolution on the crosshole section (figure 6.4a) is nearly twice that of the hole-to-surface section. The reflection at 10m depth is from the water table,

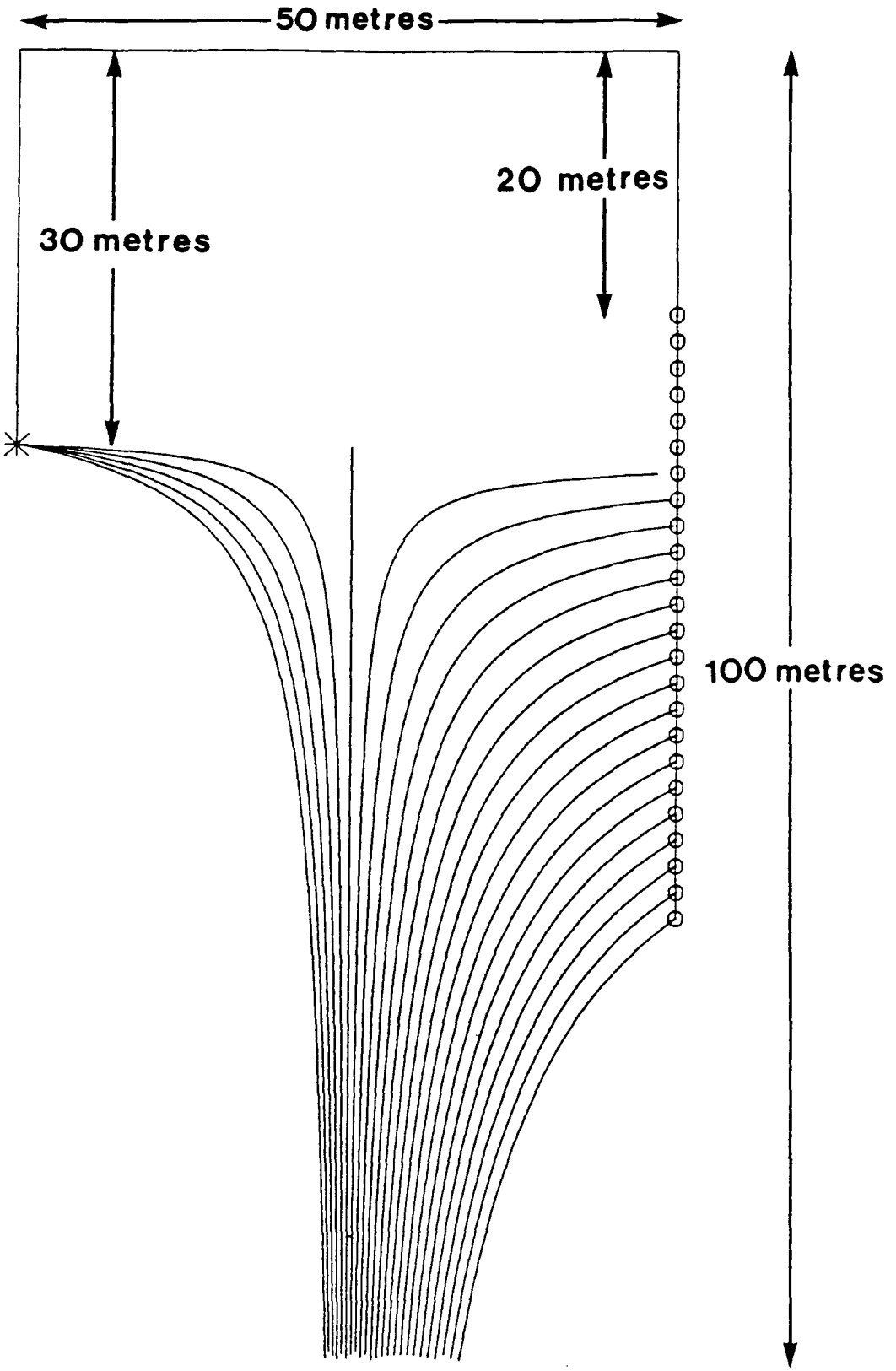

Figure 6.1 Reflection point loci for upgoing primary reflections in a common-shot gather for a crosshole survey.

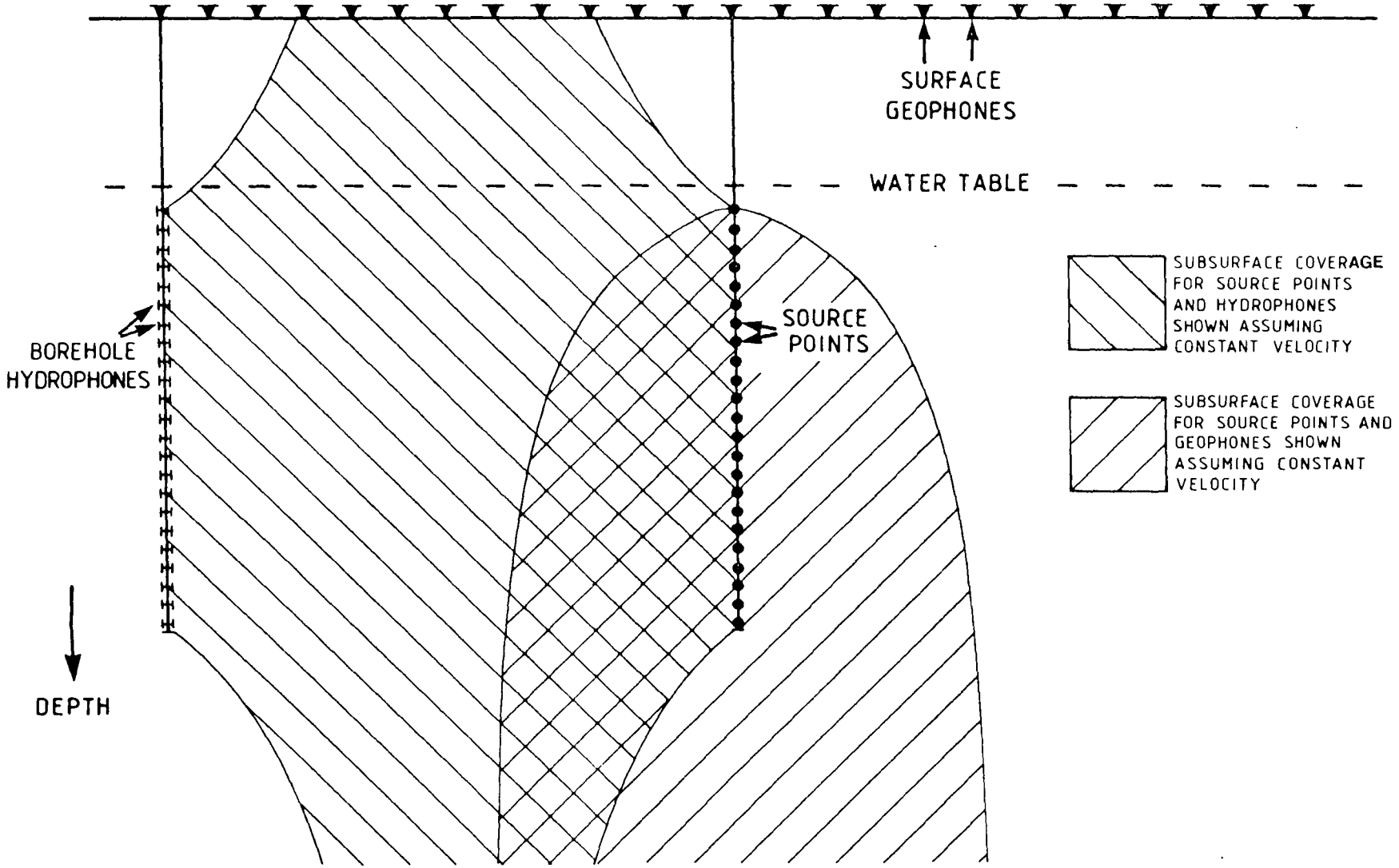

Figure 6.2 Zones of coverage obtained from processing a crosshole survey (both upward travelling and downward travelling wavefields) and from a hole-to-surface survey using one of the boreholes.

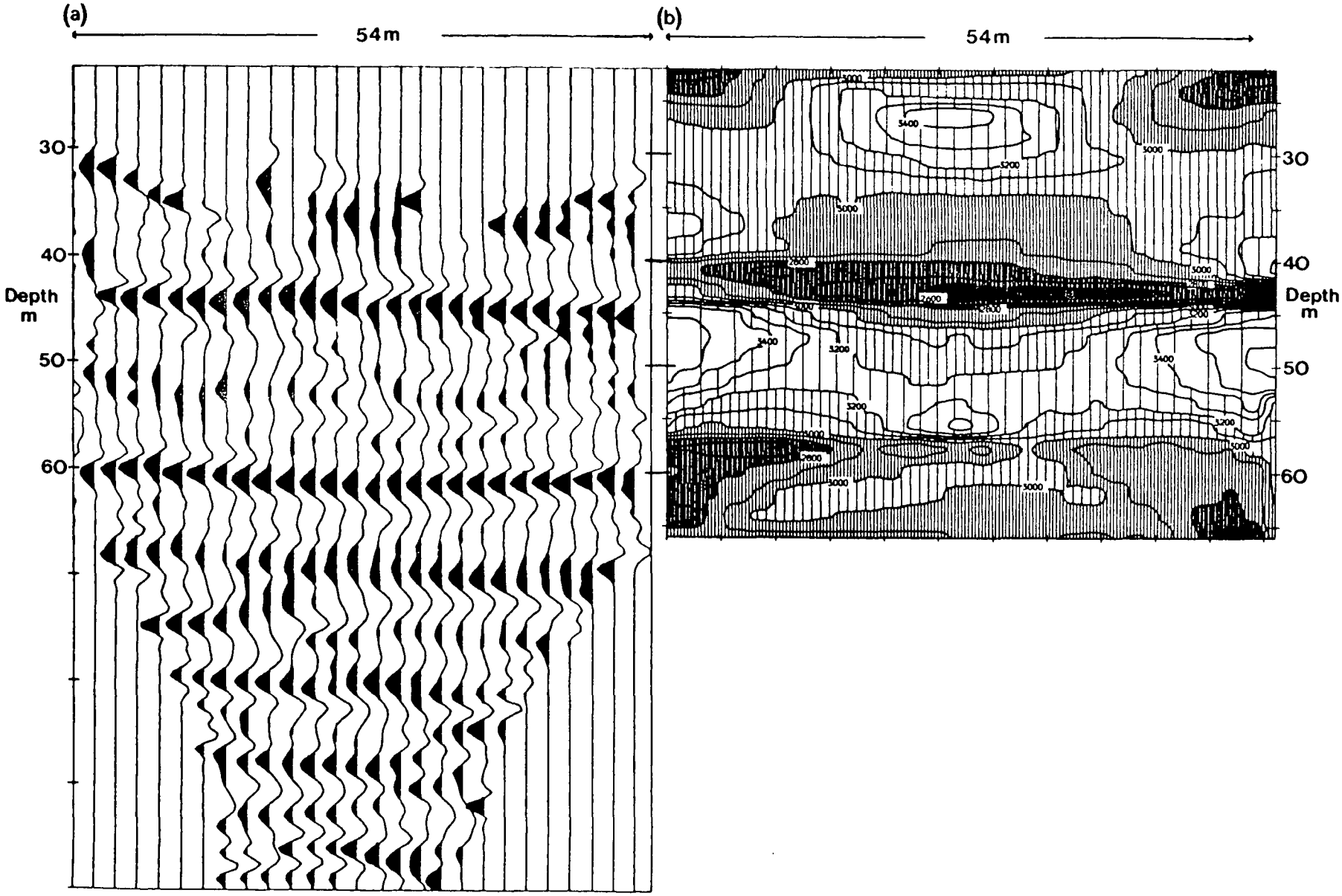

Figure 6.3 Images obtained from the crosshole dataset at Tinsley Park. (a) Stacked depth section resulting from processing the survey with the crosshole reflection method. An automatic gain control of length 30m has been applied and the trace spacing is 2m. (b) Tomographic velocity field resulting from processing the interpreted direct arrivals with the SIRT method (from figure 3.6).

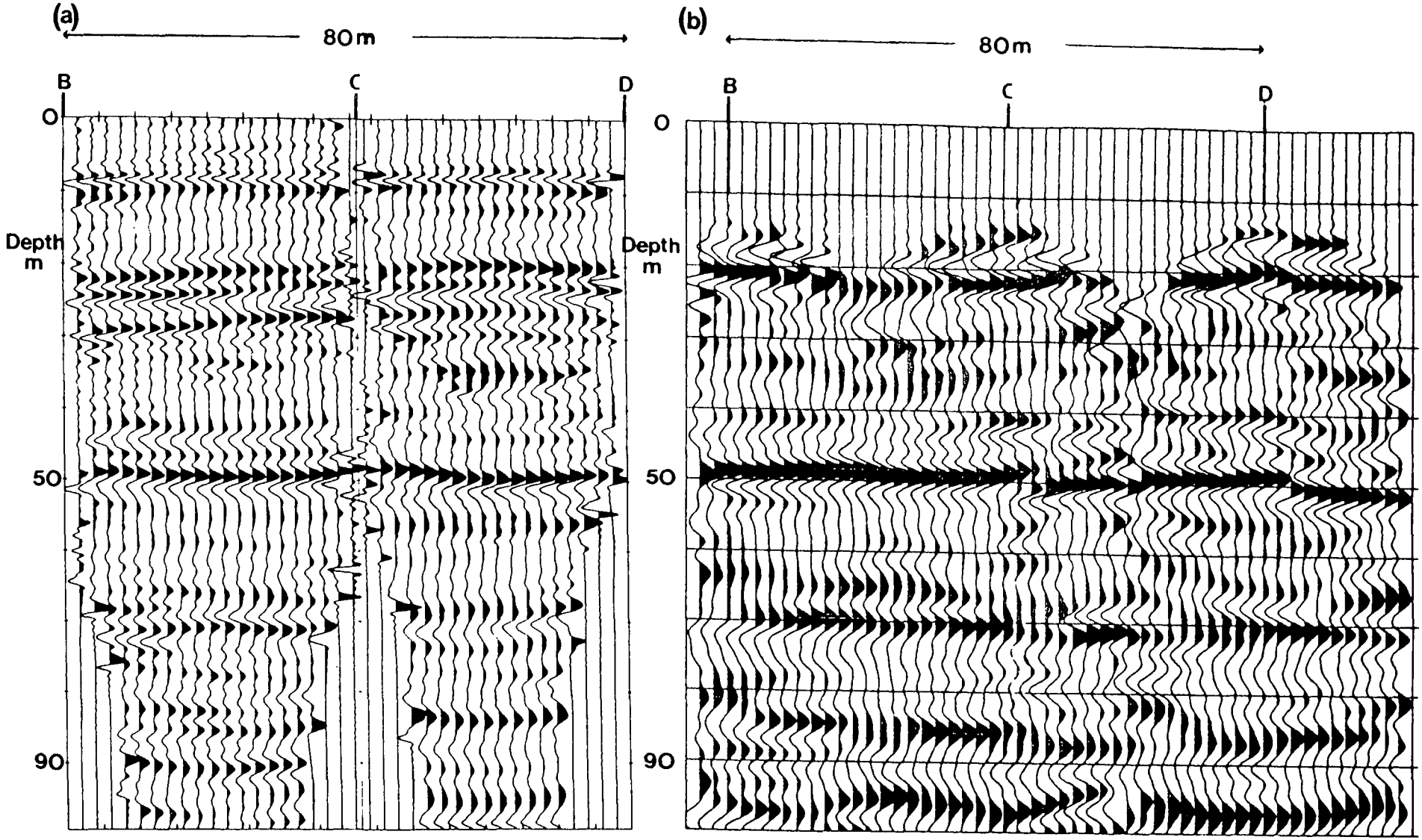

Figure 6.4 Comparison of crosshole and hole-to-surface results. (a) Depth section resulting from processing the two crosshole reflection surveys shot between boreholes B and C and boreholes C and D at Tinsley Park. An automatic gain control of 25m has been applied and the trace spacing is 2m. (b) Depth section resulting from processing the hole-to-surface surveys shot in boreholes B, C and D at Tinsley Park (figure 5.7). An automatic gain control of 30m has been applied and the trace spacing is 2m.

and the reflection at 20m depth is resolved into two separate reflectors with a third reflector seen just below. This is confirmed by borehole information. Continuous coverage is obtained on the reflector at 20m depth, though the image is poor at the borehole locations. This reflector appears to dip by a couple of metres down to the left, but should be flat according to borehole information. This dip may be due to incorrect migration velocities.

The reflector at 50m depth is seen as a continuous event on the crosshole section, though again the image is poor at the borehole locations. There is no evidence to support the small features seen on this reflector on the hole-to-surface section. The curvature on this reflector seen on the crosshole section is due to migration edge effects not cancelling out at the edges of the surveys.

The deeper events agree well on both sections, though the signal-to-noise ratio is poor. The 4m fault near borehole B between 70m and 80m depth is not seen on either section.

It was anticipated that the 2m fault just to the right of borehole D, seen on the hole-to-surface section at 50m depth, would be visible on the crosshole section cutting the shallow reflectors. This is not seen, and this suggests that the fault might be vertical, cutting the reflector at 20m depth, near borehole D, where there is a small disruption in reflector continuity. Alternatively the dislocation may not extend up to the shallow reflectors.

The disruption in the reflector just to the right of borehole C, seen on the hole-to-surface section at 50m depth, is again not confirmed by the crosshole data. It is unfortunate that this feature occurs just where the crosshole image is at its poorest. Again, no disturbances are seen cutting the shallow reflectors on the crosshole section, as might be expected if this feature were a small fault. However, if the fault was near vertical then it is unlikely that it would be apparent on the crosshole section, due to its position close to the borehole. Alternatively, its throw may decay to zero below the shallow reflectors.

Chapter VII

Conclusions and suggestions for further work

Seismic traveltime tomography does not have the resolution required to image the geological features, such as thin coal seams, washouts, and faults with throws of a couple of metres, found in shallow Coal Measures strata. Uphole surveys acquired below the water table have not shown the anticipated lowering of seismic velocity associated with collapse of strata above old workings, so the tomographic method will not have general application for detecting old workings either. However, the velocity field obtained from a tomographic survey is useful in processing the data by the crosshole seismic reflection method, and in determining whether anisotropy is present by comparing velocities with those obtained from uphole surveys.

High resolution seismic reflection sections of shallow Coal Measures strata within the uppermost 100m or so of the Earth's surface may be obtained using the hole-to-surface seismic reflection method. Several such surveys have been acquired at opencast exploration sites in Northern England, and the processed data show that the coal seams produce the strongest reflections.

The parallel development of the crosshole seismic reflection method allows an interesting comparison to be made.

There are various limitations to each method which must be understood if either is to be used on a routine basis. The methods may be summarised as follows.

The advantages of the crosshole method are:

• The vertical resolution, which essentially depends on the temporal frequency content of the data, is approximately double that of the hole-to-surface method, but the more horizontal raypaths probably mean that the lateral resolution is not much greater than the hole-to-surface method. Further surveys with common

subsurface coverage need to be acquired to demonstrate differences in resolving power more precisely.

- It may be used to obtain coverage beneath roads and rivers, where surface geophones cannot be planted.

- Coverage is obtained above the shallowest shot and receiver depths.

The disadvantages of the crosshole method are:

- Two boreholes are required, and the optimum borehole spacing is dependent on the target depth.

- The coverage is limited to the plane between the boreholes (assuming moderate dips); the image deteriorates at the boreholes, and the zone of coverage narrows above the shallowest and below the deepest source/receiver depths.

The advantages of the hole-to-surface method are:

- Only a single borehole is required.

- Coverage may be obtained where drilling access is restricted, such as beyond the edge of site boundaries.

- The survey orientation may be in any direction.

- The method may be extended to three-dimensions to obtain a bell-shaped volume of subsurface coverage, by deploying an areal array of geophones around the borehole.

The disadvantages of the hole-to-surface method are:

- The vertical resolution is approximately half that of the crosshole method.

- Coverage is limited to below the water table.

Both methods require the source and receiver positions to be below the water table. This is a fundamental limitation at present. To be able to extend the surveys above the water table, further development of the source and receivers is needed. With the hole-to-surface method, only the source is a problem. It may

be possible in certain circumstances to block the borehole with a 'packer', and to raise the water level in the borehole by simply pouring in water. This has yet to be tested, but it would only work away from levels of old workings and faults (where the water level would drain away too fast). With the crosshole method a further problem at the receiver hole might be noise due to the draining water.

Downhole sources which can work above the water table do exist (Bertrand et al. 1987, Laurent et al. 1990) and such sources should be tested. Borehole geophones could be used to extend the crosshole receiver array above the water table. However, Beattie's (1990) recent work shows that tube waves may be more of a problem on geophone receivers below the water table than on hydrophones, and it should be noted that there might be problems with merging the data recorded on two different receiver types.

Further experimentation is also required with the source to reduce the acquisition time. To date only small explosive charges have been used, and whilst these make a good impulsive source, they are slow to use. Ideally, a repeatable source is required, such as a downhole airgun or a borehole sparker (Baria et al. 1989). Both these sources only work below the level of the water table.

A further problem which needs to be solved is that of blocked boreholes. The uncased boreholes collapse and become blocked sooner or later after drilling. This is a particularly severe problem where the boreholes penetrate old workings or faults, when the boreholes may become blocked immediately after drilling. A solution to this problem may be to case the boreholes with a lightweight material such as plastic, having sufficient strength to withstand the collapse and yet having a fairly low impedance contrast with water so as not to inhibit source and receiver coupling. The casing need not be permanent, but nevertheless should be cheap because sections are liable to be lost down some boreholes. For the crosshole work, it is usually necessary to fire repeat shots at each shot position, and the sleeving would need to be able to withstand the source. This is a good reason for using some form of source other than explosives, so that the sleeving may be used more than just once. A further possibility which should be tested is to make use of the steel logging casing which is routinely used by Britsh Coal. It might be possible that it could withstand the explosive force of the detonators, with the energy still

being transferred to the surrounding rock, although intuitively one would expect tube waves to be a problem if receivers were placed inside the logging casing.

Further work planned for this research project is to test out some of the above suggestions to improve the acquisition of both the hole-to-surface and crosshole techniques, to build up a portfolio of test cases, and to develop the hole-to-surface method to three-dimensions.

References

Ahmed, H., Dillon, P. B., Johnstad, S. E. & Johnston, C. D. 1986. Northern Viking Graben multilevel three-component walkaway VSP's - a case history. *First Break*, 4(10), 8-27.

Aki, K. & Richards, P. G. 1980. *Quantitative seismology, theory and methods, Vol 1.* W. H. Freeman and Company.

Auckland, J. 1988. *P-wave anisotropy in Coal Measures rocks and its implication for seismic tomography.* M.Sc. dissertation, University of Durham.

Balch, A. H., Lee, M. W., Miller, J. J. & Taylor, R. T. 1982. The use of vertical seismic profiles in seismic investigations of the earth. *Geophysics*, 47, 906-918.

Baria, R., Jackson, P. D. & McCann, D. M. 1989. Further development of a high-frequency seismic source for use in boreholes. *Geophysical Prospecting*, 37, 31-52.

Beattie, K. 1990. *A comparison of receiver types in crosshole seismics.* M.Sc. dissertation, University of Durham.

Berkhout, A. J. 1984. *Seismic migration. Imaging of acoustic energy by wavefield extrapolation. B: Practical aspects.* Elsevier.

Berryman, J. G. 1979. Long-wave elastic anisotropy in transversely isotropic media. *Geophysics*, 44, 896-917.

Bertrand, Y., Bozetto, P., Lakshmanan, J. & Sanchez, M. 1987. The use of the Sheargun and the Sismopressiomètre in seismic studies. *First Break*, 5, 335-342.

Bregman, N. D., Hurley, P. A. & West, G. F. 1989. Seismic tomography at a fire-flood site. *Geophysics*, 54, 1082-1090.

East, R. J. R., Worthington, M. H. & Goulty, N. R. 1988. Convolutional back-projection imaging of physical models with crosshole seismic data. *Geophysical Prospecting*, 36, 139-148.

Embree, P., Burg, J. P. & Backus, M. M. 1963. Wide-band velocity filtering - the pie-slice process. *Geophysics*, 28, 948-974.

Federov, F. I. 1968. *Theory of waves in crystals.* New York, Plenum Press.

Findlay, M. J. 1987. *A curved ray iterative technique for tomographic inversion of cross-hole data.* M.Sc. dissertation, University of Durham.

Findlay, M. J. 1990. *Cross-hole seismic reflection surveying in Coal Measures.* Ph.D. dissertation, University of Durham.

Fitch, A. A. 1984. Interpretation of vertical seismic profiles. *First Break*, 2(6), 19-23.

Garrard, G. F. G. 1984. *The collapse of shallow coal mine workings.* Ph.D. dissertation, University of Durham.

Gilbert, P. 1972. An iterative method for three-dimensional reconstruction of an object from projections. *J. Theor. Biol.*, 36, 105-117.

Goossens, R. F., Smith, E. G. & Calver, M. A. 1974. *Westphalian* **in** *The Geology and mineral resources of Yorkshire.* Rayner, D. H. & Hemmingway, J. E. (Eds) Yorkshire Geological Society.

Goulty, N. R. & Brabham, P. J. 1984. Seismic refraction profiling in opencast coal exploration. *First Break*, 2(5), 26-34.

Goulty, N. R. & Ziolkowski, A. 1985. Seismic surveys applied to problems in coal mining: example from Bilsthorpe Colliery, U.K. **in** *Proceedings of the 9th Congr. Int. Stratigr. Geol. Carbonifere*, 4, 689-694.

Goulty, N. R., Thatcher, J. S., Findlay, M. J., Kragh, J. E. & Jackson, P. D. 1990. Experimental investigation of crosshole seismic techniques for shallow coal exploration. *Quarterly Journal of Engineering Geology*, 23, 217-228.

Greenhalgh, S. A. & Suprajitno, M. 1985. Vertical seismic profiling in coal. *Geophysical Prospecting*, 33, 696-715.

Hardage, B. A. 1983. *Vertical seismic profiling. Part A: Principles.* Geophysical Press.

Hatton, L., Worthington, M. H. & Makin, J. 1986. *Seismic data processing, theory and practice.* Blackwell Scientific Publications, Oxford.

Howson, M. & Sides, E. J. 1986. Borehole desurvey calculation. *Computers & Geosciences*, 12, 97-104.

Ivansson, S. 1985. A study of methods for tomographic velocity estimation in the prescence of low-velocity zones. *Geophysics*, 50, 969-988.

Jackson, P. 1985. Horizontal seismic in coal seams: Its use in the U.K. coal industry. *First Break*, 3(11), 15-24.

Jackson, P. J., Onions, K. R. & Westerman, A. R. 1989. Use of inverted VSP to enhance the exploration value of boreholes. *First Break*, 7, 233-246.

Justice, J. H., Vassilou, A. A., Singh, S., Logel, J. D., Hansen, P. A., Hall, B. R., Hutt, P. R. & Solanki, J. J. 1989. Acoustic tomography for monitoring enhanced oil recovery. *The Leading Edge*, 8(2), 12-19.

Kerner, C., Dyer, B. & Worthington, M. 1989. Wave propagation in a vertical transversely isotropic medium: field experiment and model study. *Geophysical Journal*, 97, 295-309.

Krey, Th. C. 1963. Channel waves in coal mining. *Geophysics*, 28, 701-714.

Laurent, J & Mari, J. L. 1988. *Well-to-surface seismic measurments with a downhole source.* Presented at the 50th meeting of the EAEG, The Hague.

Laurent, J., Layotte, P. C., Meynier, P. & Noual, G. 1990. *A mechanical wall-clamped borehole source and its use in inverse VSP and cross-hole seismic surveying.* Presented at the 52nd meeting of the EAEG, Copenhagen.

Layotte, P. C., Bernet Rollande, J. O., Omnes, G., Paternoster, B. & Verdier, F. 1990. *Inverse 3D borehole seismics: an experiment.* Presented at the 52nd meeting of the EAEG, Copenhagen.

Levin, F. K. 1978. The reflection, refraction and diffraction of waves in media with an elliptical velocity dependence. *Geophysics*, 43, 528-537.

Lintker, S., Reimes, L. E. & Heil, R. W. 1990. *Reverse multi-offset VSP (RMOVSP) in the Ruhr-district in West Germany.* Presented at the 52nd meeting of the EAEG, Copenhagen.

Love, A. E. H. 1944. *A treatise on the mathematical theory of elasticity.* New York, Dover Publications, Inc.

Macrides, C. G., Kanasewich, E. R. & Bharatha, S. 1988. Multiborehole seismic imaging in steam injection heavy oil recovery projects. *Geophysics*, 53, 65-75.

March, D. W. & Bailey, A. D. 1983. A review of the two-dimensional transform and its use in seismic processing. *First Break*, 1(1), 9-21.

Mason, I. M., Buchanan, D. J. & Booer, A. K. 1980. Channel wave mapping of coal seams. *Geophysics*, 45, 1131-1143.

Mason, I. M. 1981. Algebraic reconstruction of a two-dimensional inhomogeneity in the High Hazles seam of the Thoresby colliery. *Geophysics*, 46, 298-306.

McMechan, G. A. 1983. Seismic tomography in boreholes. *Geophysical J. R. astr. Soc.*, 74, 601-612.

Muftuoglu, Y. V. & Scoble, M. J. 1984. Derivation of diggability index for surface mine equipment selection. *Mining Science and Technology*, (1984), 305-322.

Noble, M. D., Lambert, R. A., Ahmed, H. & Lyons, J. 1988. The application of three-component VSP data to the interpretation of the Vulcan gas field and its impact on field development. *First Break*, 6, 131-149.

Roberts, P. 1987. *P-waves and tomography in Coal Measures rocks.* M.Sc. dissertation, University of Durham.

Robinson, E. A. & Treitel, S. 1980. *Geophysical signal analysis.* Prentice-Hall, Englewood Cliffs, N. J.

Sheriff, R. E. & Geldart, L. P. 1983. *Exploration seismology, Vol. 1*, Cambridge University Press.

Trueman. A. 1954. *The coalfields of Great Britain.* Edward Arnold.

Uhrig, L. F. & VanMelle, F. A. 1955. Velocity anisotropy in stratified media. *Geophysics*, 20, 774-779.

Wong, J., Hurley, P. & West, G. F. 1983. Cross-hole seismology and seismic imaging in crystalline rock. *Geophys. Res. letters*, 10, 686-689.

Worthington. M. H. 1984. An introduction to geophysical tomography. *First Break*, 2(11), 20-26.

Wye, R. 1986. *An investigation into the accuracy of algebraic reconstruction techniques for tomographic inversion.* M.Sc. dissertation, University of Durham.

Yilmaz, O. 1987. *Seismic data processing.* Investigations in Geophysics, Society of Exploration Geophysicists, Tulsa.

Ziolkowski, A. 1979. *Seismic profiling for coal on land.* **in** *Developments in geophysical exploration methods.* A. A. Fitch (Ed), Applied Science Publishers ltd, London.

Ziolkowski, A. 1981. *Seismic surveying in the British coal fields.* Mining Engineer, 234, 605-615.

Ziolkowski, A. & Lerwill, W. E. 1979. A simple approach to high resolution seismic profiling for coal. *Geophysical Prospecting*, 27, 360-393.

Appendix A

Computer software

A suite of computer programs was written to process the hole-to-surface seismic data.

Software is implemented on the NUMAC (Northumbrian Universities Multiple Access Computer) Amdahl 5860 mainframe, which uses the MTS (Michigan Terminal System) operating system. All programs are written in the Fortran 77 programming language. The IBM VS fortran compiler is used. MTS system subroutines are used for magnetic tape operations, and an external graphical library, *GHOST80 (Culham laboratory), is used extensively.

The software is written as a single menu driven package, with the migration as a separate program.

This appendix lists the two control menus, and the code for the three major processing steps of hole-to-surface data: f-k wavefield separation, deconvolution and migration.

MAIN MENU

1. – – – – –Read data

2. – – – – –Plot data

3. – – – – –Write data

4. – – – – –Processing menu

5. – – – – –Enter headers

6. – – – – –Print data

7. – – – – –Statistical trace summary

8. – – – – –Trace manipulation menu .. (change space s-r)

9. – – – – –Convolve data with a wavelet

10. – – – – –Save a specified trace for wavelet decon option

11. – – – – –First break menu ...auto pick...aligning data etc

12. – – – – –Calculate energy in specified window

13. – – – – –Sum traces for CDP/STACK analysis

14. – – – – –Resample data to COARSER sample rate

15. – – – – –Renumber traces of data array

00. – – – – –Exit

PROCESSING MENU

0 Return

1 Remove dc from traces

2 Filter data

3 Ramp / norm / agc /mute

5 Compute spectra

7 Edit data samples

8 Automatic spike edit

9 Shift traces within record

10 Taper traces

11 Gain recovery

12 Sum traces within record

14 Compute F-K Spectra / filter data

15 Fourier interpolation

16 Autocorrelation for display

17 Predictive deconvolution

19 Design/apply wavelet shaping filter (normal eq)

21 Flatten amp spectrum

22 Median filter a record

23 Correlate adjacent traces

```
      SUBROUTINE PRO14(N,NRECS,NKILL,NSAMS,R4DAT,DT)

C     2D-FFT AND SIMPLE FK FILTER ROUTINE
C     ***********************************

      COMPLEX CDAT(1024,64),CW2(1024),CW3(64)
      REAL*4  R4DAT(N,NRECS),XTEMP(1024),TEMAR2(1024,64)
      CHARACTER*1 ANS,VANS,FANS,IVA
      CHARACTER*20 OUTDIS
      CHARACTER*180 ACOMM

C     Set up some constants
      N2 = 64
      FNYQ = 1./(2.*DT/1000000.)
      PRINT*,'Fnyq= ',FNYQ
      NKEEP = NSAMS
      NSAMS = 1024
      PRINT*,' Padding to 1024 samples'
C     ~~~~~~~~~~~~~~~~~~~~~~~~~~~~~~~~~~~~~~~~~~~~~~~~


C     First input options
      VANS = 'N'
  124 WRITE(6,910)
      WRITE(6,911)
      WRITE(6,912)FANS
      WRITE(6,913)HCSL1,HCSL2
      WRITE(6,918)HCIN1,HCIN2
      WRITE(6,914)VCSL1,VCSL2
      WRITE(6,919)VCIN1,VCIN2
      WRITE(6,994)
      WRITE(6,915)VANS
      IF(VANS.EQ.'Y'.OR.VANS.EQ.'y')THEN
              WRITE(6,916)TFREQ
              WRITE(6,917)IVA
      ENDIF
      WRITE(6,920)DX

  910 FORMAT(  ' 0   Return')
  911 FORMAT(/,/,' 1   OK go !! ')
  912 FORMAT(/,' 2   Filter data                                  :',A1)
  913 FORMAT(/,' 3   High cut slope and taper slope (app' vel):',2F12.1)
  918 FORMAT(  ' 4   Corresponding intercepts on freq axis hz :',2F12.1)
  914 FORMAT(/,' 5    Low cut slope and taper slope (app' vel):',2F12.1)
  919 FORMAT(  ' 6   Corresponding intercepts on freq axis hz :',2F12.1)
  994 FORMAT(/,'      If slopes of passband are of opposite sign
     &               then high cut becomes low cut on +ve side and must
     &               be specified as +ve. Intercepts are zero....PIESLICE')
  915 FORMAT(/,' 7   View spectra                                 :',A1)
  916 FORMAT(/,' 8   Max freq for plot                            :',F6.1)
  917 FORMAT(/,' 9   Variable area plot                           :',A1)
  920 FORMAT(/,' 10  DX                                           :',F8.4)
      READ*, IOPT
      IF(IOPT.EQ.0) RETURN
      IF(IOPT.EQ.1) GO TO 9876
      IF(IOPT.EQ.2) READ(5,999)FANS
  999             FORMAT(A1)
      IF(IOPT.EQ.3) READ*,HCSL1,HCSL2
      IF(IOPT.EQ.4) READ*,HCIN1,HCIN2
      IF(IOPT.EQ.5) READ*,VCSL1,VCSL2
      IF(IOPT.EQ.6) READ*,VCIN1,VCIN2
      IF(IOPT.EQ.7) READ(5,999)VANS
      IF(IOPT.EQ.8) READ*,TFREQ
      IF(IOPT.EQ.9) READ(5,999)IVA
      IF(IOPT.EQ.10)READ*,DX

      GO TO 124
C     ------------------------------------------------------------

99761 CALL ZERO2C(1024,N2,CDAT)

 9876 RKNYQ = 1./(2.*DX)
      DO 111 I = 1,NRECS
             DO 222 J = 1,NSAMS
                    CDAT(J,I) = CMPLX(R4DAT(J,I),0.0)
  222        CONTINUE
  111 CONTINUE



      PRINT*,' Starting 2d fft '
      CALL FFT2D(CDAT,NSAMS,N2,-1.,-1.)
C     calls subroutine FORK ... Claerbout
      PRINT*,' ok !'

C     option to write out fk spectra for further processing
      PRINT*,' Write out raw 2d fft traces for further processing...y/n'
      READ(5,999)ANS
      IF(ANS.EQ.'Y'.OR.ANS.EQ.'y')THEN
                PRINT*,' Enter output file name'
                READ(5,899) OUTDIS
  899           FORMAT(A20)
                PRINT*,' Enter shot id no. '
                READ*,NSHOT
                IDCODE = (NSHOT - 1) * (N2+1) + 1
                LEN = (NSAMS+2) * 8
C               Complex trace therefore 8 bytes / sample
                OPEN(2,FILE=OUTDIS,STATUS='UNKNOWN',FORM='UNFORMATTED',
     1          ACCESS='DIRECT',RECL=LEN)
C
C  WRITE SEISMOGRAM RECORDS
C
                DO 132 J = 1, N2
                    NREC = IDCODE + J
                    PRINT*,'Writing channel  ',J
                    WRITE(2,REC=NREC)(CDAT(I,J),I=1,NSAMS)
  132           CONTINUE
                CLOSE(2)
      ENDIF

C     ------------------------------------------------------------
      IF(VANS.EQ.'y'.OR.VANS.EQ.'Y')THEN
C     Compute amplitude spectra and rearrange traces for view
      K=1
      DO 700 I = N2/2 +2 , N2
             DO 800 J = 1,NSAMS
             TEMAR2(J,K) = SQRT( REAL(CDAT(J,I))**2+AIMAG(CDAT(J,I))**2)
  800        CONTINUE
             K=K+1
  700 CONTINUE
```

```
      DO 770 I = 1,N2/2 +1
             DO 880 J = 1,NSAMS
             TEMAR2(J,K) = SQRT( REAL(CDAT(J,I))**2+AIMAG(CDAT(J,I))**2)
 880         CONTINUE
             K=K+1
 770   CONTINUE
      DO 779 I = 1,N2
             DO 889 J = NSAMS+1,N
             TEMAR2(J,K) = 0.0
 889         CONTINUE
             K=K+1
 779   CONTINUE


      LSAMP = INT( NSAMS/2. * (TFREQ / FNYQ)  + 1.)
      PRINT*,' LSAMP =',LSAMP
      PRINT*,' RKNYQ =',RKNYQ
      CALL TDPLOT(TEMAR2,N,N2,1,LSAMP,1,N2,3.,IVA,'N')

C     Find max of temarr
      RRM = 0.
      DO 9911 I = 1,N2
             CALL ZERO(N,XTEMP)
             DO 9912 J = 1,LSAMP
                    XTEMP(J) = TEMAR2(J,I)
 9912        CONTINUE
             CALL MAXSN(NSAMS,XTEMP,XM,II)
             IF(XM.GT.RRM)RRM = XM
 9911  CONTINUE
      PRINT*,' Max of fk = ',INT(RRM*10000.)

      ENDIF

      PRINT*, 'WRITE OUT FK SPECTRA ? 1=Y'
      READ*,IA
      IF(IA.EQ.1)THEN
      CALL OPENO(9)
      DO 777 J = 1,LSAMP
         DO 778 I = 1,N2
              WRITE(9,1817)I,J,INT(TEMAR2(J,I)*10000.)
 778     CONTINUE
 777  CONTINUE
      ENDIF

 1817 FORMAT(I6,I6,3X,I10)

C     ------------------------------------------------------------



C     Now filter
      IF(FANS.EQ.'Y'.OR.FANS.EQ.'y')THEN
C     ------------------------------------------------------------
C     Compute dip in samples/trace in FK
      NSO2 = NSAMS/2
      NSO2P1 = NSAMS/2 +1
      HSLOPE = FLOAT(NSO2/(N2/2)) * ABS(HCSL1)/(FNYQ/RKNYQ)
      HSLOP2 = FLOAT(NSO2/(N2/2)) * ABS(HCSL2)/(FNYQ/RKNYQ)
      VSLOPE = FLOAT(NSO2/(N2/2)) * ABS(VCSL1)/(FNYQ/RKNYQ)
      VSLOP2 = FLOAT(NSO2/(N2/2)) * ABS(VCSL2)/(FNYQ/RKNYQ)
      PRINT*,' HSLOPE = ',HSLOPE
      PRINT*,' HSLOP2 = ',HSLOP2
      PRINT*,' VSLOPE = ',VSLOPE
      PRINT*,' VSLOP2 = ',VSLOP2

      IF(VCSL1.GE.0.0.AND.HCSL1.GE.0.0)THEN
C     Filter +ve dips-----------------------------------------------

      DO  444  I = 1, N2/2+1
C     Now samples to filter
            IS1 = VSLOPE*(I-1)+1 + INT(VCIN1*NSO2/FNYQ)
            IS2 = HSLOPE*(I-1)+1 + INT(HCIN1*NSO2/FNYQ)
            IS11= VSLOP2*(I-1)+1 + INT(VCIN2*NSO2/FNYQ)
            IS22= HSLOP2*(I-1)+1 + INT(HCIN2*NSO2/FNYQ)
            NTEM= IS1-IS11 + 1
            NTEM2=IS22-IS2 + 1
            PRINT*,' IS1 IS2 IS11 IS22 = ',IS1,IS2,IS11,IS22
            PRINT*,' NTEM NTEM2 = ',NTEM,NTEM2

            DO 5551  JJ  =  1,NSAMS
                   CW2(JJ)  =  CDAT(JJ,I)
 5551       CONTINUE

C           First do tapers:
            DO 5552 K = 1,NTEM
             IF(NTEM.GT.1.AND.VSLOPE.GT.0.0.AND.IS11+K.LT.NSO2P1)THEN
                A = FLOAT(NTEM-K)*COS(ATAN(VSLOPE))
                B = FLOAT(K)*COS(ATAN(VSLOPE))/COS(ATAN(VSLOPE-VSLOP2))
                WT= 1.-(A/(A+B))
                CW2(IS11+K)=CW2(IS11+K)*CMPLX(WT,0.0)
             ENDIF
 5552       CONTINUE

            DO 5559 K = 1,NTEM2
           IF(NTEM2.GT.1.AND.HSLOPE.LT.NSO2P1.AND.IS2+K.LT.NSO2P1)THEN
                A = FLOAT(NTEM2-K)*COS(ATAN(HSLOPE))
                B = FLOAT(K)*COS(ATAN(HSLOP2))/COS(ATAN(HSLOPE-HSLOP2))
                WT= (A/(A+B))
                CW2(IS2+K)=CW2(IS2+K)*CMPLX(WT,0.0)
             ENDIF
 5559       CONTINUE

            DO  5553  JJ = 1,NSAMS
               CDAT(JJ,I) = CW2(JJ)
 5553       CONTINUE

            IF(IS11.LT.NSO2P1)THEN
            DO 555  J  =  1 , IS11
                   CDAT(J,I)  =  CMPLX(0.0,0.0)
 555        CONTINUE
            ELSE
            DO 545  J  =  1 , NSO2P1
                   CDAT(J,I)  =  CMPLX(0.0,0.0)
 545        CONTINUE
            ENDIF

            IF(IS22.LT.NSO2P1)THEN
                   DO 5133 J = IS22 ,NSAMS
```

```
                  CDAT(J,I) = CMPLX(0.0,0.0)
 5133             CONTINUE
          ELSE
                  DO 6284 J = NSAMS/2 +1 ,NSAMS
                     CDAT(J,I) = CMPLX(0.0,0.0)
 6284             CONTINUE
           ENDIF


 444   CONTINUE

 C     Add a simple spatial taper
 C     This one seems about right with 64 traces and typical passbands
       DO 1838 J  = 1,NSAMS
               CDAT(J,1) = CDAT(J,1) * CMPLX(.1,0.0)
               CDAT(J,2) = CDAT(J,2) * CMPLX(.3,0.0)
               CDAT(J,3) = CDAT(J,3) * CMPLX(.5,0.0)
               CDAT(J,4) = CDAT(J,4) * CMPLX(.7,0.0)
               CDAT(J,5) = CDAT(J,5) * CMPLX(.8,0.0)
               CDAT(J,6) = CDAT(J,6) * CMPLX(.9,0.0)
               CDAT(J,N2/2+1) = CDAT(J,N2/2+1) * CMPLX(.1,0.0)
               CDAT(J,N2/2  ) = CDAT(J,N2/2  ) * CMPLX(.3,0.0)
               CDAT(J,N2/2-1) = CDAT(J,N2/2-1) * CMPLX(.5,0.0)
               CDAT(J,N2/2-2) = CDAT(J,N2/2-2) * CMPLX(.7,0.0)
               CDAT(J,N2/2-3) = CDAT(J,N2/2-3) * CMPLX(.8,0.0)
               CDAT(J,N2/2-4) = CDAT(J,N2/2-4) * CMPLX(.9,0.0)
  1838 CONTINUE

 C     Now do -ve frequencies
       ITR = 2
       DO 11 I = N2 , N2/2+2 , -1
             ISAM = 2
             DO 12 J = NSAMS , 1 ,-1
                   CDAT(J,I) = CONJG(CDAT(ISAM,ITR))
                   ISAM = ISAM + 1
  12         CONTINUE
       ITR = ITR + 1
  11   CONTINUE

       ENDIF
 C     end +ve dips
 C     ----------------------------------------------------------------




       IF(VCSL1.LE.0.0.AND.HCSL1.LE.0.0)THEN
 C     Filter -ve dips
       KTR = 1

       DO  292  I = N2 , N2/2+1 , -1
 C     Now samples to filter
             IS1 = VSLOPE* KTR +1 + INT(VCIN1*NSO2/FNYQ)
             IS2 = HSLOPE* KTR +1 + INT(HCIN1*NSO2/FNYQ)
             IS11= VSLOP2* KTR +1 + INT(VCIN2*NSO2/FNYQ)
             IS22= HSLOP2* KTR +1 + INT(HCIN2*NSO2/FNYQ)
             NTEM= IS1-IS11 + 1
             NTEM2=IS22-IS2 + 1
             PRINT*,' IS1 IS2 IS11 IS22 = ',IS1,IS2,IS11,IS22
             PRINT*,' NTEM NTEM2 = ',NTEM,NTEM2

       DO 223  JJ  =  1,NSAMS
               CW2(JJ)  =  CDAT(JJ,I)
  223  CONTINUE

 C     First do tapers:
       DO 224 K = 1,NTEM
        IF(NTEM.GT.1.AND.VSLOPE.GT.0.0.AND.IS11+K.LT.NSO2P1)THEN
            A = FLOAT(NTEM-K)*COS(ATAN(VSLOPE))
            B = FLOAT(K)*COS(ATAN(VSLOPE))/COS(ATAN(VSLOPE-VSLOP2))
            WT= 1.-(A/(A+B))
            CW2(IS11+K)=CW2(IS11+K)*CMPLX(WT,0.0)
        ENDIF
  224  CONTINUE

       DO 225 K = 1,NTEM2
       IF(NTEM2.GT.1.AND.HSLOPE.LT.NSO2P1.AND.IS22-K.LT.NSO2P1)THEN
            A = FLOAT(NTEM2-K)*COS(ATAN(HSLOPE))
            B = FLOAT(K)*COS(ATAN(HSLOPE2))/COS(ATAN(HSLOPE-HSLOP2))
            WT= 1.-(A/(A+B))
            CW2(IS22-K)=CW2(IS22-K)*CMPLX(WT,0.0)
        ENDIF
  225  CONTINUE

       DO  226  JJ = 1,NSAMS
           CDAT(JJ,I) = CW2(JJ)
  226  CONTINUE

       IF(IS11.LT.NSO2P1)THEN
       DO 227  J  =  1 , IS11
              CDAT(J,I)  =  CMPLX(0.0,0.0)
  227  CONTINUE
       ELSE
       DO 228  J  =  1 , NSO2P1
              CDAT(J,I)  =  CMPLX(0.0,0.0)
  228  CONTINUE
       ENDIF

       IF(IS22.LT.NSO2P1)THEN
              DO 229 J = IS22 ,NSAMS
                 CDAT(J,I) = CMPLX(0.0,0.0)
   229        CONTINUE
       ELSE
              DO 285 J = NSAMS/2 , NSAMS
                 CDAT(J,I) = CMPLX(0.0,0.0)
  285         CONTINUE
       ENDIF

       KTR = KTR + 1
  292  CONTINUE

 C     Must filter k=0 trace also
       IF(HSLOPE.LT.NSO2P1)THEN
             IS11 = INT(VCIN2*NSO2/FNYQ) + 1
             IS22 = INT(HCIN2*NSO2/FNYQ) + 1
             DO 138 J = IS22 , NSAMS-IS22
                    CDAT(J,1) = CMPLX(0.0,0.0)
  138        CONTINUE
             IF(IS11.GT.1)THEN
             DO 338 J = 1,IS11
```

```
                CDAT(J,1) = CMPLX(0.0,0.0)
 338        CONTINUE
            DO 438 J = NSAMS-IS11+1,NSAMS
                CDAT(J,1) = CMPLX(0.0,0.0)
 438        CONTINUE
            ENDIF
      ENDIF
C     Add a simple spatial taper
C     Seems ok with 64 traces and typical passbands
      DO 1839 J  = 1,NSAMS
            CDAT(J,1)    = CDAT(J,1)    * CMPLX(.1,0.0)
            CDAT(J,N2)   = CDAT(J,N2)   * CMPLX(.3,0.0)
            CDAT(J,N2-1)= CDAT(J,N2-1)* CMPLX(.5,0.0)
            CDAT(J,N2-2)= CDAT(J,N2-2)* CMPLX(.7,0.0)
            CDAT(J,N2-3)= CDAT(J,N2-3)* CMPLX(.8,0.0)
            CDAT(J,N2-4)= CDAT(J,N2-4)* CMPLX(.9,0.0)
            CDAT(J,N2/2+1) = CDAT(J,N2/2+1) * CMPLX(.1,0.0)
            CDAT(J,N2/2+2) = CDAT(J,N2/2+2) * CMPLX(.3,0.0)
            CDAT(J,N2/2+3) = CDAT(J,N2/2+3) * CMPLX(.5,0.0)
            CDAT(J,N2/2+4) = CDAT(J,N2/2+4) * CMPLX(.7,0.0)
            CDAT(J,N2/2+5) = CDAT(J,N2/2+5) * CMPLX(.8,0.0)
            CDAT(J,N2/2+6) = CDAT(J,N2/2+6) * CMPLX(.9,0.0)
 1839  CONTINUE

C     Now do -ve frequencies
      ITR = N2
      DO 18 I = 2 , N2/2+1
            ISAM = 2
            DO 19 J = NSAMS , 1 , -1
                  CDAT(J,I) = CONJG(CDAT(ISAM,ITR))
                  ISAM = ISAM + 1
 19         CONTINUE
      ITR = ITR - 1
 18   CONTINUE


      ENDIF
C     end -ve dips
C     ------------------------------------------------------------




      IF(VCSL1*HCSL1.LT.0.0)THEN
C     Standard pi slice ... the "high cut" is treated as the low cut
C     on the +ve side and the "low cut" is the low cut on the -ve side
C     The intercepts must be zero with the freq axis
C     ------------------------------------------------------------------

      DO  744  I = 1, N2/2+1
C     Now samples to filter
            IS1 = HSLOPE*(I-1)+1 + INT(HCIN1*NSO2/FNYQ)
            IS11= HSLOP2*(I-1)+1 + INT(HCIN2*NSO2/FNYQ)
            NTEM= IS1-IS11 + 1

            DO 7551  JJ  =  1,NSAMS
                  CW2(JJ)  =  CDAT(JJ,I)
 7551       CONTINUE
C           First do tapers:
            DO 7552 K = 1,NTEM
             IF(NTEM.GT.1.AND.HSLOPE.GT.0.0.AND.IS11+K.LT.NSO2P1)THEN
                A = FLOAT(NTEM-K)*COS(ATAN(HSLOPE))
                B = FLOAT(K)*COS(ATAN(HSLOPE))/COS(ATAN(HSLOPE-HSLOP2))
                WT= 1.-(A/(A+B))
                CW2(IS11+K)=CW2(IS11+K)*CMPLX(WT,0.0)
             ENDIF
 7552       CONTINUE

            DO  7553  JJ = 1,NSAMS
                CDAT(JJ,I) = CW2(JJ)
 7553       CONTINUE

            IF(IS11.LT.NSO2P1)THEN
            DO 755  J  =  1 , IS11
                  CDAT(J,I)  =  CMPLX(0.0,0.0)
 755        CONTINUE
            ELSE
            DO 745  J  =  1 , NSO2P1
                  CDAT(J,I)  =  CMPLX(0.0,0.0)
 745        CONTINUE
            ENDIF

 744  CONTINUE

C     Now do -ve frequencies
      ITR = 2
      DO 71 I = N2 , N2/2+2 , -1
            ISAM = 2
            DO 72 J = NSAMS , 1 ,-1
                  CDAT(J,I) = CONJG(CDAT(ISAM,ITR))
                  ISAM = ISAM + 1
 72         CONTINUE
      ITR = ITR + 1
 71   CONTINUE

C     end +ve side of pi slice


C     Now filter -ve dips
      KTR = 1

      DO  492  I = N2 , N2/2+1 , -1
C     Now samples to filter
            IS1 = VSLOPE* KTR +1 + INT(VCIN1*NSO2/FNYQ)
            IS11= VSLOP2* KTR +1 + INT(VCIN2*NSO2/FNYQ)
            NTEM= IS1-IS11 + 1

            DO 423  JJ  =  1,NSAMS
                  CW2(JJ)  =  CDAT(JJ,I)
 423        CONTINUE

C           First do tapers:
            DO 424 K = 1,NTEM
             IF(NTEM.GT.1.AND.VSLOPE.GT.0.0.AND.IS11+K.LT.NSO2P1)THEN
                A = FLOAT(NTEM-K)*COS(ATAN(VSLOPE))
                B = FLOAT(K)*COS(ATAN(VSLOPE))/COS(ATAN(VSLOPE-VSLOP2))
                WT= 1.-(A/(A+B))
                CW2(IS11+K)=CW2(IS11+K)*CMPLX(WT,0.0)
```

```
            ENDIF
 424        CONTINUE

            DO  426  JJ = 1,NSAMS
                CDAT(JJ,I) = CW2(JJ)
 426        CONTINUE

            IF(IS11.LT.NSO2P1)THEN
            DO 427  J  =  1 , IS11
                   CDAT(J,I)  =  CMPLX(0.0,0.0)
 427        CONTINUE
            ELSE
            DO 428  J  =  1 , NSO2P1
                   CDAT(J,I)  =  CMPLX(0.0,0.0)
 428        CONTINUE
            ENDIF

            KTR = KTR + 1
  492  CONTINUE

C       Now do -ve frequencies
        ITR = N2
        DO 48 I = 2 , N2/2+1
              ISAM = 2
              DO 49 J = NSAMS , 1 , -1
                    CDAT(J,I) = CONJG(CDAT(ISAM,ITR))
                    ISAM = ISAM + 1
   49         CONTINUE
        ITR = ITR - 1
   48   CONTINUE


        ENDIF
C       end -ve side of pi slice

C       finished pi slice
C       ------------------------------------------------------------




C       ------------------------------------------------------------
        IF(VANS.EQ.'y'.OR.VANS.EQ.'Y')THEN
C       Compute amplitude spectra and rearrange traces for view
        K=1
        DO 701 I = N2/2 +2 , N2
              DO 801 J = 1,NSAMS
              TEMAR2(J,K) = SQRT( REAL(CDAT(J,I))**2+AIMAG(CDAT(J,I))**2)
   801        CONTINUE
              K=K+1
   701  CONTINUE

        DO 771 I = 1,N2/2 + 1
              DO 881 J = 1,NSAMS
              TEMAR2(J,K) = SQRT( REAL(CDAT(J,I))**2+AIMAG(CDAT(J,I))**2)
   881        CONTINUE
              K=K+1
   771  CONTINUE

        LSAMP = INT( NSAMS/2. * (TFREQ / FNYQ)  + 1.)
```

```
        CALL TDPLOT(TEMAR2,N,N2,1,LSAMP,1,N2,3.,IVA,'N')

C       Find max of temarr
        RRM = 0.
        DO 9611 I = 1,N2
              CALL ZERO(NSAMS,XTEMP)
              DO 9612 J = 1,LSAMP
                    XTEMP(J) = TEMAR2(J,I)
 9612         CONTINUE
              CALL MAXSN(NSAMS,XTEMP,XM,II)
              IF(XM.GT.RRM)RRM = XM
 9611   CONTINUE
        PRINT*,' Max of fk filtered = ',INT(RRM*1000.)
        ENDIF
C       end view option

        PRINT*, 'WRITE OUT FK SPECTRA ? 1=Y'
        READ*,IA
        IF(IA.EQ.1)THEN
        CALL OPENO(8)
        DO 177 J = 1,LSAMP
           DO 178 I = 1,N2
                 WRITE(8,1817)I,J,INT(TEMAR2(J,I) * 1000.)
  178      CONTINUE
  177   CONTINUE
        ENDIF

        ENDIF
C       end filter option
C       ------------------------------------------------------------


C       ------------------------------------------------------------
C       Now filter back
        CALL FFT2D(CDAT,NSAMS,N2,1.,1.)
C       calls subroutine FORK... Claerbout

        DO 77 J = 1,NSAMS
              DO 66 I = 1,NRECS
                 R4DAT(J,I) = REAL(CDAT(J,I))
   66         CONTINUE
   77   CONTINUE
        DO 37 J = 1,NSAMS
              DO 46 I = 1,N2
                TEMAR2(J,I) = REAL(CDAT(J,I))
   46         CONTINUE
   37   CONTINUE

C       CALL TDPLOT(TEMAR2,N,N2,1,NSAMS,1,N2,3.,'N','N')
C       CALL TDPLOT(TEMAR2,N,N2,1,NSAMS,1,N2,3.,'N','Y')

C       OK all done !

        NSAMS = NKEEP
        RETURN
        END
```

```
      SUBROUTINE PRO19(N,NRECS,NKILL,NSAMS,R4DAT,DT,XTEMP)

C     WAVELET DECONVOLUTION
C     *********************

C     This subroutine will extract a wavelet from a record using an
C     autocorrelation sum ... then finding minimum phase wavelet.
C     A desired output wavelet can then be specified in the frequency domain,
C     and a filter is then designed which can be applied to the whole data.
C
C     Optionally a wavelet can be supplied on earlier menu
C
C     The desired output wavelet is a butterworth filter (zero or min phase)
C     optionally desired output can have same spectrum as input wavelet

C     Method of filter calculation is standard normal equations

      REAL R4DAT(N,NRECS),TEMP(1024),AUTO(1024),X(1024),BUTT(1024)
      REAL BUTT2(1024),FILT(1024),PLOT1(1024,4),PLOT2(1024,4)
      REAL TEMP2(2048),XTEMP(1024),FILT2(1024),ERRARR(100),TRACE(1024)
      INTEGER LAGARR(100)

      COMPLEX CFILT(1024),CBUTT(1024),CTEMP(1024)
      COMPLEX CTEMP2(1024),CTEMP3(1024)
      CHARACTER*1 FAPPLY,IVA,WSAVE,WSUPP,IPWAV,ZPONLY
      CHARACTER*30 TITLE

C     some defaults
      WTNSE = 0.02
      FAPPLY = 'n'
      NTAP = 0
      ISAVE = 0
      ILAG = 0
      IPHASE = 0

C     zero some arrays
      CALL ZERO(NSAMS,TEMP)
      CALL ZERO(NSAMS,AUTO)
      CALL ZERO(NSAMS,FILT)
      CALL ZERO(NSAMS,BUTT)
      CALL ZERO(NSAMS,BUTT2)
      CALL ZERO(NSAMS,TEMP2)

  111 WRITE(6,100)
      WRITE(6,101)
      WRITE(6,102)AUTT1,AUTT2
      WRITE(6,103)WAVT1,WAVT2
      WRITE(6,104)BUT1,BUT2
      WRITE(6,105)BUT3,BUT4
      WRITE(6,106)WTNSE
      WRITE(6,107)FAPPLY
      WRITE(6,108)IVA
      WRITE(6,109)NTAP1,NTAP2
      WRITE(6,110)WSAVE
      WRITE(6,112)WSUPP
      WRITE(6,113)IPWAV
      WRITE(6,114)ZPONLY
      WRITE(6,115)ILAG
      WRITE(6,116)RLSQER
      WRITE(6,117)IPHASE
      WRITE(6,118)WIND1,WIND2

  100 FORMAT('     0      Return')
  101 FORMAT('     1      ok go !')
  102 FORMAT(/,'     2      Taper on trace for applying filter:',2F8.4)
  103 FORMAT('     3      Taper on wavelet  millisec         :',2F8.4)
  104 FORMAT('     4      Butterworth lc and slope db/oct    :',2F9.1)
  105 FORMAT('     5      Butterworth hc and slope db/oct    :',2F9.1)
  106 FORMAT('     6      White noise add       1=100%       :',F7.5)
  107 FORMAT('     7      Apply filter ?   (No plots)        :',A1)
  108 FORMAT('     8      Variable area plots ?              :',A1)
  109 FORMAT('     9      Filter tap st/fn from end in sam   :',2I5)
  110 FORMAT('     10     Save wavelet                       :',A1)
  112 FORMAT('     11     Wavelet supplied ?                 :',A1)
  113 FORMAT('     12     Plot wavlet ?                      :',A1)
  114 FORMAT('     13     Zero phase conversion only ?       :',A1)
  115 FORMAT('     14     Lag in samples of desired ouput    :',I4)
  117 FORMAT('     15     Zero phase (0) or min phase (1)    :',I4)
  118 FORMAT('     16     Window for wavelet extraction ms   :',2F8.4)
  116 FORMAT(/,'            Least square error                 :',F8.4)

      READ*,IOPT
      IF(IOPT.EQ.0)RETURN
      IF(IOPT.EQ.1)GO TO 999
      IF(IOPT.EQ.2)READ*,AUTT1,AUTT2
      IF(IOPT.EQ.3)READ*,WAVT1,WAVT2
      IF(IOPT.EQ.4)READ*,BUT1,BUT2
      IF(IOPT.EQ.5)READ*,BUT3,BUT4
      IF(IOPT.EQ.6)READ*,WTNSE
      IF(IOPT.EQ.7)THEN
          READ(5,1543)FAPPLY
          PRINT*,' 1=  Test filter with spike at sample 200 '
          PRINT*,' 2=  Test input wavelet with spike at sample 200 '
          PRINT*,' 3=  Test desired wavelet with spike at sample 200 '
          PRINT*,'     else filter data '
          READ*, ITEST
      ENDIF
      IF(IOPT.EQ.8)READ(5,1543)IVA
      IF(IOPT.EQ.9)READ*,NTAP1,NTAP2
      IF(IOPT.EQ.10)READ(5,1543)WSAVE
      IF(IOPT.EQ.11)READ(5,1543)WSUPP
      IF(IOPT.EQ.12)READ(5,1543)IPWAV
      IF(IOPT.EQ.13)READ(5,1543)ZPONLY
      IF(IOPT.EQ.14)THEN
                    PRINT*,' Enter 1 for optimum lag calculation'
                    READ*, IOPTL
                    IF(IOPTL.EQ.1)THEN
                         PRINT*,' Enter 1st lag   no lags and lag step'
                            READ*, LAG1,NLAG,DLAG
                            LAGK = 0
                            ILAG = LAG1
                    ELSE
                            PRINT*,' Enter lag'
                            READ(5,*)ILAG
                    ENDIF
      ENDIF
      IF(IOPT.EQ.15)READ(5,*)IPHASE
      IF(IOPT.EQ.16)READ(5,*)WIND1,WIND2
 1543 FORMAT(A1)
      GO TO 111
```

```
999  CONTINUE
     PRINT*,' DT = ',DT
     FNYQ = 1./(2.*DT/1000000.)
     DF = FNYQ/(FLOAT(NSAMS/2))
     PRINT*,' FNYQ = ',FNYQ
     PRINT*,' DF = ',DF
     PRINT*,' NSAMS =',NSAMS
     NT1 = INT(AUTT1/(DT/1000.)) +1
     NT2 = INT(AUTT2/(DT/1000.)) +1
     NWT1 = INT(WAVT1/(DT/1000.)) +1
     NWT2 = INT(WAVT2/(DT/1000.)) +1
     IW1 = INT(WIND1/(DT/1000.)) +1
     IW2 = INT(WIND2/(DT/1000.)) +1
     PRINT*,' NWT1 =',NWT1
     PRINT*,' NWT2 =',NWT2

     IF(WSUPP.EQ.'Y'.OR.WSUPP.EQ.'y')THEN
                          DO 2657 J = 1,NSAMS
                                  AUTO(J) = XTEMP(J)
2657                      CONTINUE
                          CALL LINTAP(NSAMS,AUTO,0,0,NWT1,NWT2)
                          CALL MAXSN(NWT2,AUTO,XB,II)
                          DO 2658 J = 1,NSAMS
                                  AUTO(J) = AUTO(J)/XB
2658                      CONTINUE
                          IF(IPWAV.EQ.'Y'.OR.IPWAV.EQ.'y')THEN
                          TITLE='WAVELET'
                          CALL SBPLOT(AUTO,NWT2,X,0,TITLE)
                          ENDIF
                          GOTO 5559
     ENDIF

C    Extract wavelet
     IF(ISAVE.EQ.0)THEN
     PRINT*,' Extracting wavelet !'
     CALL ZERO(NSAMS,TEMP2)
     DO 1234 I = 1,NRECS
          DO 200 J = IW1,IW2
                 TEMP(J) = R4DAT(J,I)
                 X(J) = FLOAT(J)
200       CONTINUE
          CALL CROSS(NSAMS,TEMP,NSAMS,TEMP,NSAMS,AUTO)
C         From TSASUB Adrian Bowen
          IF(AUTO(1).NE.0.0)THEN
          DO 340 J = 1,NSAMS
                 TEMP2(J) = TEMP2(J)+(AUTO(J)/AUTO(1))
340       CONTINUE
          ENDIF
1234  CONTINUE

C    Now do min phase conversion
     CALL MINPH(TEMP2,NWT2)
C    Finds minph wavelet from autocorrelation ... Claerbout
     PRINT*,'AFTER MINPH'
     CALL LINTAP(NSAMS,TEMP2,0,0,NWT1,NWT2)
     IF(IPWAV.EQ.'Y'.OR.IPWAV.EQ.'y')THEN
     TITLE='MINPH'
     CALL SBPLOT(TEMP2,NWT2,X,0,TITLE)
     ENDIF

     DO 5356 J = NWT2+1,NSAMS
            TEMP2(J) = 0.0
5356 CONTINUE
     DO 5556 J = 1,NSAMS
             AUTO(J) = TEMP2(J)
5556 CONTINUE
C    wavelet extracted----------------------------------------

     IF(WSAVE.EQ.'Y'.OR.WSAVE.EQ.'y')ISAVE=1

     ENDIF

C    Now work out butterworth wavelet spectrum
5559 IF(ZPONLY.EQ.'Y'.OR.ZPONLY.EQ.'y')GO TO 9752
C    Zp conversion only

C    High cut
     RNL = ALOG10((2.*(10.**(BUT4/10.))) -1.)
     RNL = RNL / (2.*ALOG10(2.))
     DO 300 J = 1,NSAMS/2+1
            RFR = DF*FLOAT(J-1)
            TEM = 1./(1.+((RFR/BUT3)**(2.*RNL)))
            BUTT(J) = SQRT(TEM)
300  CONTINUE

C    Low cut
     RNL = ALOG10((2.*(10.**(BUT2/10.)))-1.)
     RNL = RNL / (2.*ALOG10(2.))
     PRINT*,' RNL = ',RNL

     BUTT2(1) = 0.0
     DO 400 J = 2,NSAMS/2+1
            RFR = DF*FLOAT(J-1)
            TEM = 1./(1.+((BUT1/RFR)**(2.*RNL)))
            BUTT2(J) = SQRT(TEM)
400  CONTINUE


     DO 500 J = 1,NSAMS/2+1
            BUTT(J) = BUTT(J) * BUTT2(J)
500  CONTINUE

C    Setup desired putput .....zponly
9752 IF(ZPONLY.EQ.'Y'.OR.ZPONLY.EQ.'y')THEN
             DO 3826 J = 1,NSAMS
                     CTEMP(J) = CMPLX(AUTO(J),0.0)
3826         CONTINUE
             CALL FORK(NSAMS,CTEMP,-1.)
C            Claerbout
             DO 6548 J = 1,NSAMS
                     BUTT(J) = CABS(CTEMP(J))
6548         CONTINUE
C            Same amp spectrum as wavelet
     ENDIF

C    put desired output in time domain.............................
C    -ve frequencies (zero phase)
     IF(ZPONLY.EQ.'Y'.OR.ZPONLY.EQ.'y')GO TO 6723
     ISAM = 2
     DO 754 J = NSAMS , NSAMS/2+2 , -1
```

```
                BUTT(J) = BUTT(ISAM)
                ISAM = ISAM + 1
 754  CONTINUE
C     set up complex arrays for fft
6723  DO 889 J = 1,NSAMS
            CBUTT(J) = CMPLX(BUTT(J),0.0)
 889  CONTINUE
      CALL FORK(NSAMS,CBUTT,1.)
C     Claerbout
      DO 9726 J = 1,NSAMS
             BUTT2(J)=REAL(CBUTT(J))
 9726 CONTINUE


C     Convert desired output to min phase if required
      IF(IPHASE.EQ.1) THEN
                      PRINT*,' NSAMS = ',NSAMS
C                     Now shift desired output in order to compute the
C                     correct autocorrelation
                      CALL ZERO(NSAMS,TEMP)
                      DO 1469 J = 1,NSAMS/2
                           TEMP(J) = BUTT2(NSAMS-NSAMS/2+J)
 1469                 CONTINUE
                      DO 1470 J = NSAMS/2+1,NSAMS
                           TEMP(J) = BUTT2(J-NSAMS/2)
 1470                 CONTINUE
                      DO 1471 J = 1,NSAMS
                           BUTT2(J) = TEMP(J)
 1471                 CONTINUE
C                     shift done
                      CALL CROSS(NSAMS,BUTT2,NSAMS,BUTT2,NSAMS,TEMP)
C                     From TSASUB Adrian Bowen
                      DO 3322 J = NSAMS/10+1,NSAMS
                           TEMP(J) = 0.
 3322                 CONTINUE
                      CALL MINPH(TEMP,NSAMS/10)
C                     finds minph wavelet from autocorrelation .. Claerbout
                      TITLE = 'Min phase version of Butt'
                      CALL SBPLOT(TEMP,NSAMS/10,X,0,TITLE)
                      CALL ZERO(NSAMS,BUTT2)
                      DO 5498 J = 1,NSAMS
                           BUTT2(J) = TEMP(J)
 5498                 CONTINUE
                      PRINT*,' Enter taper in samples '
                      READ*,NN1,NN2
                      CALL LINTAP(NSAMS,BUTT2,0,0,NN1,NN2)
      ENDIF


C     Now shift desired output by ILAG samples
      IF(ILAG.GT.0)THEN
                   CALL ZERO(NSAMS,TEMP)
                   DO 5469 J = 1,ILAG
                           TEMP(J) = BUTT2(NSAMS-ILAG+J)
 5469              CONTINUE
                   DO 5470 J = ILAG+1,NSAMS
                           TEMP(J) = BUTT2(J-ILAG)
 5470              CONTINUE
                   DO 5471 J = 1,NSAMS
                           BUTT2(J) = TEMP(J)
 5471              CONTINUE
      ENDIF


C     Now do autocorrelation of wavelet
      CALL NORMAN(NWT2,AUTO)
      DO 7654 J = NWT2+1,NSAMS
            AUTO(J) = 0.0
 7654 CONTINUE
      CALL CROSS(NSAMS,AUTO,NSAMS,AUTO,NSAMS,TEMP2)
C     From TSASUB Adrian Bowen
      DO 3654 J = NWT2+1,NSAMS
            TEMP2(J) = 0.0
 3654 CONTINUE

C     Now do crosscorrelation of wavelet+desired output (butt)
      CALL CROSS(NSAMS,BUTT2,NSAMS,AUTO,NSAMS,TEMP)
C     From TSASUB Adrian Bowen

C     add white noise
      TEMP2(1) = TEMP2(1) + TEMP2(1)*WTNSE


C     solve normal equations
      CALL EUREKA(NSAMS,TEMP2,TEMP,FILT,FILT2)
C     From TSASUB Adrian Bowen

C     Now tranform filter and wavelet into the frequency domain
      DO 600 J = 1,NSAMS
            CFILT(J) = CMPLX(FILT(J),0.0)
            CTEMP(J) = CMPLX(AUTO(J),0.0)
 600  CONTINUE
      CALL FORK(NSAMS,CFILT,-1.)
      CALL FORK(NSAMS,CTEMP,-1.)
C     Claerbout


C     Test filter....
      DO 7263 J = 1,NSAMS
            CTEMP3(J) = CFILT(J) * CTEMP(J)
 7263 CONTINUE
      CALL FORK(NSAMS,CTEMP3,1.)
C     Claerbout
      DO 7264 J = 1,NSAMS
            TEMP(J) = REAL(CTEMP3(J))
 7264 CONTINUE


C     Calculate least square error
      RLSQER = 0.0
      CALL NORMAN(NSAMS,BUTT2)
      CALL NORMAN(NSAMS,TEMP)
      DO 4865 J = 1,NSAMS
            RLSQER = RLSQER + ((BUTT2(J) - TEMP(J))**2 )
 4865 CONTINUE



C     Now set up arrays for plotting
      DO 900 J = 1 , NSAMS/2-1
```

```
            PLOT1(J,1) = AUTO(J+NSAMS/2+1)
            PLOT1(J,2) = BUTT2(J+NSAMS/2+1)
            PLOT1(J,3) = FILT(J+NSAMS/2+1)
            PLOT1(J,4) = REAL(CTEMP3(J+NSAMS/2+1))
 900  CONTINUE
      DO 922 J = NSAMS/2 , NSAMS
            PLOT1(J,1) = AUTO(J-NSAMS/2+1)
            PLOT1(J,2) = BUTT2(J-NSAMS/2+1)
            PLOT1(J,3) = FILT(J-NSAMS/2+1)
            PLOT1(J,4) = REAL(CTEMP3(J-NSAMS/2+1))
 922  CONTINUE
C     put tes out put in freq
      CALL FORK(NSAMS,CTEMP3,-1.)
C     Claerbout
      DO 950 J = 1 , NSAMS
            PLOT2(J,1) = CABS(CTEMP(J))
            PLOT2(J,2) = BUTT(J)
            PLOT2(J,3) = CABS(CFILT(J))
            PLOT2(J,4) = CABS(CTEMP3(J))
 950  CONTINUE

C     Store fft of wav in ctemp3
      DO 7623 J = 1,NSAMS
            CTEMP3(J) = CTEMP(J)
 7623 CONTINUE

      IF(IOPTL.NE.1)THEN
      IF(FAPPLY.EQ.'N'.OR.FAPPLY.EQ.'n')THEN
      IF(IVA.EQ.'Y'.OR.IVA.EQ.'y')THEN
      CALL TDPLOT(PLOT1,NSAMS,4,NSAMS/3,NSAMS-NSAMS/3,1,4,-1.8,'Y','Y')
      CALL TDPLOT(PLOT2,NSAMS,4,1,NSAMS/4,1,4,-1.8,'Y','Y')
      ELSE
      CALL TDPLOT(PLOT1,NSAMS,4,NSAMS/3,NSAMS-NSAMS/3,1,4,-1.8,'N','Y')
      CALL TDPLOT(PLOT2,NSAMS,4,1,NSAMS/4,1,4,-1.8,'N','Y')
      ENDIF
      ENDIF
      ENDIF

C     apply filter
      IF(FAPPLY.EQ.'Y'.OR.FAPPLY.EQ.'y')THEN
C           Taper filter if required
            DO 1098 J = 1,NSAMS
                  TEMP(J) = FILT(J)
 1098       CONTINUE
        CALL LINTAP(NSAMS,TEMP,0,0,NSAMS/2+1-NTAP1,NSAMS/2+1-NTAP2)
            DO 1038 J = 1,NSAMS
                  TEMP2(J) = FILT(J)
 1038       CONTINUE
        CALL LINTAP(NSAMS,TEMP2,NSAMS/2+2+NTAP2,NSAMS/2+2+NTAP1,0,0)
            DO 1236 J = 1,NSAMS
                  CFILT(J) = CMPLX(TEMP(J)+TEMP2(J),0.0)
 1236       CONTINUE
C           Put filter into freq domain
            CALL FORK(NSAMS,CFILT,-1.)
C           Claerbout

C           do convolution
            DO 4365 I = 1,NRECS
C              Taper trace
               DO 1658 J = 1,NSAMS
                     TEMP(J) = R4DAT(J,I)
 1658          CONTINUE
               CALL LINTAP(NSAMS,TEMP,0,0,NT1,NT2)
               DO 1001 J = 1,NSAMS
               CTEMP(J) = CMPLX(TEMP(J),0.0)
               IF(ITEST.EQ.1.OR.ITEST.EQ.2)CTEMP(J) = CMPLX(0.0,0.0)
               IF(ITEST.EQ.3)CTEMP(J) = CMPLX(0.0,0.0)
 1001          CONTINUE
                  IF(ITEST.EQ.1)CTEMP(200) = CMPLX(1.0,0.0)
                  IF(ITEST.EQ.2)CTEMP(200) = CMPLX(1.0,0.0)
                  IF(ITEST.EQ.3)CTEMP(200) = CMPLX(1.0,0.0)
                  CALL FORK(NSAMS,CTEMP,-1.)
C                 Claerbout
               DO 1083 J = 1,NSAMS
                  IF(ITEST.EQ.1)CTEMP(J) = CTEMP(J) * CFILT(J)
                  IF(ITEST.EQ.2)CTEMP(J) = CTEMP(J) * CTEMP3(J)
                  IF(ITEST.EQ.3)CTEMP(J) = CTEMP(J) * BUTT(J)
                  IF(ITEST.EQ.0)CTEMP(J) = CTEMP(J) * CFILT(J)
 1083          CONTINUE
               PRINT*,' Convolution  ',I,' ok'
               CALL FORK(NSAMS,CTEMP,1.)
C              Claerbout
C              must now shift trace by the lag
               DO 7372 J = 1,NSAMS
                  TRACE(J) = REAL(CTEMP(J))
 7372          CONTINUE
               DO 6402 J = 1,NSAMS-ILAG
                     R4DAT(J,I) = TRACE(J+ILAG)
 6402          CONTINUE
C              now the wraparound
               DO 6020 J = 1,IABS(ILAG)
                     R4DAT(NSAMS-ILAG+J,I) = TRACE(J)
 6020          CONTINUE
               PRINT*,' Trace ',I,' shifted by -ve ',ILAG
 4365       CONTINUE

      RETURN

      ELSE
            IF(IOPTL.EQ.1)THEN
                  LAGK = LAGK+1
                  LAGARR(LAGK) = LAG1
                  ERRARR(LAGK) = RLSQER
                  PRINT*,' LAG1 = ',LAG1
                  PRINT*,' ILAG  = ',ILAG
                  PRINT*,' ERR  = ',RLSQER
                  ILAG = ILAG+DLAG
                  PRINT*,' LAGK = ',LAGK
                  IF(LAGK.EQ.NLAG)THEN
                        CALL MINSN(NLAG,ERRARR,XM,II)
               PRINT*,' OPT LAG CHOSEN = ',LAG1+ (II-1)*DLAG
                        ILAG = LAG1+ (II-1)*DLAG
                        IOPTL = 0
                  IF(FAPPLY.EQ.'Y'.OR.FAPPLY.EQ.'y')GO TO 999
                        GO TO 111
                  ENDIF
                  GO TO 999
            ENDIF
            GO TO 111
      ENDIF
```

```
RETURN
END
```

```
      PROGRAM VSPMIG

C     Migration is performed on common shot gathers. One downhole shot
C     with an array of surface receivers.
C     Follows the method of Berkhout (1984), and uses F-K wavefield
C     extrapolation .. see Claerbout I.E.I.
C     Berkhout (1984) "Seismic migration"


      PARAMETER(N=256,M=64,NR=48)
C     NR should be same as PROC program when the CS gather was output
C     ~~~~~~~~~~~~~~~~~~~~~~~~~~~~~~~~~~~~~~~~~~~~~~~~~~~~~~~~~~~~~~~~

      REAL RECDAT(N,M),SORDAT(N,M),OUTDAT(500,M),PLOT(N,M),BUTT(N)
      REAL R4DAT(1024,NR),V(500),TEMP(1024),AMP(N),PHZ(N),BUTT2(N)
      COMPLEX CREC(N,M),CSOR(N,M),C,NC,COMI,IMAGE(500,M),CTEM(M)
      COMPLEX COREL(N,M),CTR(M),CTS(M),CTEMP(N)

C     Reflection point mute arrays:
      REAL THICK(N),VREF(N),X(52000),Z(52000),DEP(N)

C     Input output arrays:
      CHARACTER*20 IPDISC,OPDISC,WFILE
      CHARACTER*180 A
      REAL RECDEP(NR),DBGAIN(NR),GCMSCL(NR)
      INTEGER IDPROC(5,24),NFIRST(NR),NCR(2)


C     ---------------------------------------------------------------
C     First read in input file
C     ---------------------------------------------------------------
537   WRITE(6,241)
      WRITE(6,242)NSHOT
      WRITE(6,243)IPDISC
      WRITE(6,244)NSAMS
      WRITE(6,245)NRECS
      WRITE(6,246)IFTR
      WRITE(6,247)M
      WRITE(6,248)ISPACE
      WRITE(6,249)
      WRITE(6,250)

241   FORMAT(/,' 1.     OK ! read      ')
242   FORMAT(/,' 2.     File # i.d.    ',I4)
243   FORMAT(/,' 3.     Disc to read   ',A12)
244   FORMAT(/,' 4.     No. samples    ',I4)
245   FORMAT(/,' 5.     No. channels   ',I4)
246   FORMAT(/,' 6.     Read trace 1 of the data to trace ',I3)
247   FORMAT(/,'        of the ',I1,' trace migration array')
248   FORMAT(/,' 7.     Data spacing within the migration array ',I3)
249   FORMAT(/,'        1=adjacent 2=every other ...etc ')
250   FORMAT(/,'        nrecsout = nrecs * this value   ')
      PRINT*,'  '
      PRINT*,'          Enter option ... <RETURN> then input '

      READ*,NOPT

      IF(NOPT.EQ.1) GO TO 1212
      IF(NOPT.EQ.2) READ(5,*  )NSHOT
      IF(NOPT.EQ.3) READ(5,899)IPDISC
      IF(NOPT.EQ.4) READ(5,*  )NSAMS
      IF(NOPT.EQ.5) READ(5,*  )NRECS
      IF(NOPT.EQ.6) READ(5,*  )IFTR
      IF(NOPT.EQ.7) READ(5,*  )ISPACE
899   FORMAT(A20)
      GO TO 537

1212  IDCODE= (NSHOT-1) * (NRECS+1) + 1
      LEN = (NSAMS+2) * 4

      OPEN(10,FILE=IPDISC,STATUS='OLD',ACCESS='DIRECT',RECL=LEN)
      READ(10,REC=IDCODE)A,SORPOS,NDUMM,RECDEP,DBGAIN,GCMSCL,NFIRST,
     &                   NCR,NPROCS,IDPROC,DUM
      DO 345 J = 1, NRECS
         NREC = IDCODE + J
         READ(10,REC=NREC)(R4DAT(I,J),I=1,NSAMS)
345   CONTINUE
      CLOSE(10)
C     read done!
C     ---------------------------------------------------------------



C     Max apparent dip to migrate ..... in apparent velocity
C     Rarely used
C     VAPP = 1.0/(DIPMX*1.0E-3)
C     VAPP = 0.0
C     PRINT*,'VAPP  = ',VAPP

C     ---------------------------------------------------------------

C     Set up some constants
      PI  = ACOS(-1.)
      PI2 = PI/2.0
      N2  = M
      NSARR = N
      ILTR = IFTR + (NRECS-1)*ISPACE

C     Zero arrays
      CALL ZERO2(N,M,RECDAT)
      CALL ZERO2(N,M,SORDAT)
      CALL ZERO2C(500,M,IMAGE)
      CALL ZERO2(500,M,OUTDAT)


C     set up migration parameters
799   WRITE(6,800)
      WRITE(6,801)
      WRITE(6,802) DMIG
      WRITE(6,803) DD
      WRITE(6,805) DT
      WRITE(6,806) SDEP
      WRITE(6,807) DX
      WRITE(6,810) IPPP
      WRITE(6,811) STR
      WRITE(6,812)
      WRITE(6,813) III
800   FORMAT(/,' 0          Return')
801   FORMAT(/,' 1          OK Migrate! ')
802   FORMAT(/,' 2          Total depth to migrate              :',F5.1)
```

```
803   FORMAT(/,' 3         Depth sample rate                  :',F5.1)
805   FORMAT(/,' 5         DT   in micro secs                 :',F5.1)
806   FORMAT(/,' 6         Source depth                       :',F5.1)
807   FORMAT(/,' 7         DX                                 :',F5.1)
810   FORMAT(/,' 9         Plot data to migrate 1=y           :',I1)
811   FORMAT(/,' 10        Tr no of source in migration array :',F5.1)
812   FORMAT(/,'           Source:                             ')
813   FORMAT(/,' 11        1=spike  2=sine wave  3=file read  :',I1)

      READ*, IOPT

      IF(IOPT.EQ.0) STOP
      IF(IOPT.EQ.1) GO TO 9999
      IF(IOPT.EQ.2) READ(5,*  )DMIG
      IF(IOPT.EQ.3) READ(5,*  )DD
      IF(IOPT.EQ.5) READ(5,*  )DT
      IF(IOPT.EQ.6) READ(5,*  )SDEP
      IF(IOPT.EQ.7) READ(5,*  )DX
      IF(IOPT.EQ.9) READ(5,*  )IPPP
      IF(IOPT.EQ.10)READ(5,*  )STR
      IF(IOPT.EQ.11)THEN
                    READ(5,*  )III
                    ISPH = 1
                    IF(III.EQ.2)THEN
                              PRINT*,'Enter freq of sine wave'
                              READ*,SFR
                    ENDIF
                    IF(III.EQ.3)THEN
                              PRINT*,'id=1  NRECS=1  NSAMS=1024'
                              PRINT*,'Enter file with source wavelet'
                              READ(5,5238)WFILE
 5238                         FORMAT(A20)
                              PRINT*,'Zero phase (0)  min phase (1) ?'
                              READ*,ISPH
                    ENDIF
      ENDIF

      GO TO 799

 9999 CONTINUE

C     Input now complete
C     ------------------------------------------------------------
      DTS = DT/1000000.
C     This is DT in seconds!!
C     ------------------------------------------------------------

C     Set up source function
C     The source is specified as either a spike, a sinwave or a wavelet (above).
C     This is specified over THREE traces in the source array (4m), weighted as
C     (0.5,1.0,0.5). Verticalilty may be specified by assigning the source to a
C     fraction trace no. (eg: 40.5). The weighting function (0.5,1.0,0.5) is
C     shifted laterally and interpolated appropriately.

      ISTR = INT(STR)
C     This will always round down

C     Interpolation of source function laterally
      SC  = (STR-FLOAT(ISTR)) * 0.5
      SC2 = (1.0-(STR-FLOAT(ISTR))) * 0.5

      IF(III.EQ.1)THEN
C     Source is spike
                    SORDAT(1,ISTR-1) = 0.5 - SC
                    SORDAT(1,ISTR  ) = 1.0 - SC
                    SORDAT(1,ISTR+1) = 1.0 - SC2
                    SORDAT(1,ISTR+2) = 0.5 - SC2
      ENDIF
      IF(III.EQ.2)THEN
C     sinewave as source-------------------
                    PI = ACOS(-1.)
                    T = 1./SFR
                    NS = INT(T/DTS)
                    DO 2932 I = 1,NS+1
            SORDAT(I,ISTR-1) = (0.5-SC )*SIN(2.*PI*SFR*FLOAT(I-1)*DTS)
            SORDAT(I,ISTR  ) = (1.0-SC )*SIN(2.*PI*SFR*FLOAT(I-1)*DTS)
            SORDAT(I,ISTR+1) = (1.0-SC2)*SIN(2.*PI*SFR*FLOAT(I-1)*DTS)
            SORDAT(I,ISTR+2) = (0.5-SC2)*SIN(2.*PI*SFR*FLOAT(I-1)*DTS)
 2932               CONTINUE
      ENDIF
      IF(III.EQ.3)THEN
C     Source in file WFILE   id=1 NRECS=1 NSAMS=1024   -------
      OPEN(11,FILE=WFILE,STATUS='OLD',ACCESS='DIRECT',RECL=LEN)
      READ(11,REC=1)A
      NSAMW = 1024
      NREC = 2
      READ(11,REC=NREC)(TEMP(I),I=1,NSAMW)
C     normalise TEMP:
      CALL NORMAN(NSAMW,TEMP)
      DO 6533 I = 1,N
              SORDAT(I,ISTR-1) = TEMP(I) * (0.5-SC)
              SORDAT(I,ISTR)   = TEMP(I) * (1.0-SC)
              SORDAT(I,ISTR+1) = TEMP(I) * (1.0-SC2)
              SORDAT(I,ISTR+2) = TEMP(I) * (0.5-SC2)
 6533 CONTINUE

      IF(ISPH.EQ.0)THEN
              KK=2
              DO 9912 I=N,N/2,-1
                 SORDAT(I,ISTR-1) = TEMP(KK) * (0.5-SC)
                 SORDAT(I,ISTR)   = TEMP(KK) * (1.0-SC)
                 SORDAT(I,ISTR+1) = TEMP(KK) * (1.0-SC2)
                 SORDAT(I,ISTR+2) = TEMP(KK) * (0.5-SC2)
                 KK = KK+1
 9912            CONTINUE
      ENDIF

      CLOSE(11)

      ENDIF
C     Source is done!
C     ------------------------------------------


C     ------------------------------------------------
C     put data to migrate into recdat
C     apply taper to edge traces ... seems to help rid some noise
      K = 1
 319  DO 913 I = IFTR,IFTR+NRECS-1
         DO 912 J = 1,NSARR
```

```
            IF(I.EQ.IFTR)          R4DAT(J,K)=R4DAT(J,K)*.4
            IF(I.EQ.IFTR+1)        R4DAT(J,K)=R4DAT(J,K)*.7
            IF(I.EQ.IFTR+NRECS-2)R4DAT(J,K)=R4DAT(J,K)*.7
            IF(I.EQ.IFTR+NRECS-1)R4DAT(J,K)=R4DAT(J,K)*.4
            RECDAT(J,I+(K-1)*(ISPACE-1)) = R4DAT(J,K)
 912     CONTINUE
         K = K + 1
 913  CONTINUE



C     If IPPP = 1 plot data to migrate
      IF(IPPP.EQ.1)THEN
         CALL TDPLOT(RECDAT,N,M,1,NSARR,1,N2,2.,'N','N')
         CALL TDPLOT(SORDAT,N,M,1,NSARR,ISTR-2,ISTR+2,2.,'N','N')
      ENDIF


C     set up velocity field
      CALL MIGVEL(V,N,VREF,NLAY,THICK,DD)


C     set up complex arrays for source and receiver wavefields
      DO 911 I = 1,N2
             DO 922 J = 1,NSARR
                      CREC(J,I) = CMPLX(RECDAT(J,I),0.0)
                      CSOR(J,I) = CMPLX(SORDAT(J,I),0.0)
 922         CONTINUE
 911  CONTINUE



C     Freq step (My INFO only !!!)
 333  DF   = (1./(2.*DTS)) / (FLOAT(NSARR)/2.)
      PRINT*,'DX = ',DX
      PRINT*,'DF = ',DF



C     Transform to f-k space
      CALL FFT2D(CSOR,NSARR,N2,-1.,-1.)
      CALL FFT2D(CREC,NSARR,N2,-1.,-1.)
C     FFT2d calls subroutine FORK ... Claerbout


C     Source depth in samples
      ISDEP = INT(SDEP/DD)
      PRINT*,' DD = ',DD
      PRINT*,' Source depth ISDEP = ',ISDEP


      PRINT*,' Plot 2dfft ?   1=y '
      READ*, IP
      IF(IP.EQ.1)THEN
      DO 444 I = 1,N2
         DO 445 J = 1,NSARR
              RECDAT(J,I) = CABS(CREC(J,I))
              SORDAT(J,I) = CABS(CSOR(J,I))
  445    CONTINUE
  444  CONTINUE
       CALL TDPLOT(SORDAT,N,M,1,NSARR,1,N2,2.,'N','N')
       CALL TDPLOT(RECDAT,N,M,1,NSARR,1,N2,2.,'N','N')
       ENDIF



C     ---------------------------------------------------------------------
C     Enter the values for the output wavelet shaping

C     The amplitude spectrum only is shaped to a butterworth impulse
      WRITE(6,*)' Enter high cut for wavelet shaping '
      READ(5,*)RHC
C     If the high cut is entered as 0 then no shaping is done
      WRITE(6,*)' Enter low cut for wavelet shaping '
      READ(5,*)RLC
      WRITE(6,*)' Enter high cut slope (db/oct)      '
      READ(5,*)SHC
      WRITE(6,*)' Enter low cut slope (db/oct)       '
      READ(5,*)SLC

C     Now calculate the amplitude spectrum of the butterworth impulse
      IF(RHC.NE.0.0)THEN
C     High cut
      RBH = ALOG10((2.*(10.**(SHC/10.))) -1.)
      RBH = RBH / (2.*ALOG10(2.))
C     Low cut
      RBL = ALOG10((2.*(10.**(SLC/10.)))-1.)
      RBL = RBL / (2.*ALOG10(2.))

      DO 1758 J = 1,NSARR/2 +1
              W = 2.*PI *FLOAT(J-1) / FLOAT(NSARR)
              IF(W.GT.PI)W=W-(2.*PI)
              F = (W/(2.*PI))/DTS
              TEM = 1./(1.+((F/RHC)**(2.*RBH)))
              BUTT(J) = SQRT(TEM)
              IF(F.EQ.0.0)THEN
                      TEM = 0.0
              ELSE
                      TEM = 1./(1.+((RLC/F)**(2.*RBL)))
              ENDIF
              BUTT2(J) = SQRT(TEM)
              BUTT(J) = BUTT(J) * BUTT2(J)
 1758 CONTINUE
      ENDIF


C     ---------------------------------------------------------------------
C     First of all the receivers must be reverse extrapolated to the source
C     depth .... the migration can then proceed as a 'normal' shot record

      IF(SDEP.GT.0.0)THEN

C     find the source layer
      CALL ZERO(N,DEP)
      DDUMMY = 0.0
C     DEP is depth to bottom of a layer
      DO 8583 I = 1,NLAY
              DEP(I) = DDUMMY + THICK(I)
              PRINT*,'DEP(I) ',DEP(I)
```

```
            DDUMMY = DEP(I)
            IF(SDEP.LE.DEP(I))THEN
                    SLAY = I
                    GO TO 8534
            ENDIF
 8583 CONTINUE
 8534 CONTINUE
      PRINT*,' SOURCE DEPTH = ',SDEP
      PRINT*,' SOURCE LAYER = ',SLAY

      DO 501 ID = 1,INT(SLAY)
         DO 502 ITRACE = 1,N2
            RKX = 2.*PI*FLOAT(ITRACE-1) / FLOAT(N2)
            IF(RKX.GT.PI)RKX=RKX-(2.*PI)
            RKX = RKX / DX
            DO 503 IFR = 1,NSARR/2+1
                   W = 2.*PI *FLOAT(IFR-1) / FLOAT(NSARR)
                   W = W/DTS
        IF(ABS(W).GT.ABS(VREF(ID)*RKX).AND.ABS(W).GT.ABS(VAPP*RKX))THEN
C                     reverse extrapolation of the receiver
                      COMI = CMPLX(0.0,+1.0)
                      TEM = SQRT(1.-(VREF(ID)**2*RKX**2 / W**2) )
                      IF(ID.EQ.INT(SLAY).AND.ID.NE.1)THEN
                          C =CEXP(COMI*W*(SDEP-DEP(ID-1))*TEM/VREF(ID))
                      ELSEIF(ID.EQ.INT(SLAY).AND.ID.EQ.1)THEN
                          C =CEXP(COMI*W*SDEP*TEM/VREF(ID))
                      ELSE
                          C =CEXP(COMI*W*(THICK(ID))*TEM/VREF(ID))
                      ENDIF
                      CREC(IFR,ITRACE) = CREC(IFR,ITRACE) * C
                   ELSE
                      CREC(IFR,ITRACE) = CMPLX(0.0,0.0)
                   ENDIF
  503         CONTINUE
  502       CONTINUE
  501  CONTINUE
       ENDIF
C      ---------------------------------------------------------------



C      ---------------------------------------------------------------
C      Start migration down depth axis as for finite offset shot record
       DO 200 ID = ISDEP+1,INT(DMIG/DD)

          DO 202 ITRACE = 1,N2

             RKX = 2.*PI*FLOAT(ITRACE-1) / FLOAT(N2)
             IF(RKX.GT.PI)RKX=RKX-(2.*PI)
             RKX = RKX / DX
             DO 203 IFR = 1,NSARR/2+1
                    W = 2.*PI *FLOAT(IFR-1) / FLOAT(NSARR)
                    W = W/DTS
         IF(ABS(W).GT.ABS(V(ID)*RKX).AND.ABS(W).GT.ABS(VAPP*RKX))THEN
C                      forward extrapolation of the source
                       COMI = CMPLX(0.0,-1.0)
                       TEM = SQRT(1.-(V(ID)**2*RKX**2 / W**2) )
                       C =CEXP(COMI*W*DD*TEM/V(ID))
                       CSOR(IFR,ITRACE) = CSOR(IFR,ITRACE) * C
C                      reverse extrapolation of the receiver
                       COMI = CMPLX(0.0,1.0)
                       C =CEXP(COMI*W*DD*TEM/V(ID))
                       CREC(IFR,ITRACE) = CREC(IFR,ITRACE) * C
                    ELSE
                       CSOR(IFR,ITRACE) = CMPLX(0.0,0.0)
                       CREC(IFR,ITRACE) = CMPLX(0.0,0.0)
                    ENDIF
  203         CONTINUE
  202       CONTINUE



C         Now correlate the wavefields by multiplication in the f-x domain
C         with one field time reversed (conjugate).
          DO 1987 J = 1,NSARR/2+1
                  DO 1789 I = 1,N2
                          CTR(I) = CREC(J,I)
                          CTS(I) = CSOR(J,I)
 1789             CONTINUE
                  CALL FORK(N2,CTR,1.)
                  CALL FORK(N2,CTS,1.)
C                 Subroutine from Claerbout

                  DO 1777 I = 1,N2
                          COREL(J,I) = CTS(I) * CONJG(CTR(I))
 1777             CONTINUE
 1987     CONTINUE



C     Now shape the amplitude spectrum of the correlated wavefield to
C     a specified butterworth impulse
C     If the high cut was entered as zero then no shaping is done
      IF(RHC.EQ.0.0)GOTO 3155

      DO 3154 I = 1,N2
              DO 3758 J = 1,NSARR/2+1
                      CTEMP(J) = COREL(J,I)
 3758         CONTINUE
              CALL POLAR(NSARR,CTEMP,AMP,PHZ)
C             Subroutine from Findlay computes amp and phase

              CALL MAXSN(NSARR,AMP,XM,II)
              DO 8758 J = 1,NSARR/2 +1
                      RE = BUTT(J)*XM*COS(PHZ(J))
                      AI = BUTT(J)*XM*SIN(PHZ(J))
                      COREL(J,I) = CMPLX(RE,AI)
                      CTEMP(J)   = COREL(J,I)
 8758         CONTINUE

C             DO 3958 J = 1,NSARR
C                     PLOT(J,1) = CABS(CTEMP(J))
C3958         CONTINUE
 3154  CONTINUE
```

```
C         Now extract t=zero component by frequency summation
 3155     DO 1954 I = 1,N2
             DO 1955 J = 1,NSARR/2+1
                   IMAGE(ID,I)=IMAGE(ID,I)+COREL(J,I)
 1955        CONTINUE
 1954     CONTINUE


      DO 302 II  = 1,N2
             OUTDAT(ID,II) = REAL(IMAGE(ID,II))
 302  CONTINUE

C     One depth step ID now complete
      WRITE(6,*)
     &'Depth step ',ID-ISDEP,' complete...image to ',ID/DD,' metres.'
 200  CONTINUE

C     For the mute set ISTR as nearest trace to STR.
      ISTR = NINT(STR)

      WRITE(6,*)' IFTR   ISTR   ILTR  '
      WRITE(6,*) IFTR, ' ',ISTR,'  ',ILTR

C     Now do the mute calling refmut
      WRITE(6,*)' Do you want to mute the output?  ...   1=Y'
      READ(5,*)IM
      IF(IM.EQ.1)THEN
      XOFFST = ABS(IFTR-ISTR)*DX
      CALL  REFMUT(X,Z,XOFFST,VREF,THICK,NLAY,SDEP,NRET)
C     Subroutine is adapted from program by Findlay

      DO 700 J = 1,ISTR
             OFF = ABS(ISTR-J)
             OFF = OFF * DX
             XTEST = DX
             ZMUTE = 0.0
             DO 701 JJ = 1,NRET
                    DIFF = ABS(X(JJ)-OFF)
                    IF(DIFF.LT.XTEST)THEN
                           ZMUTE  = Z(JJ)
                           XTEST = DIFF
                     ENDIF
 701         CONTINUE
             IMUTE = INT(ZMUTE/DD)
             IF(IMUTE.EQ.0.AND.OFF.GT.XOFFST/2.0)IMUTE=500
             PRINT*,' Trace ',J,' offset ',OFF,' mute = ',IMUTE*DD,' m'
             DO 702 I = 1,IMUTE
                    OUTDAT(I,J) = 0.0
 702         CONTINUE
 700  CONTINUE

C     Now the second half of the survey
      XOFFST = ABS(ISTR-ILTR)*DX
      CALL  REFMUT(X,Z,XOFFST,VREF,THICK,NLAY,SDEP,NRET)
C     Subroutine is adapted from program by Findlay

      DO 900 J = ISTR+1,N2
             OFF = ABS(ISTR-J)
             OFF = OFF * DX
             XTEST = DX
             ZMUTE = 0.0
             DO 901 JJ = 1,NRET
                    DIFF = ABS(X(JJ)-OFF)
                    IF(DIFF.LT.XTEST)THEN
                           ZMUTE  = Z(JJ)
                           XTEST = DIFF
                     ENDIF
 901         CONTINUE
             IMUTE = INT(ZMUTE/DD)
             IF(IMUTE.EQ.0.AND.OFF.GT.XOFFST/2.0)IMUTE=500
             PRINT*,' Trace ',J,' offset ',OFF,' mute = ',IMUTE*DD,' m'
             DO 902 I = 1,IMUTE
                    OUTDAT(I,J) = 0.0
 902         CONTINUE
 900  CONTINUE
C     muting done
      WRITE(6,*)' Muting ok'
      ENDIF



      PRINT*,' Plot migrated data  ?   1=y '
      READ*, IP
      IF(IP.EQ.1)THEN
      CALL TDPLOT(OUTDAT,500,M,1,200,1,N2,1.0,'N','Y')
      CALL TDPLOT(OUTDAT,500,M,1,200,1,N2,1.0,'N','N')
      CALL TDPLOT(OUTDAT,500,M,1,200,1,N2,1.0,'Y','N')
      ENDIF



C---------------------Now write out file-------------------
      PRINT*,' Enter output file name '
      READ(5,899)OPDISC
      NRECS = NRECS*ISPACE
      PRINT*,'Enter the number of output depth samples'
      READ*,NSAMS

      LEN = (NSAMS+2)*4
      IDCODE = (NSHOT - 1) * (NRECS+1) + 1
      OPEN(2,FILE=OPDISC,STATUS='UNKNOWN',FORM='UNFORMATTED',
     1        ACCESS='DIRECT',RECL=LEN)

C     Output headers
      WRITE(2,REC=IDCODE)A,SORPOS,NRECS,RECDEP,DBGAIN,GCMSCL,NFIRST,
     1                     NCR,NPROCS,IDPROC,DT

C     Write seismogram records
         DO 132 J = 1,  NRECS
            NREC = IDCODE + J
            WRITE(2,REC=NREC)(OUTDAT(I,J+IFTR-1),I=1,NSAMS)
  132    CONTINUE
      CLOSE(2)

      STOP
```